Champs Magnétiques et Effet Dynamo dans les Corps Célestes

Dr. Allan Sacha Brun
Service d'Astrophysique, CEA Saclay
(lcd-www.colorado.edu/sabrun & sacha.brun@cea.fr)

Magnétohydrodynamique, Effet Dynamo et Théorie du champ moyen

- Les équations du mouvement ou hydrodynamiques
- Les équations de Maxwell et d'induction
- Théorie des champs moyens, effet dynamo, effets α et ω

The Dynamo Effect what is it exactly?

The main source of magnetic filed in the Universe is the due to dynamo action:

A definition: this is the property that a conducting fluid possesses to generate a magnetic field B via its motions (self-induction) and to sustain it against Ohmic dissipation

This is intrinsically a tri dimensional effect, there is for exemple an anti-dynamo Theorem (Cowling's theorem) forbidding purely axisymmetric dynamos

Some References:

MHD: Cowling (1957), Moffatt (1978), Radler & Krause (1981), Parker (1989), Chouduri (1997), Davidson (2000),
Cosmic Magnetism: Zeldovich et al. (1983), Parker (1989), Hollerbach & Rudiger (2004),
Turbulence and fluid dynamics: Kundu & Cohen (2003), Rieutord (1995), Lesieur 1999, Frisch 1999

Equations du Mouvement

$$\frac{\partial \rho}{\partial t} = -\boldsymbol{\nabla} \cdot (\rho \mathbf{v}), \quad (1)$$

$$\rho \frac{\partial \mathbf{v}}{\partial t} = -\rho(\mathbf{v} \cdot \boldsymbol{\nabla})\mathbf{v} - \boldsymbol{\nabla} P + \rho \mathbf{g} - 2\rho \boldsymbol{\Omega_o} \times \mathbf{v} - \boldsymbol{\nabla} \cdot \boldsymbol{\mathcal{D}}, \quad (2)$$

$$\rho T \frac{\partial S}{\partial t} = -\rho T(\mathbf{v} \cdot \boldsymbol{\nabla})S + \boldsymbol{\nabla} \cdot (\kappa_r \rho c_p \boldsymbol{\nabla} T) + 2\rho\nu \left[e_{ij} e_{ij} - 1/3(\boldsymbol{\nabla} \cdot \mathbf{v})^2 \right] + \rho\epsilon, \quad (3)$$

Tenseur visqueux:

$$\mathcal{D}_{ij} = -2\rho\nu[e_{ij} - 1/3(\boldsymbol{\nabla} \cdot \mathbf{v})\delta_{ij}],$$

Maxwell's Equation (cgs)

$$\nabla \cdot \mathbf{E} = 4\pi\rho, \quad (4)$$

$$\nabla \times \mathbf{E} = -\frac{1}{c}\frac{\partial \mathbf{B}}{\partial t}, \quad (5)$$

$$\nabla \cdot \mathbf{B} = 0, \quad (6)$$

$$\nabla \times \mathbf{B} = \frac{4\pi}{c}\mathbf{J} + \frac{1}{c}\frac{\partial \mathbf{E}}{\partial t} \quad (7)$$

Remark: 3 types of magnetic materials ($\boldsymbol{B}=\mu\boldsymbol{H}$, $\boldsymbol{B}$ magnetic field):
Diamagnetism (magnetic permeability $\mu<1$): most materials are diamagnetic (water for ex) (repulsion limits externally imposed field) (electronic levels full)
Paramagnetic ($\mu>1$): weak attraction (electronic levels not full) (aluminium for ex)
Ferromagnetic ($\mu>>1$): strong attraction, existence of magnetic domains through self organization/orientation of magnetic spins, residual magnetism (hysteresis) (iron for ex).

Induction Equations

From Maxwell's equations (5) & (7), and in the case where the displacement current is negligeable (i.e v << c):

$$\frac{\partial \mathbf{B}}{\partial t} = -c\boldsymbol{\nabla} \times \mathbf{E} \text{ and } \mathbf{J} = \frac{c}{4\pi}(\boldsymbol{\nabla} \times \mathbf{B}),$$

And using Ohm's law, for a moving conducting fluid with velocity $\mathbf{v}$:

$$\mathbf{J} = \sigma \left(\mathbf{E} + \frac{\mathbf{v} \times \mathbf{B}}{c} \right)$$

One can deduce the Induction equation:

Induction Equation

$$\frac{\partial \mathbf{B}}{\partial t} = -c\boldsymbol{\nabla}\times\mathbf{E} = -\boldsymbol{\nabla}\times\left(\frac{c\mathbf{J}}{\sigma} - \mathbf{v}\times\mathbf{B}\right)$$

$$= -\boldsymbol{\nabla}\times\left(\frac{c^2}{4\pi\sigma}\boldsymbol{\nabla}\times\mathbf{B} - \mathbf{v}\times\mathbf{B}\right)$$

$$\boxed{\frac{\partial \mathbf{B}}{\partial t} = \boldsymbol{\nabla}\times(\mathbf{v}\times\mathbf{B}) - \boldsymbol{\nabla}\times(\eta\boldsymbol{\nabla}\times\mathbf{B})} \quad (8)$$

with $\eta = c^2/4\pi\sigma$ the magnetic diffusivity,

$$\frac{\partial \mathbf{B}}{\partial t} = \boldsymbol{\nabla}\times(\mathbf{v}\times\mathbf{B}) + \eta\Delta\mathbf{B}, \text{ if } \eta = cst.$$

Equations de la Magnétohydrodynamique

Continuité, Navier-Stokes, Energie (+ force de Laplace + diffusion Ohmique):

$$\frac{\partial \rho}{\partial t} = -\boldsymbol{\nabla}\cdot(\rho\mathbf{v}), \qquad (1)$$

$$\rho\frac{\partial \mathbf{v}}{\partial t} = -\rho(\mathbf{v}\cdot\boldsymbol{\nabla})\mathbf{v} - \boldsymbol{\nabla}P + \rho\mathbf{g} - 2\rho\boldsymbol{\Omega_o}\times\mathbf{v}$$

$$- \boldsymbol{\nabla}\cdot\boldsymbol{\mathcal{D}} + \boxed{\frac{1}{4\pi}(\boldsymbol{\nabla}\times\mathbf{B})\times\mathbf{B}}, \qquad (2)$$

$$\rho T\frac{\partial S}{\partial t} = -\rho T(\mathbf{v}\cdot\boldsymbol{\nabla})S + \boldsymbol{\nabla}\cdot(\kappa_r\rho c_p\boldsymbol{\nabla}T) + \boxed{\frac{4\pi\eta}{c^2}\mathbf{J}^2}$$

$$+ 2\rho\nu\left[e_{ij}e_{ij} - 1/3(\boldsymbol{\nabla}\cdot\mathbf{v})^2\right] + \rho\epsilon, \qquad (3)$$

plus induction:

$$\frac{\partial \mathbf{B}}{\partial t} = \boldsymbol{\nabla}\times(\mathbf{v}\times\mathbf{B}) - \boldsymbol{\nabla}\times(\eta\boldsymbol{\nabla}\times\mathbf{B}) \qquad (8)$$

Diffusivités dans le Soleil

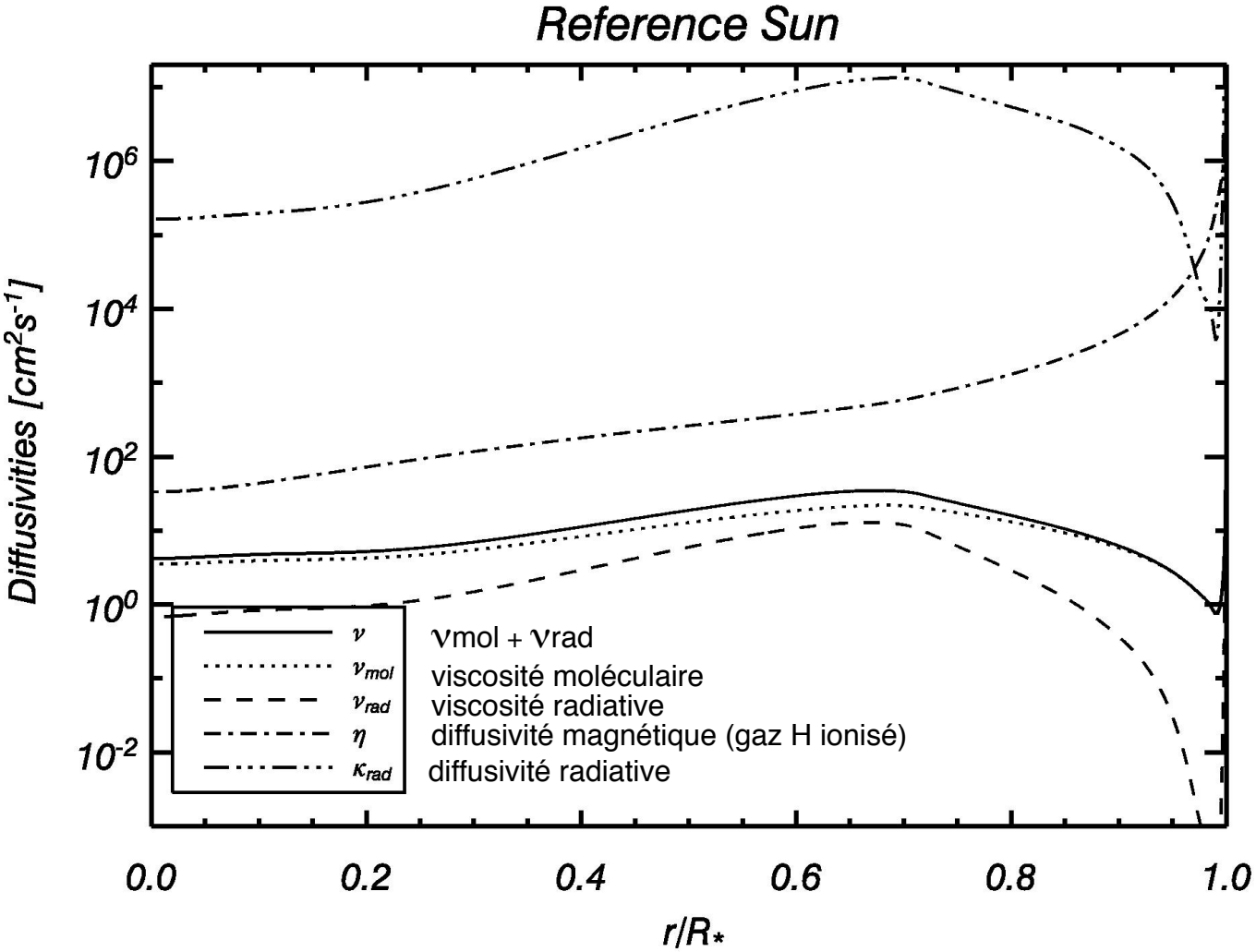

$$\nu_{rad} = \frac{4}{15}\frac{a}{c}\frac{T^4}{\rho^2\kappa_{opa}} \qquad \nu_{mol} = \frac{2.2\,10^{-15}}{\ln\Lambda}\frac{T^{5/2}}{\rho} \qquad \eta = 5.2\,10^{11}\ln\Lambda\, T^{-3/2}$$

$$\kappa_{rad} = \frac{\chi}{\rho c_p} = \frac{4}{3}\frac{acT^3}{\rho^2 c_p \kappa_{opa}}$$

See Zeldovich et al. 1983, for a discussion of the formula of ν, η, κ

Nombres de Prandtl (Pr), Prandtl magnétique (Pm) & Roberts (Q)

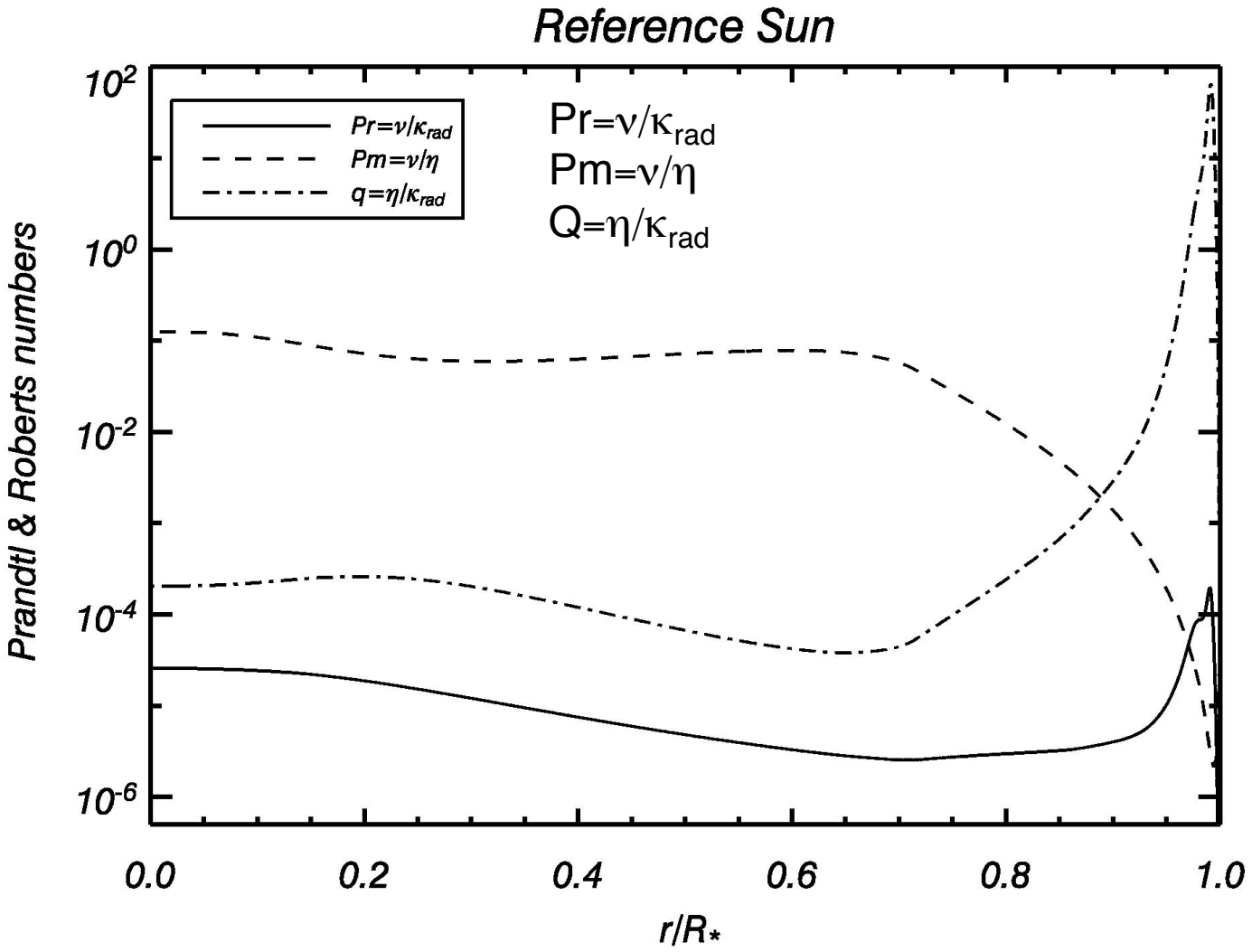

Few Remarks on the Induction Equation

$$\frac{\partial \mathbf{B}}{\partial t} = \boldsymbol{\nabla} \times (\mathbf{v} \times \mathbf{B}) + \eta \Delta \mathbf{B}$$

If the fluide is at rest, the equation simplifies to: $\frac{\partial \mathbf{B}}{\partial t} = \eta \Delta \mathbf{B}$

this is a diffusion equation, the magnetic field **B** decays in an uniform sphere of radius R in an Ohmic time scale:

$$\tau_\eta = \frac{R^2}{\pi^2 \eta}$$

In laboratory conductors, τ_η is small (10 s for a 1-m copper sphere), but in cosmic conductors, it can be Huge (> 10^{10} years)

On the contrary if the fluid is in motion (and its resistance negligeable), then the equation reads:

$$\frac{\partial \mathbf{B}}{\partial t} = \boldsymbol{\nabla} \times (\mathbf{v} \times \mathbf{B})$$

This means that the magnetic fields lines are « frozen » in the fluid

Few Remarks on the Induction Equation

The Magnetic Reynolds number Rm=νL/η is useful to assess in which of two previous regimes the system under study is, it is generally small in laboratory experiments (Rm ~1 et < 50) & big in cosmic bodies. Theoretically there is a dynamo if Rm is big enough (above a certain threshold)

This means that even though the electric currents in laboratory conductors are mainly determined by the conductivity σ, in a cosmic body σ has little influence on the amplitude of the electric current flowing, a change for exemple by a factor of 10 of σ, will not induce a significant change of $\mathbf{B}$. the conductivity is only setting the electric field $\mathbf{E}$ (weak) necessary to the existence of the currents (Cowling 1957).

Remark: the first term of the RHS of the induction equation can be split in two parts:

$$\boldsymbol{\nabla} \times (\mathbf{v} \times \mathbf{B}) = (\mathbf{B} \cdot \boldsymbol{\nabla})\mathbf{v} - (\mathbf{v} \cdot \boldsymbol{\nabla})\mathbf{B}$$

a term (first) for the distortion and shearing of $\mathbf{B}$ and a term for its advective transport.

Anelastic MHD Equations

$$\boxed{\nabla \cdot (\bar{\rho}\mathbf{v}) = 0}, \qquad \boxed{\nabla \cdot \mathbf{B} = 0},$$

$$\bar{\rho}\left(\frac{\partial \mathbf{v}}{\partial t} + (\mathbf{v}\cdot\nabla)\mathbf{v} + 2\boldsymbol{\Omega_o}\times\mathbf{v}\right) = -\nabla P + \rho\mathbf{g}$$

$$+\boxed{\frac{1}{4\pi}(\nabla\times\mathbf{B})\times\mathbf{B}} - \nabla\cdot\bar{\mathcal{D}} - [\nabla\bar{P} - \bar{\rho}\mathbf{g}],$$

$$\bar{\rho}\bar{T}\frac{\partial S}{\partial t} + \bar{\rho}\bar{T}\mathbf{v}\cdot\nabla(\bar{S}+S) = \boxed{\frac{4\pi\eta}{c^2}\mathbf{j}^2} + \boxed{\bar{\rho}\epsilon},$$

$$+\nabla\cdot(\kappa_r\bar{\rho}c_p\nabla(\bar{T}+T)) + \boxed{\nabla\cdot(\kappa\bar{\rho}\bar{T}\nabla(\bar{S}+S))}$$

$$+2\bar{\rho}\nu[e_{ij}e_{ij} - 1/3(\nabla\cdot\mathbf{v})^2]$$

$$\frac{\partial \mathbf{B}}{\partial t} = \nabla\times(\mathbf{v}\times\mathbf{B}) - \nabla\times(\eta\nabla\times\mathbf{B})$$

$$\bar{\mathcal{D}}_{ij} = -2\bar{\rho}\nu[e_{ij} - 1/3(\nabla\cdot\mathbf{v})\delta_{ij}],$$

Case of a Stratified Compressible Fluid under the influence of Rotation and Magnetic field

Kinematic vs Dynamic (nonlinear) Dynamo

If the Lorentz force can be neglected in Navier-Stokes equations, we speak about *kinematic dynamo*, the instability is linear with an exponential growth

On the contrary (which occurs for finite amplitude B fields), we speak of *dynamical dynamo*, there is a feedback of the Lorentz force on the fluid motions, the instability saturates and the magnetic fields reach a given value. The magnetic energy ME=$\mathrm{B}^2/8\pi$ is near (or larger then) an equipartition value with the kinetic energy KE=$0.5\rho \mathrm{v}^2$ of the fluid.

Remark: The Lorentz force can be split in 2 parts,

$$\mathbf{F} = \frac{1}{c}\mathbf{J}\times\mathbf{B} = \frac{1}{4\pi}(\boldsymbol{\nabla}\times\mathbf{B})\times\mathbf{B}$$
$$= \boxed{\frac{1}{8\pi}\boldsymbol{\nabla}\mathbf{B}^2}_a - \boxed{\frac{1}{4\pi}(\mathbf{B}\cdot\boldsymbol{\nabla})\mathbf{B}}_b$$

A magnetic pressure (term a) perpendicular to the magnetic field lines and a magnetic tension (term b) along them.

Kinematic Mean Field Theory

Starting point is the magnetic induction equation of MHD:

$$\frac{\partial \mathbf{B}}{\partial t} = \nabla \times (\mathbf{u} \times \mathbf{B}) + \eta \nabla^2 \mathbf{B},$$

where **B** is the magnetic field, **u** is the fluid velocity and η is the magnetic diffusivity (assumed constant for simplicity).

Assume scale separation between large- and small-scale field and flow:

$$\mathbf{B} = \mathbf{B}_0 + \mathbf{b}, \quad \mathbf{U} = \mathbf{U}_0 + \mathbf{u},$$

where **B** and **U** vary on some large length scale L, and **u** and **b** vary on a much smaller scale l.

$$\langle \mathbf{B} \rangle = \mathbf{B}_0, \quad \langle \mathbf{U} \rangle = \mathbf{U}_0,$$

where averages are taken over some intermediate scale $l \ll a \ll L$.

For simplicity, ignore large-scale flow, for the moment.

Induction equation for mean field:

$$\frac{\partial \mathbf{B}_0}{\partial t} = \nabla \times \mathbf{E} + \eta \nabla^2 \mathbf{B}_0,$$

where mean emf is $\mathcal{E} = \langle \mathbf{u} \times \mathbf{b} \rangle.$

This equation is exact, but is only useful if we can relate $\mathcal{E}$ to $\mathbf{B}_0$.

Consider the induction equation for the fluctuating field:

$$\frac{\partial \mathbf{b}}{\partial t} = \nabla \times (\mathbf{u} \times \mathbf{B}_0) + \nabla \times \mathbf{G} + \eta \nabla^2 \mathbf{b},$$

Where $\mathbf{G} = \mathbf{u} \times \mathbf{b} - \langle \mathbf{u} \times \mathbf{b} \rangle$. "pain in the neck term"

Si, G est petit, alors la force électromotrice moyenne (mean emf), peut être développée en fonction de <B>$_\phi$:

$$< \mathcal{E}_i >_\phi = < (u \times b)_i >_\phi = \alpha_{ij} < B_j >_\phi + \beta_{ijk} \frac{\partial < B_j >_\phi}{\partial x_k} + \ldots$$

BASIC PROPERTIES OF THE MEAN FIELD EQUATIONS

Add back in the mean flow U_0 and the mean field equation becomes

$$\frac{\partial \mathbf{B}_0}{\partial t} = \nabla \times (\alpha \mathbf{B}_0 + \mathbf{U}_0 \times \mathbf{B}_0) + (\eta + \beta)\nabla^2 \mathbf{B}_0.$$

ici α et β considérés isotropes

Now consider simplest case where $\alpha = \alpha_0 \cos\theta$ and $U_0 = U_0 \sin\theta\, \mathbf{e}_\phi$

In contrast to the induction equation, this can be solved for axisymmetric mean fields of the form $\mathbf{B}_0 = B_{0t}\mathbf{e}_\varphi + \nabla \times (A_{0P}\mathbf{e}_\varphi)$

The Ω effect

Conversion of poloidal to toroidal field by differential rotation.

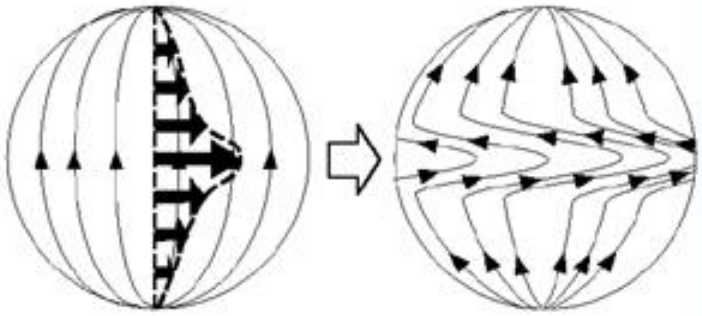

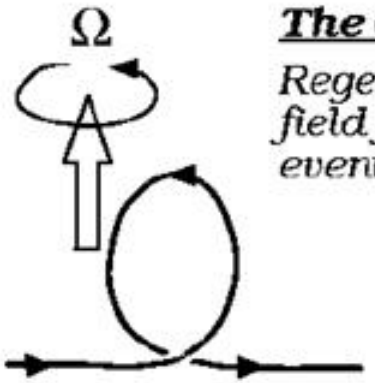

The α effect

Regeneration of poloidal field from toroidal by cyclonic events in rotating convection.

Transport et génération du champ toroidal Btor

Effet Omega (Ω): enroulement des lignes de champ

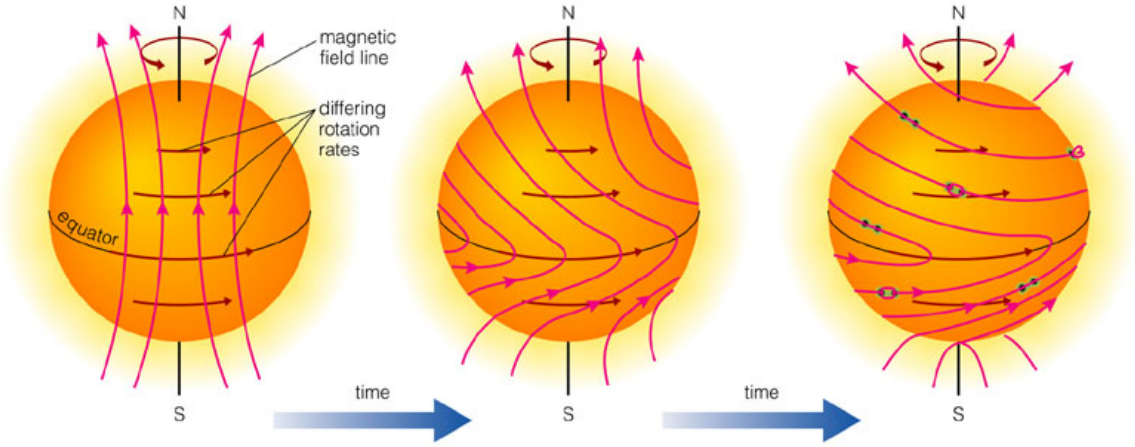

Jouve & Brun 2007, 2009

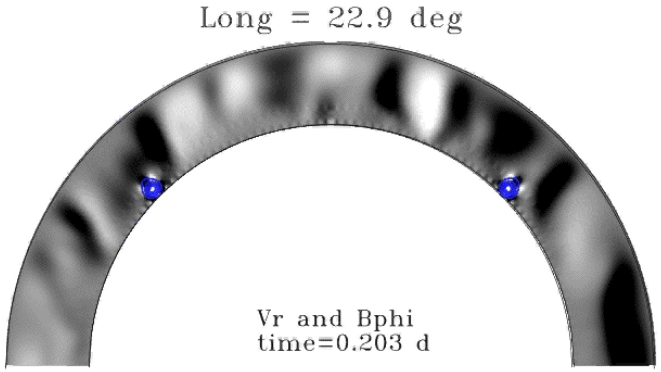

Simulations CEA projet STARS2

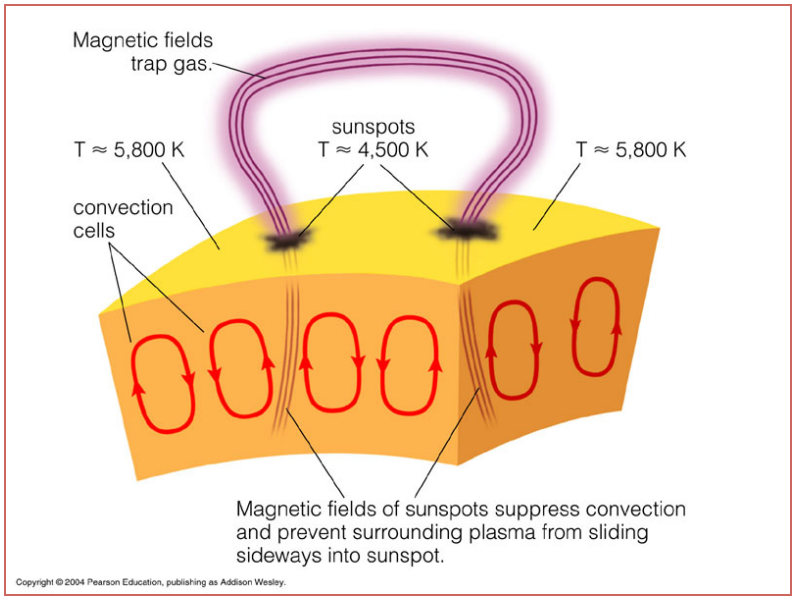

Babcock-Leighton Mechanism and Polar Cap Reversal

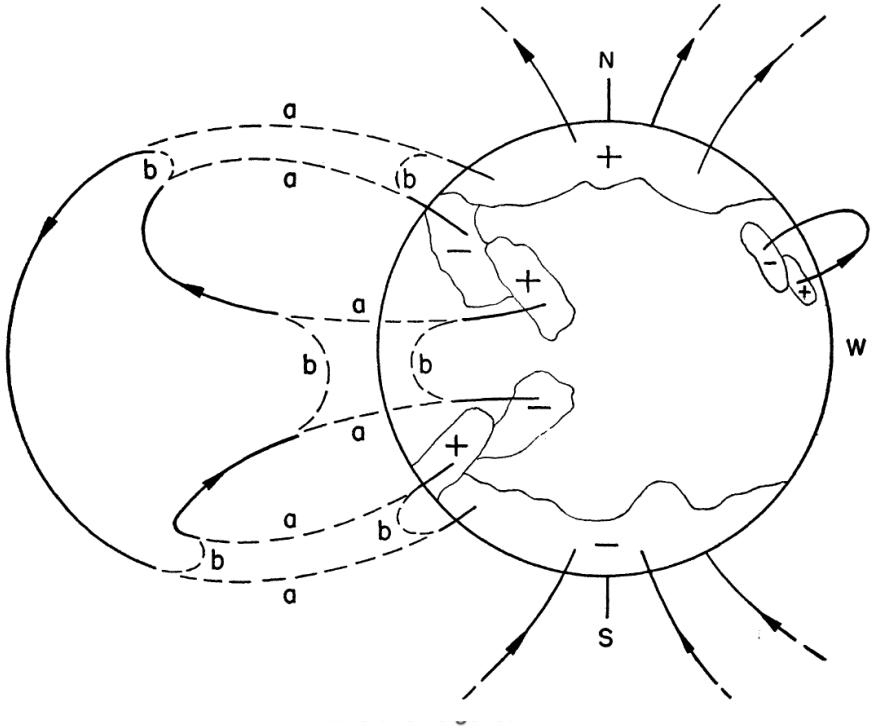

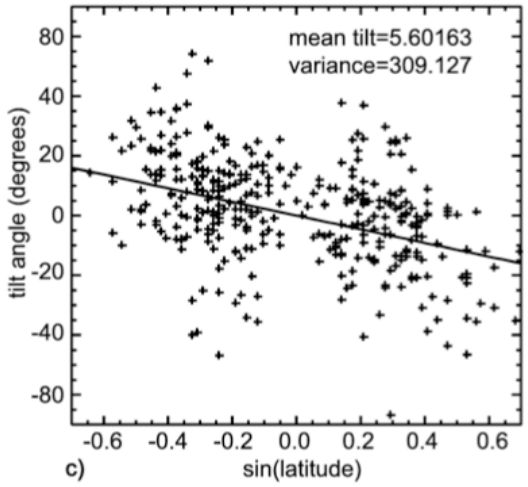

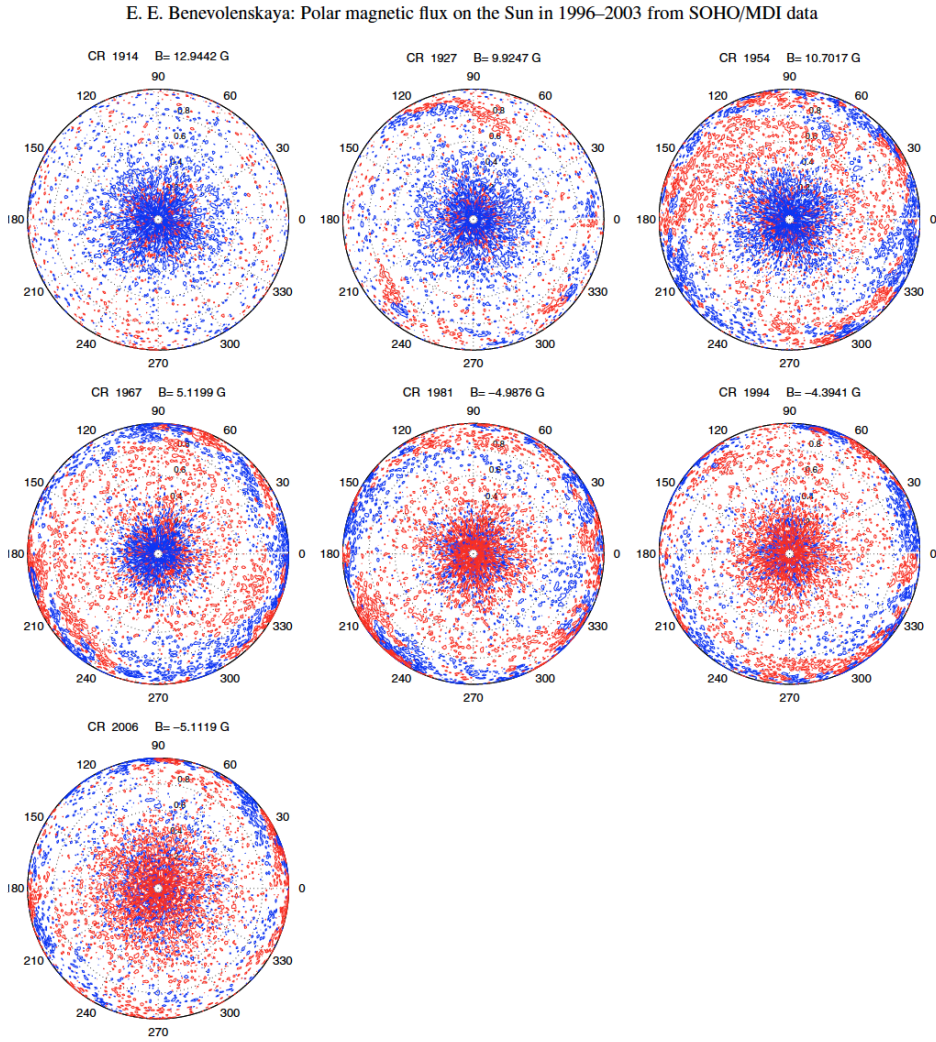

Joy's Law
Tilt of AR

How important is it to get the 11yr dynamo?

Modèles de Dynamo cinématique
2-D MHD axisymmétrique du Soleil

- Distributed dynamo: fails
- Interface dynamo:

  1) alpha-omega $\alpha\omega$

  2) Babcock-Leigthon (flux transport)

  3) mixed of both! (best model so far)

$\alpha-\Omega$ vs Babcock-Leighton dynamo mechanisms

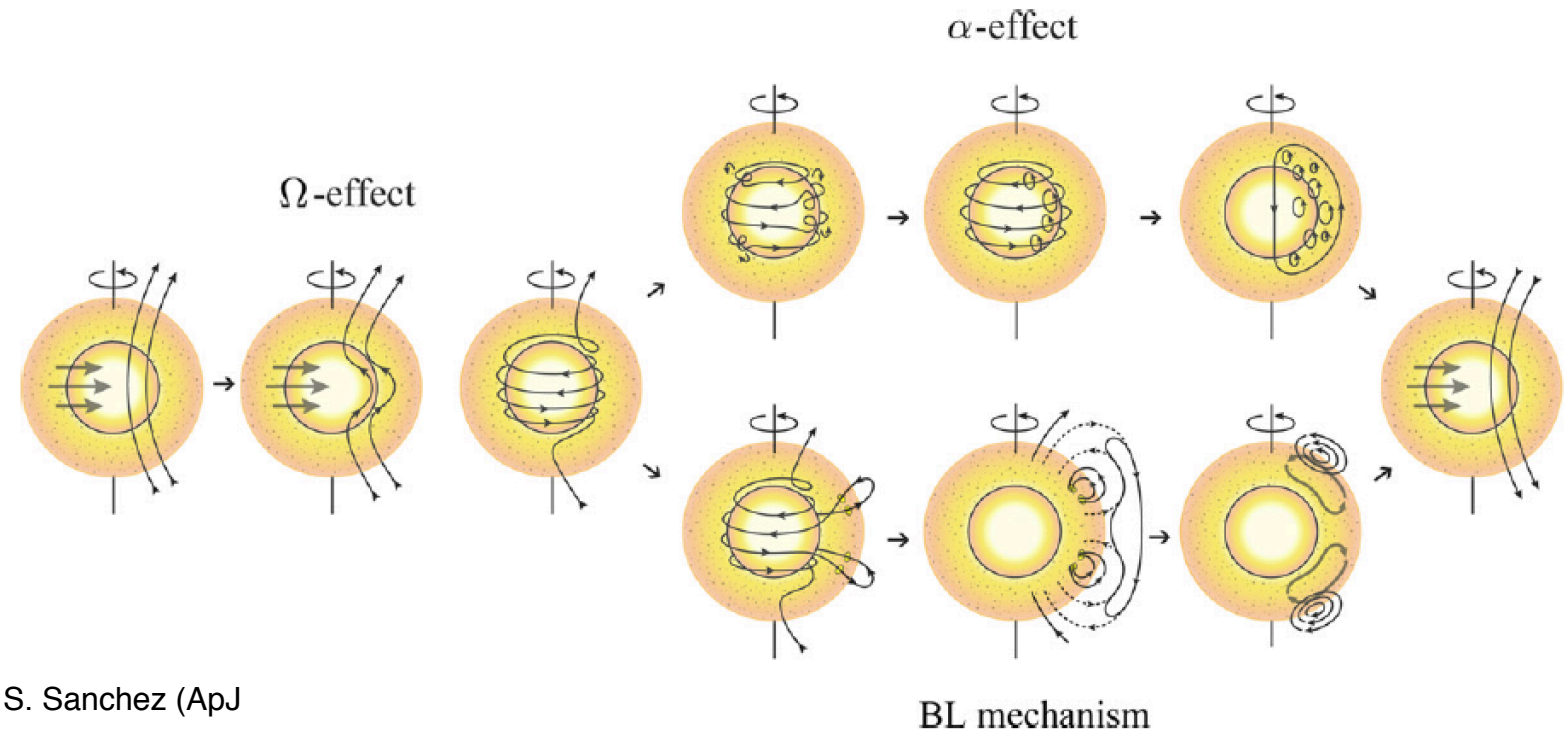

Courtesy: S. Sanchez (ApJ

Figure 1. Sketch of the main processes at work in our solar dynamo model. The Ω-effect (left) depicts the transformation of a primary poloidal field into a toroidal field by means of the differential rotation. The poloidal field regeneration is next accomplished either by the α-effect (top) and/or by the Babcock-Leighton mechanism (bottom). In the α-effect case, the toroidal field at the base of the convection zone is subject to cyclonic turbulence. Secondary small-scale poloidal fields are thereby created, and produce on average a new, large-scale, poloidal field. In the Babcock-Leighton mechanism, the primary process for poloidal field regeneration is the formation of sunspots at the solar surface from the rise of buoyant toroidal magnetic flux tubes from the base of the convection zone. The magnetic fields of those sunspots nearest to the equator in each hemisphere diffuse and reconnect, while the field due to those sunspots closer to the poles has a polarity opposite to the current one, which initiates a polarity reversal. The newly formed polar magnetic flux is transported by the meridional flow to the deeper layers of the convection zone, thereby creating a new large-scale poloidal field.

Modèles Dynamo Champs Moyens:

- Résolvent équation d'induction en axisymmétrique (donc introduction d'un terme pour satisfaire Cowling anti-dynamo théoreme)
- C'est l'effet alpha , toroidal -> poloidal
- Ou un terme source de surface S, toroidal -> poloidal
- Considère un profil de rotation => effet Omega (pol->tor)
- Régime cinématique (pas de retour sur champ de vitesse)
- Certains modèles prescrivent aussi une circulation méridienne

Plus: rapide donc large étude d'espace de paramètres
paramétrisation de alpha permet un réglage fin, résultats comparable aux observations

Moins: cinématique, prescrit alpha, Omega (éventuellement déduit de l'héliosismologie), MC (si présente) et mag diffusivité de manière non consistante

2D Mean Field models: Babcock-Leighton

1 single cell per hemisphere

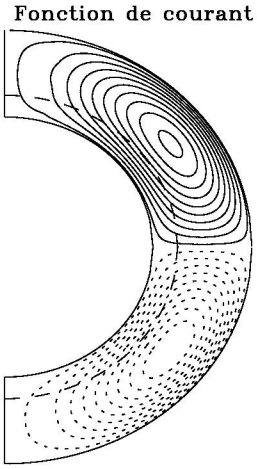

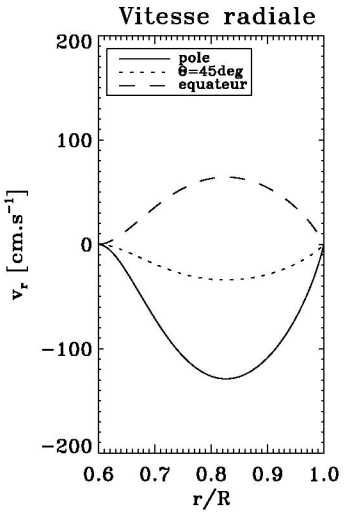

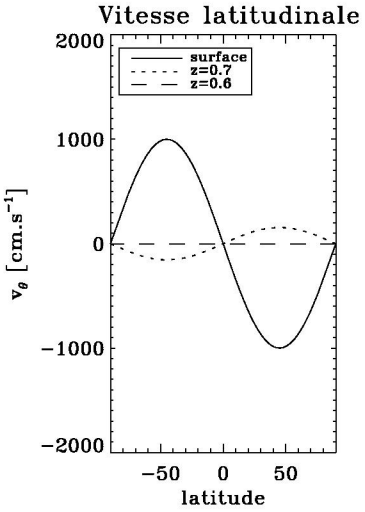

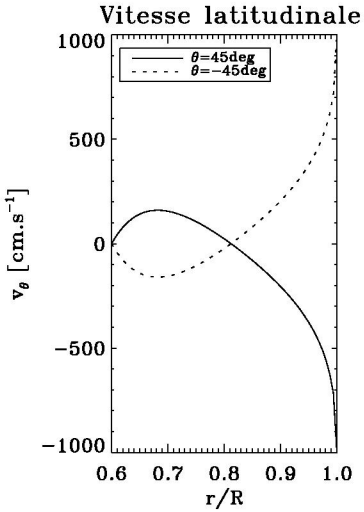

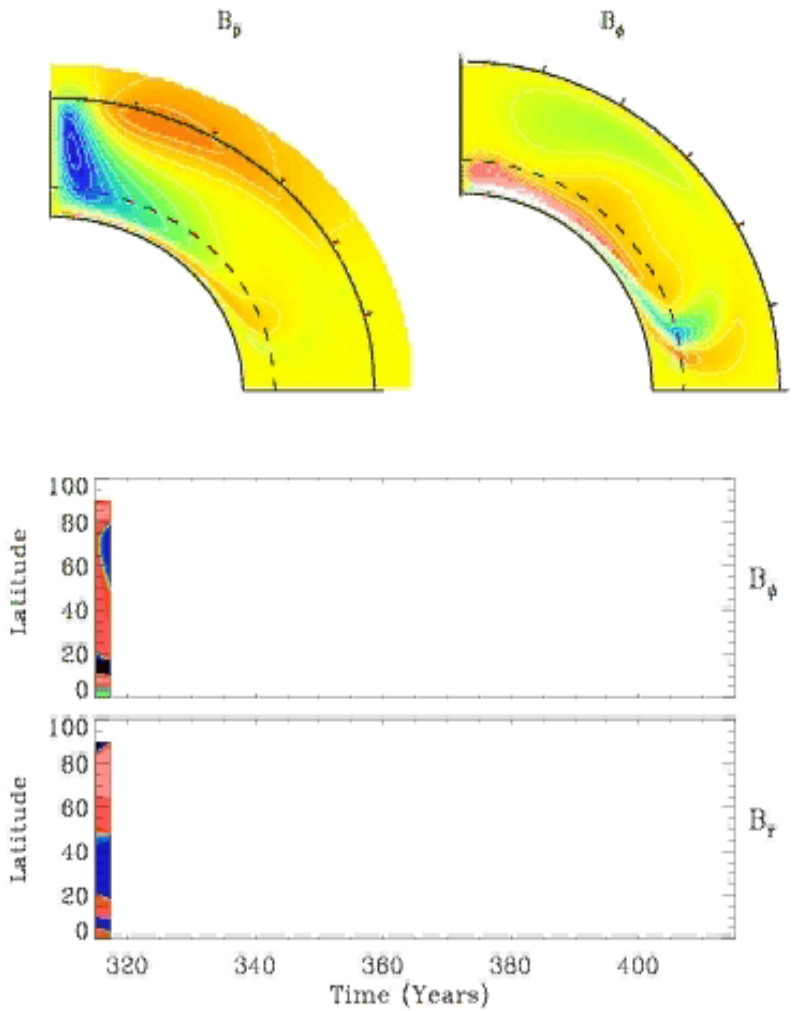

Jouve & Brun, 2007 A&A

Circulation Méridienne du Soleil

(Données MDI)

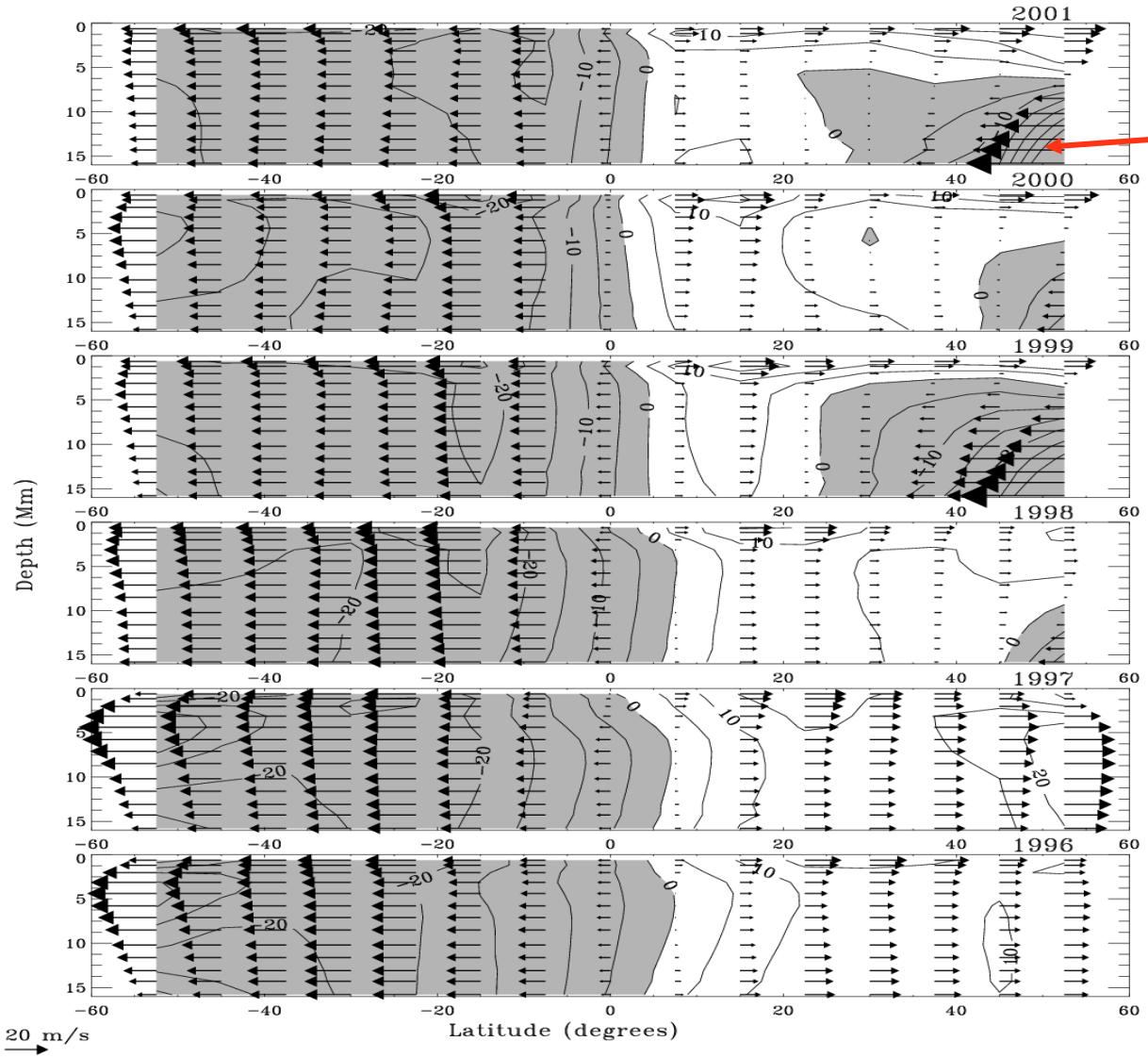

Apparition d'une contre cellule dans l'hémisphère nord lors du cycle 23.

Pb dynamo Babcock-Leighton qui assume 1 cellule

(Haber et al. 2002)

2D Mean Field models: Babcock-Leighton

2 cells in latitude, 2 in radius per hemisphere

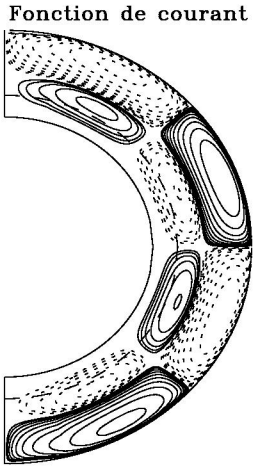

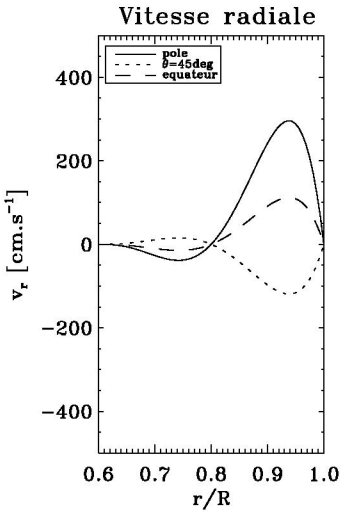

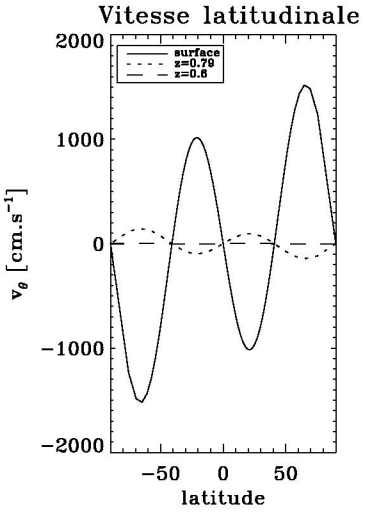

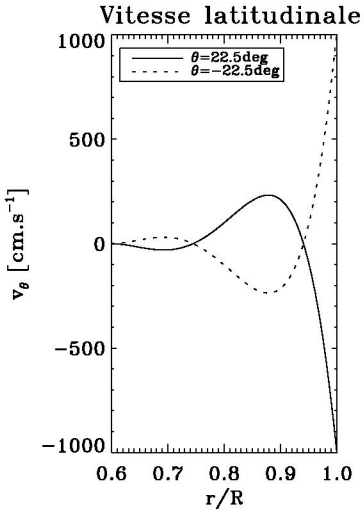

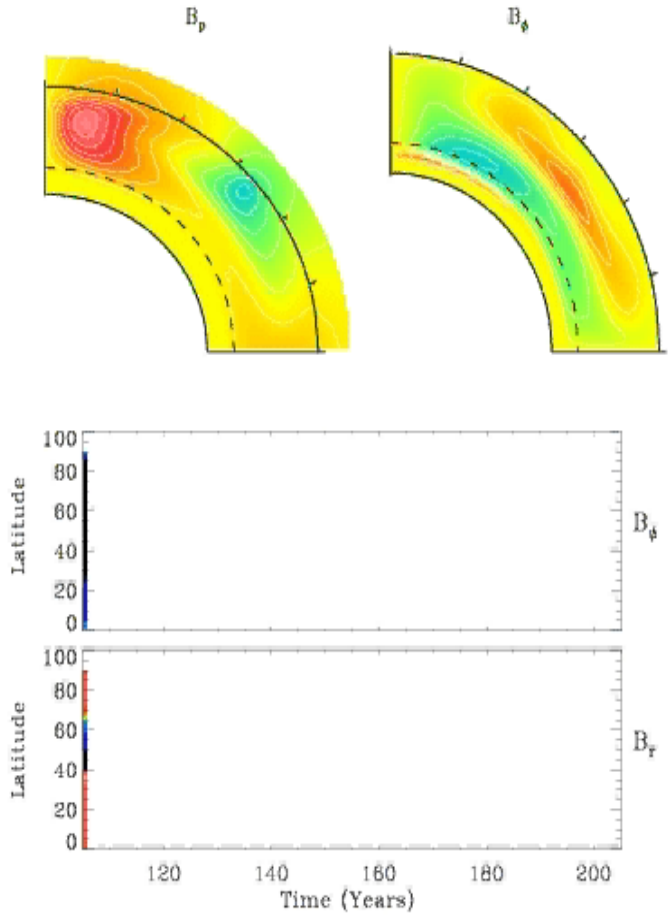

Slow down cycle period:

$T=\exp(22.84)v_0^{-0.35}\eta_t^{-0.68}s_0^{0.017}$

For parameter values Identical to 1 cell case, find T=45 yr instead of 22

Jouve & Brun 2007, A&A, 474, 239

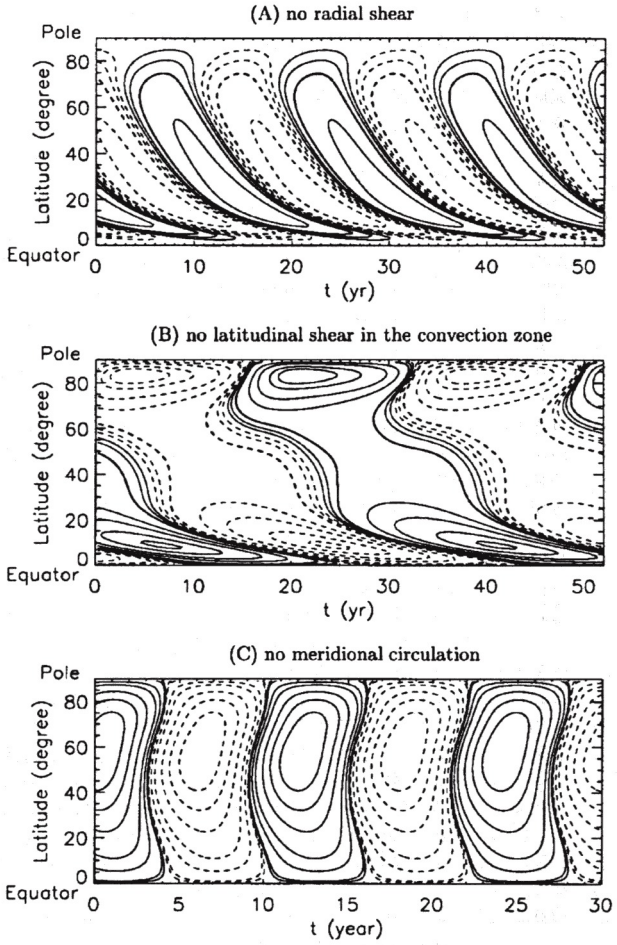

FIG. 4.—Three toroidal field butterfly diagrams resulting from various numerical "surgical" experiments. The format is the same as in Fig. 3*a*. (*a*) Solution where the radial shear was artificially shut off, with only the latitudinal shear left to contribute to the generation of toroidal fields. (*b*) Opposite experiment, i.e., the latitudinal shear has been artificially shut off. For these two solutions all parameter values are otherwise identical to the reference solution of Figs. 2 and 3. (*c*) Solution where the meridional circulation has been turned off. The resulting butterfly diagram bears a striking resemblance to that produced by mean field interface dynamos (see text).

Diagramme papillon

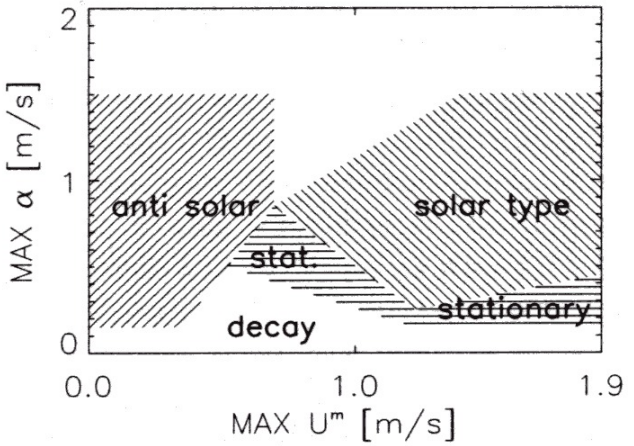

Fig. 11. The different types of solution found for varying strengths of the α-effect and the flow speed. The terms *solar type* and *anti solar* refer to equatorward and poleward drifting field belts, respectively, while *stationary* refers to a stationary field. The magnetic diffusivity always has a value of 10^{11} cm^2/s.

(Charbonneau et Dikpati 2001, Kuker et al. 2002)

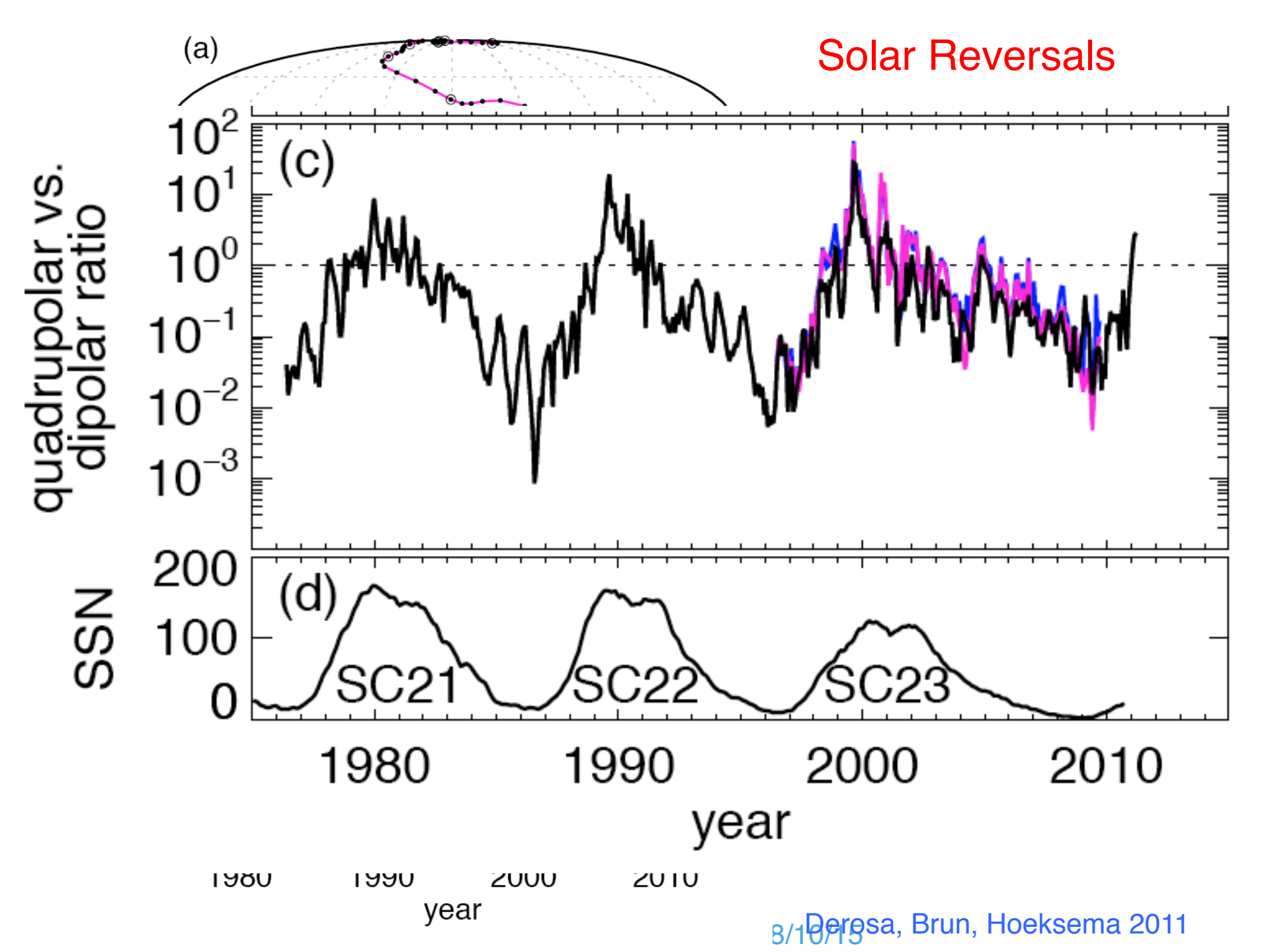
Solar Reversals
(a)
(c)
(d)
quadrupolar vs.
dipolar ratio
10^2
10^1
10^0
10^{-1}
10^{-2}
10^{-3}
SSN
200
100
0
SC21
SC22
SC23
1980
1990
2000
2010
year
Derosa, Brun, Hoeksema 2011

Reversals vs Excursions

Petrelis & Fauve 2009
Tobias & Weiss 2000

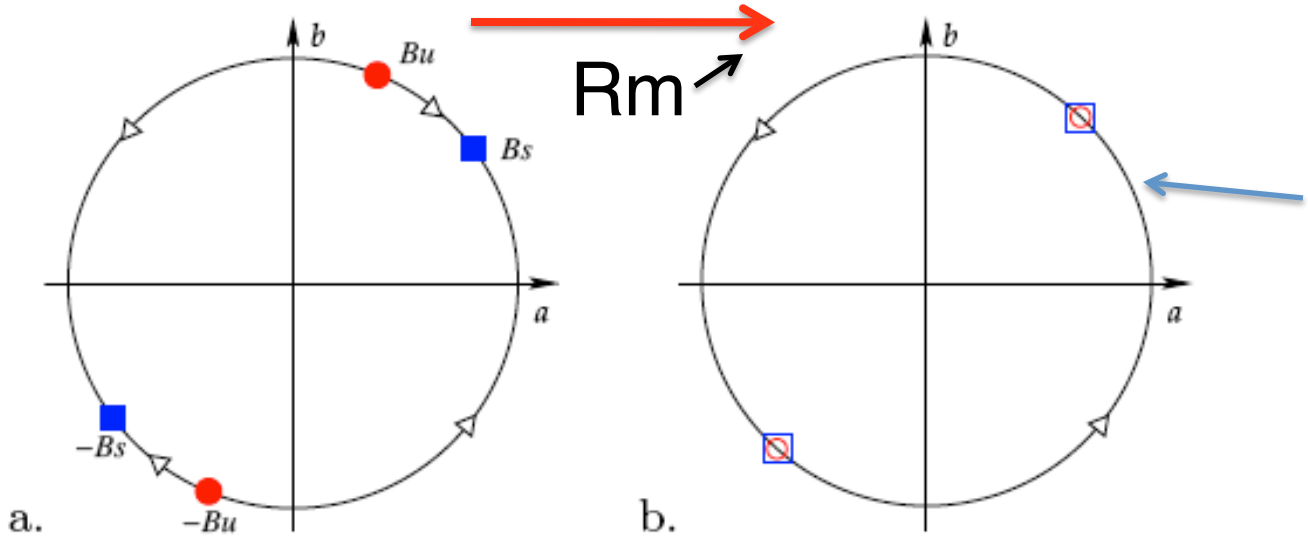

FIG. 1: Phase space of a system invariant under $\mathbf{B} \rightarrow -\mathbf{B}$ and displaying a saddle-node bifurcation: (a) below the on-

Coupling a Dipole to a Quadrupole => A= D + i Q yields a dynamical system with a 2-D phase space describing a saddle node bifurcation (with stable/unstable fixed points)

Coupling of both families via either nonlinear effects or symmetry breaking in the flow (Roberts & Stix 1972, Mc Fadden et al. 1991)

Limit cycle above the saddle node bifurcation, leads Cyclic dynamo solution.

The Sun with large Rm is above the instability, whereas the Earth isn't, explaining the failed reversals (excursions)

In order to get irregular Cycles, one needs to have a time dependent control Parameter (Rm, Re…) that makes the Sun goes On and Off (Spiegel 2009) Or to have a hopf type Bifurcation with period doubling and chaos

Such behavior is expected from the Sun's nonlinear dynamo, or by stochasticity

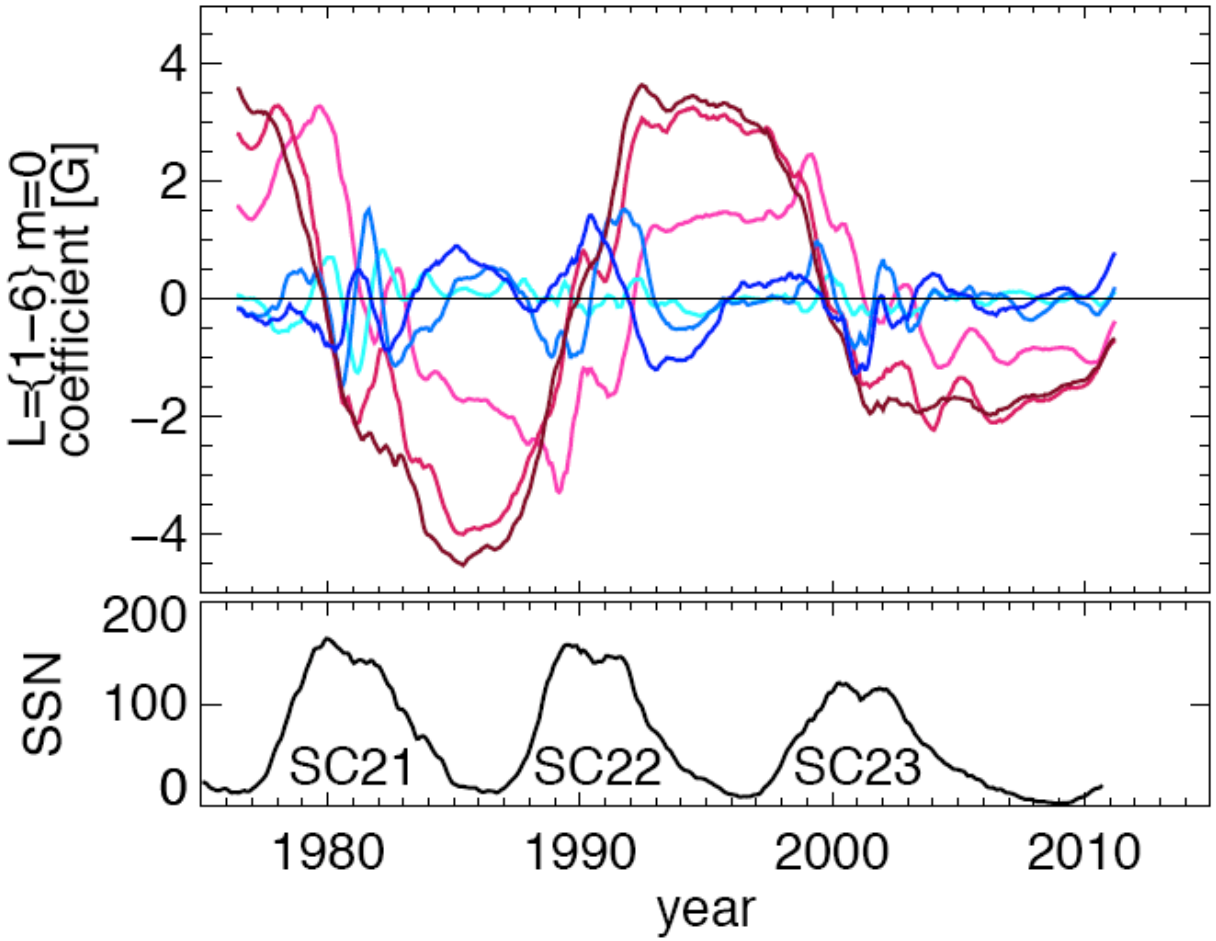

Axisymmmetric Modes

Quad ~ 25% Dip
Except at reversal where it dominates.

Fig. 10.— [XXX Energy in the first 3 odd ($\ell = \{1, 3, 5\}$ are {dark red, red, light red}) and even ($\ell = \{2, 4, 6\}$ are {dark blue, blue, light blue}) axisymmetric (m=0) degrees ℓ as a function of time for Wilcox.]

Derosa, Brun, Hoeksema 2011

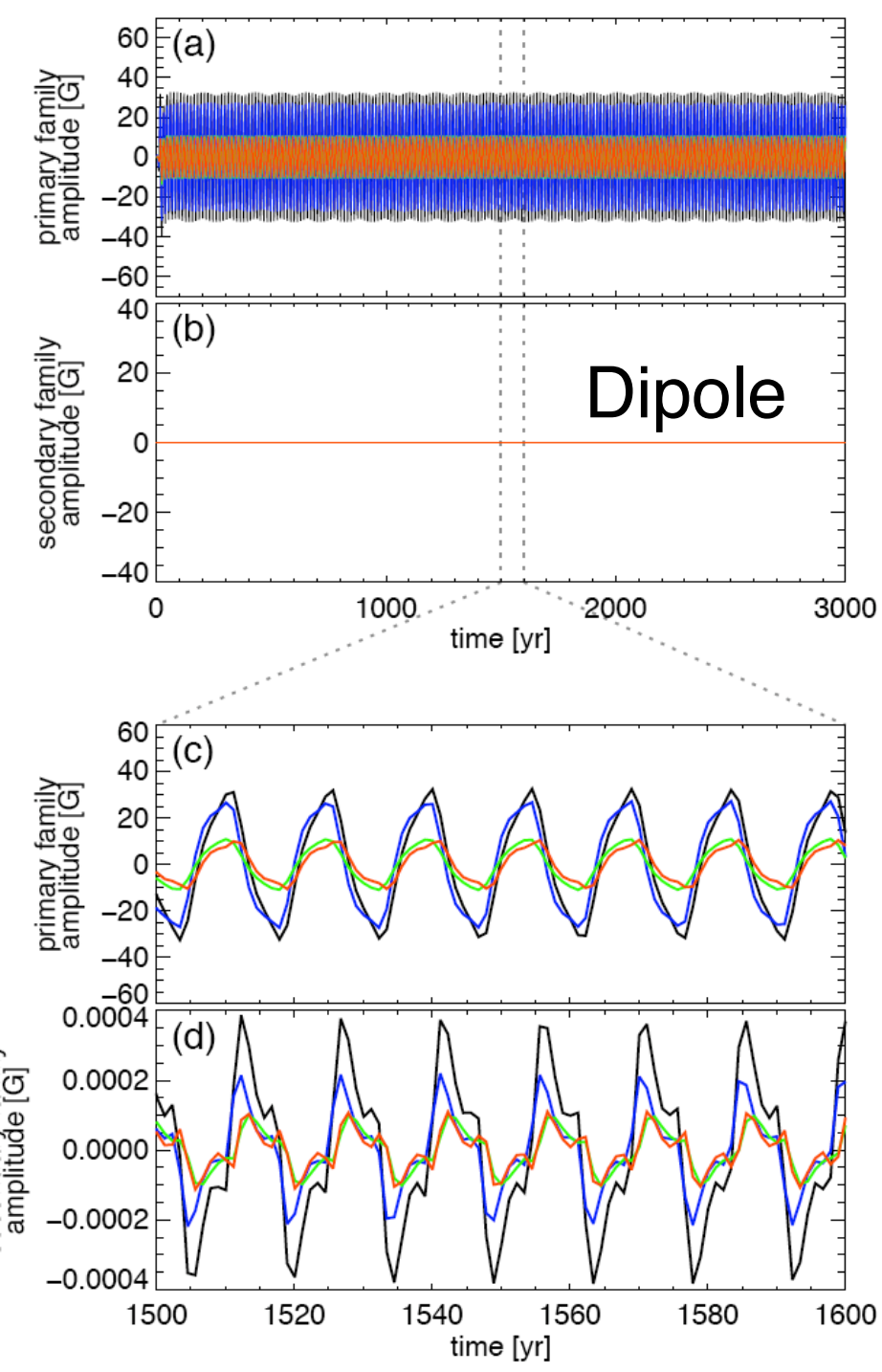
(a)
primary family amplitude [G]
(b)
Dipole
secondary family amplitude [G]
time [yr]
(c)
(d)

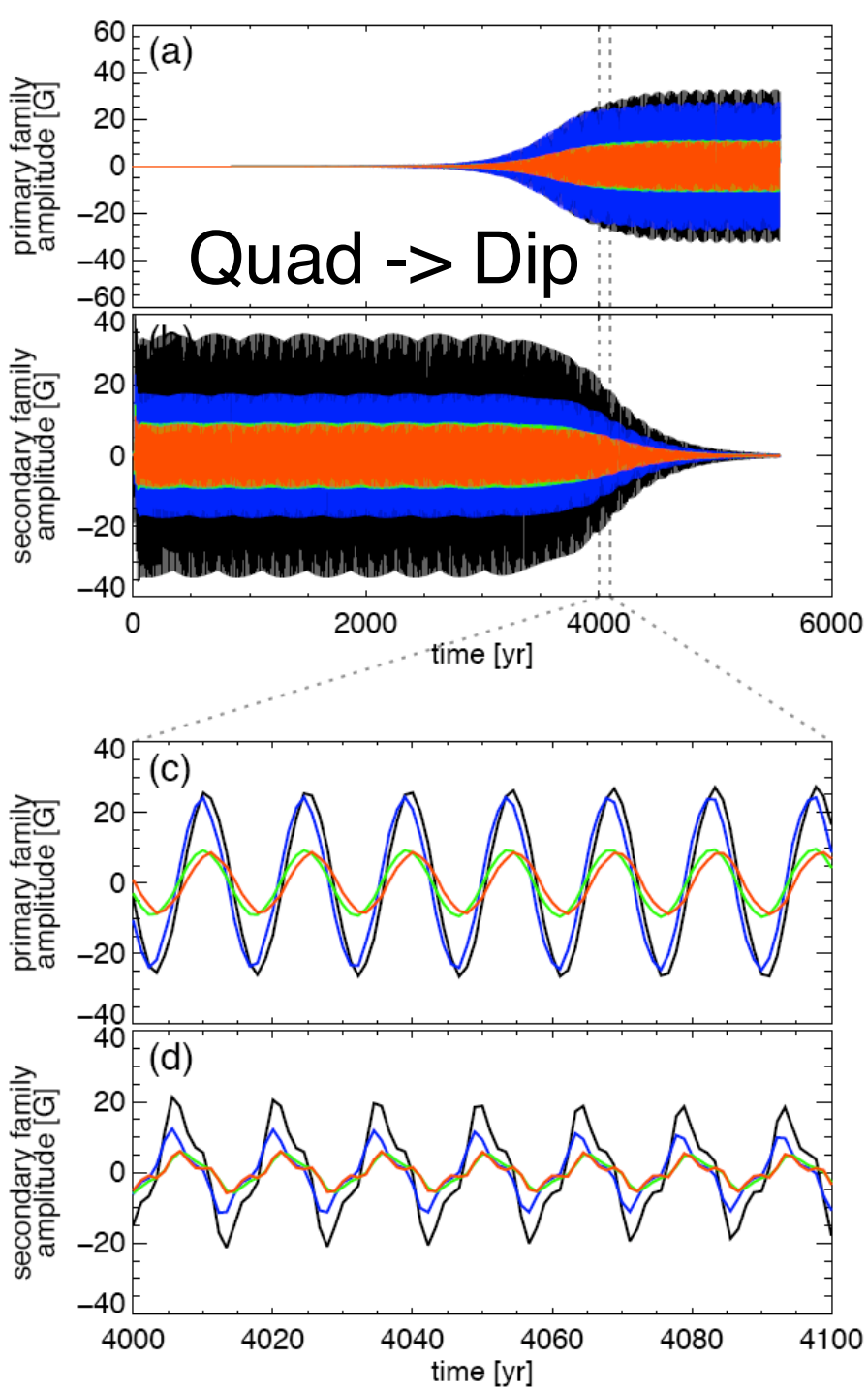
(a)
primary family amplitude [G]
Quad -> Dip
secondary family amplitude [G]
time [yr]
(c)
(d)

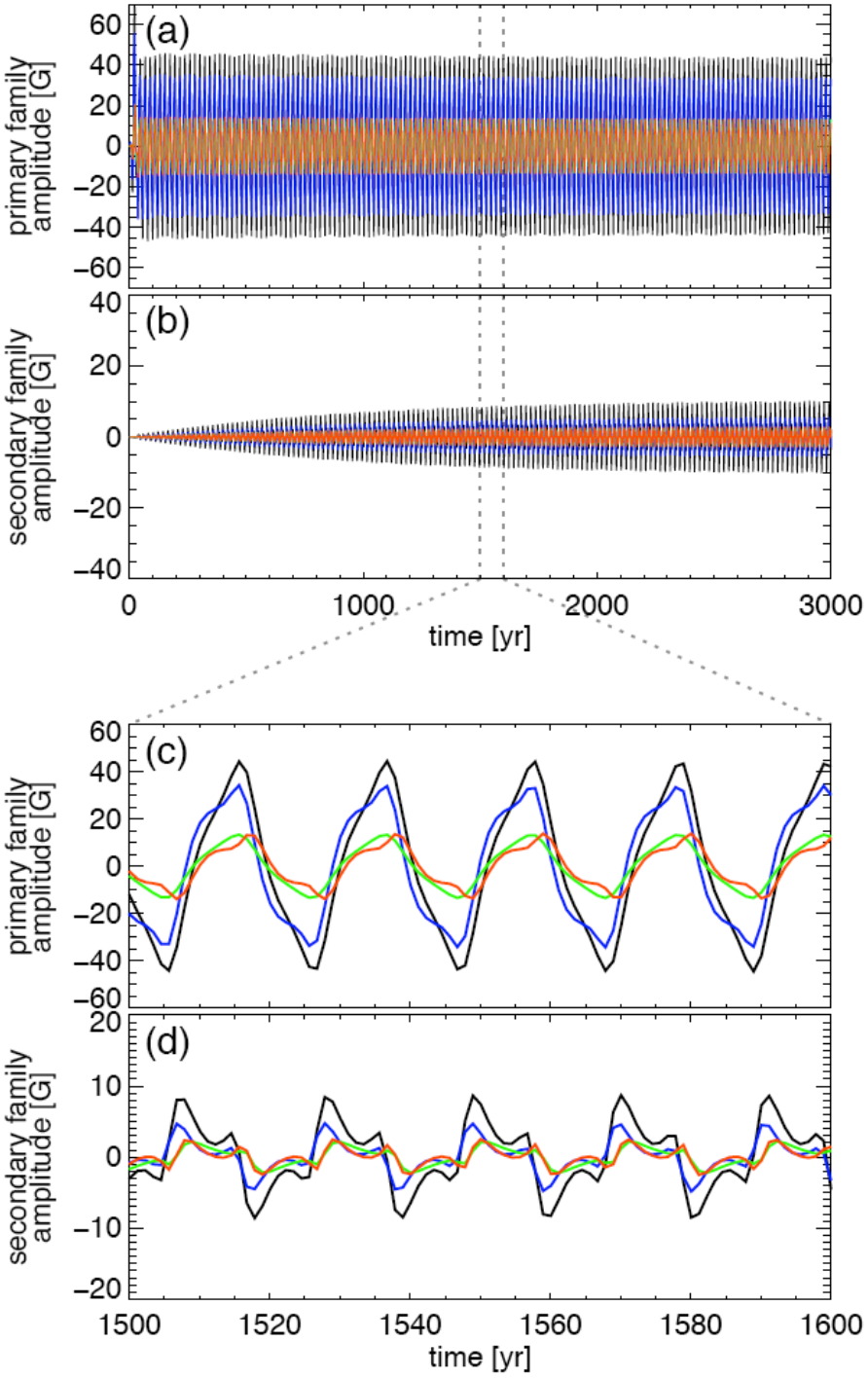

Asymmetry of Babcock-Leigthon term of 0.1%

Could be Meridional Flow.

Dip + Quad !

Derosa, Brun, Hoeksema 2011

Energy Reservoirs in a Magnetized Convection Zone

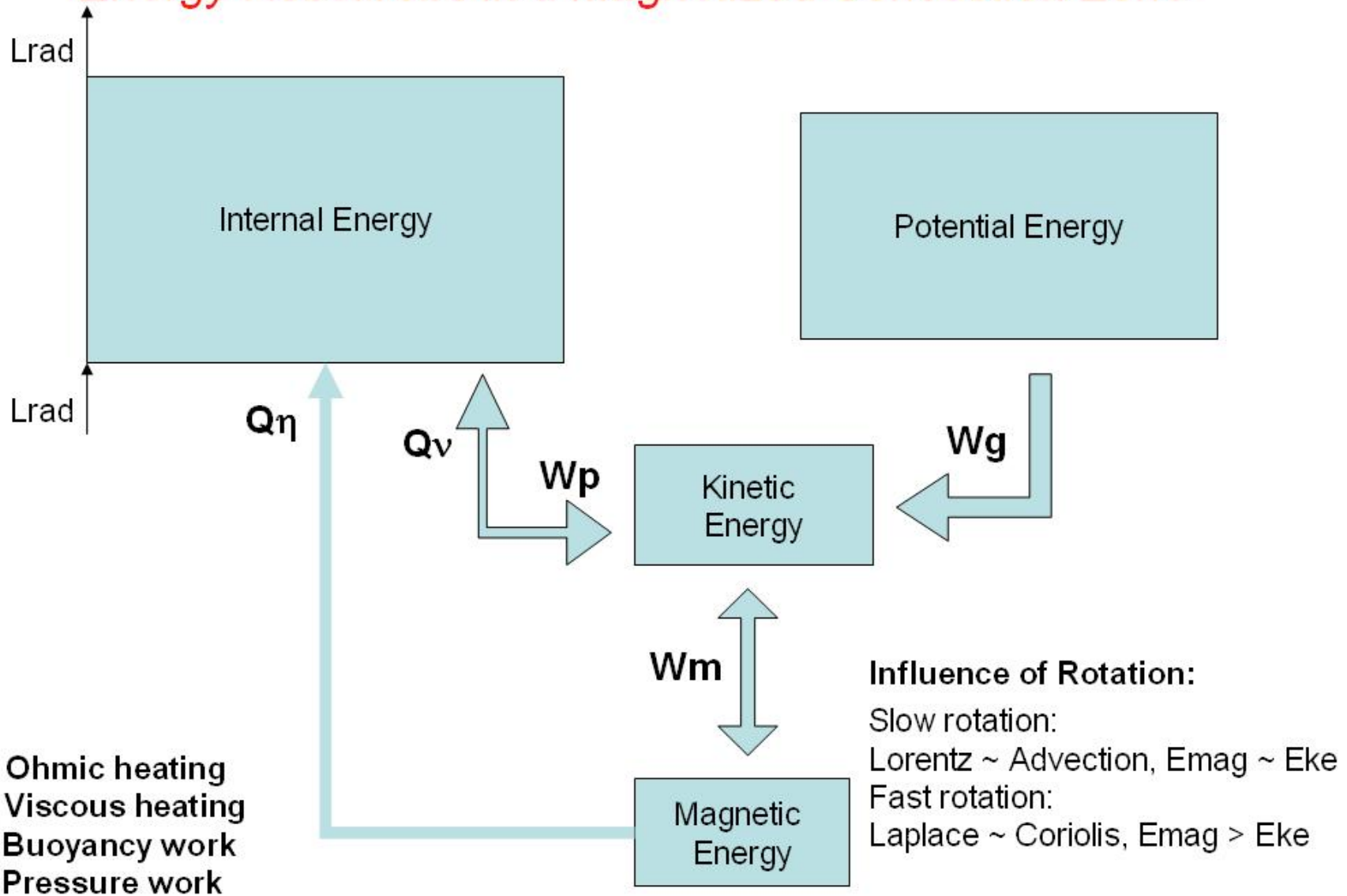

Various Dynamo Regimes and Scalings

Equilibrium field : $B_{eq} \sim \mathrm{sqrt}(8\pi P_{gaz}) \sim \mathrm{sqrt}(\rho_*)$

If magnetic Reynolds number Rm ~1 , $\nu = \eta/L$, then

Laminar (weak) scaling: Lorentz ~ diffusion =>

$$B^2_{weak} \sim \rho\nu\eta/L^2$$

Turbulent (equipartition) scaling: Lorentz ~ advection =>

$$B^2_{turb} \sim \rho v^2 \sim \rho\eta^2/L^2 \Leftrightarrow |B_{weak}| \sim |B_{turb}| P_m^{1/2}$$

Magnetostrophic (strong) scaling: Lorentz ~ Coriolis =>

$$B^2_{strong} \sim \rho\Omega\eta$$

With ρ density, ν kinematic viscosity, η magnetic diffusivity, Ω rotation rate, v, L characteristic velocity & length scales, $P_m = \nu/\eta$ the magnetic Prandtl nb

Fauve et al. 2010, Christensen 2010, Brun et al. 2013

Dynamo cinématique vs dynamique (nonlinéaire)

Si la force de Laplace peut être négligé dans l'équation de Navier-Stokes, on parle alors de *dynamo cinématique*, l'instabilité est linéaire avec une croissance exponentielle

Dans le cas contraire (ce qui arrive pour des champs B d'amplitudes finies), on parle de *dynamo dynamique*, il y a rétroaction de la force de Laplace sur les mouvements, l'instabilité sature et le champ magnétique atteint une amplitude finie. L'énergie magnétique ME=$\mathrm{B}^2/8\pi$ est proche de l'équipartition avec l'énergie cinétique KE=$0.5\rho \mathrm{v}^2$ des mouvements fluides.

Remarque: la force de la Laplace peut se décomposer en 2 parties,

$$\mathbf{F} = \frac{1}{c}\mathbf{J}\times\mathbf{B} = \frac{1}{4\pi}(\boldsymbol{\nabla}\times\mathbf{B})\times\mathbf{B}$$

$$= \boxed{-\frac{1}{8\pi}\boldsymbol{\nabla}\mathbf{B}^2}_a + \boxed{\frac{1}{4\pi}(\mathbf{B}\cdot\boldsymbol{\nabla})\mathbf{B}}_b$$

Une pression magnétique (terme a) perpendiculaire aux lignes de champ magnétique et une tension magnétique (terme b) le long de celles-ci.

Modèles Dynamo Non-linéaires (cf. cours 3b):

- Résolvent les équations de la Magnétohydrodynamiques (donc pas de terme extra)
- Régime dynamique (retour sur champ de vitesse par Lorentz)
- Modèles avec ou sans convection
- Certains modèles prescrivent le cisaillement dans la tachocline

Moins: lent donc petite étude d'espace de paramètres, 'Building block' pas de modèle complet (pour l'instant), donc comparaison avec observations moins directes

Plus: dynamique, effet alpha, Omega et MC de manière consistante, 3D (variations longitudes)

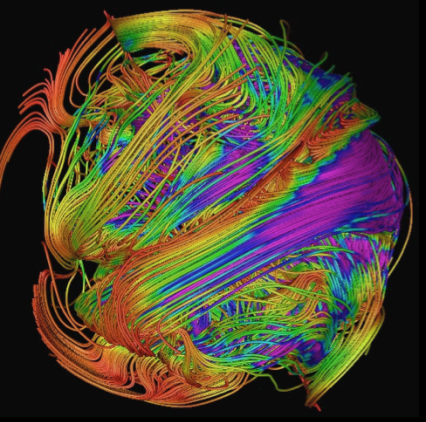

The Solar-Stellar Connection

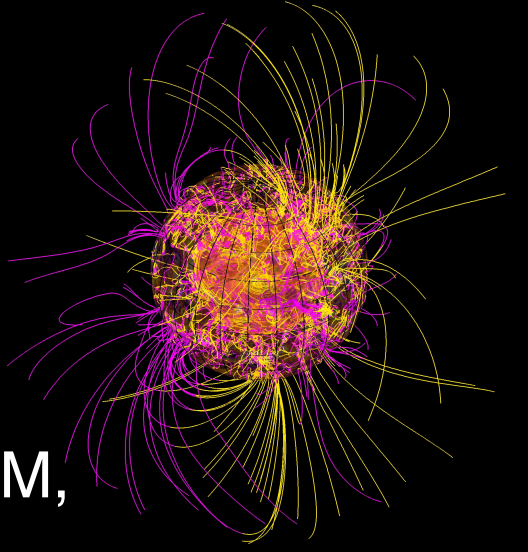

Allan Sacha Brun

Service d' Astrophysique/UMR AIM,
CEA-Saclay

with J. Toomre, J.P. Zahn, M. Browning, K. Augustson, B. Brown, A. Strugarek, L. Jouve, J. Varela, C. Emeriau, S. Matt, and the STARS2 Team

- Mean flows
- Dynamo action in solar-like stars

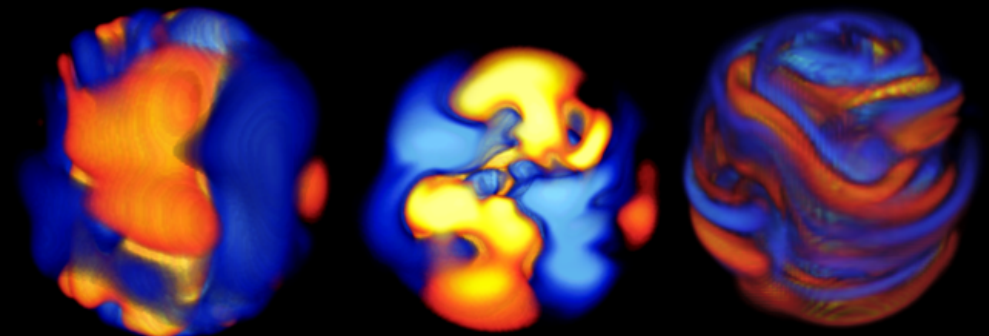

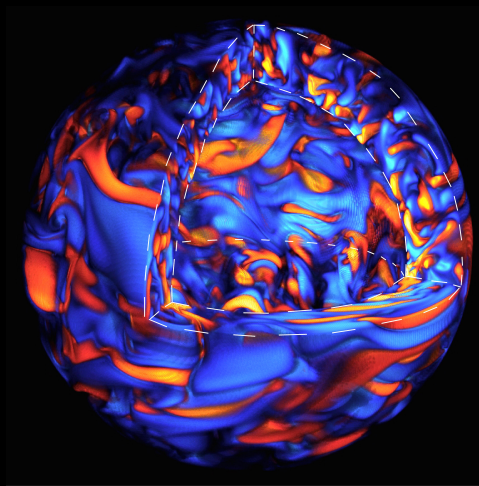

School, 28/10/15

The Sun: the closest magnetic star

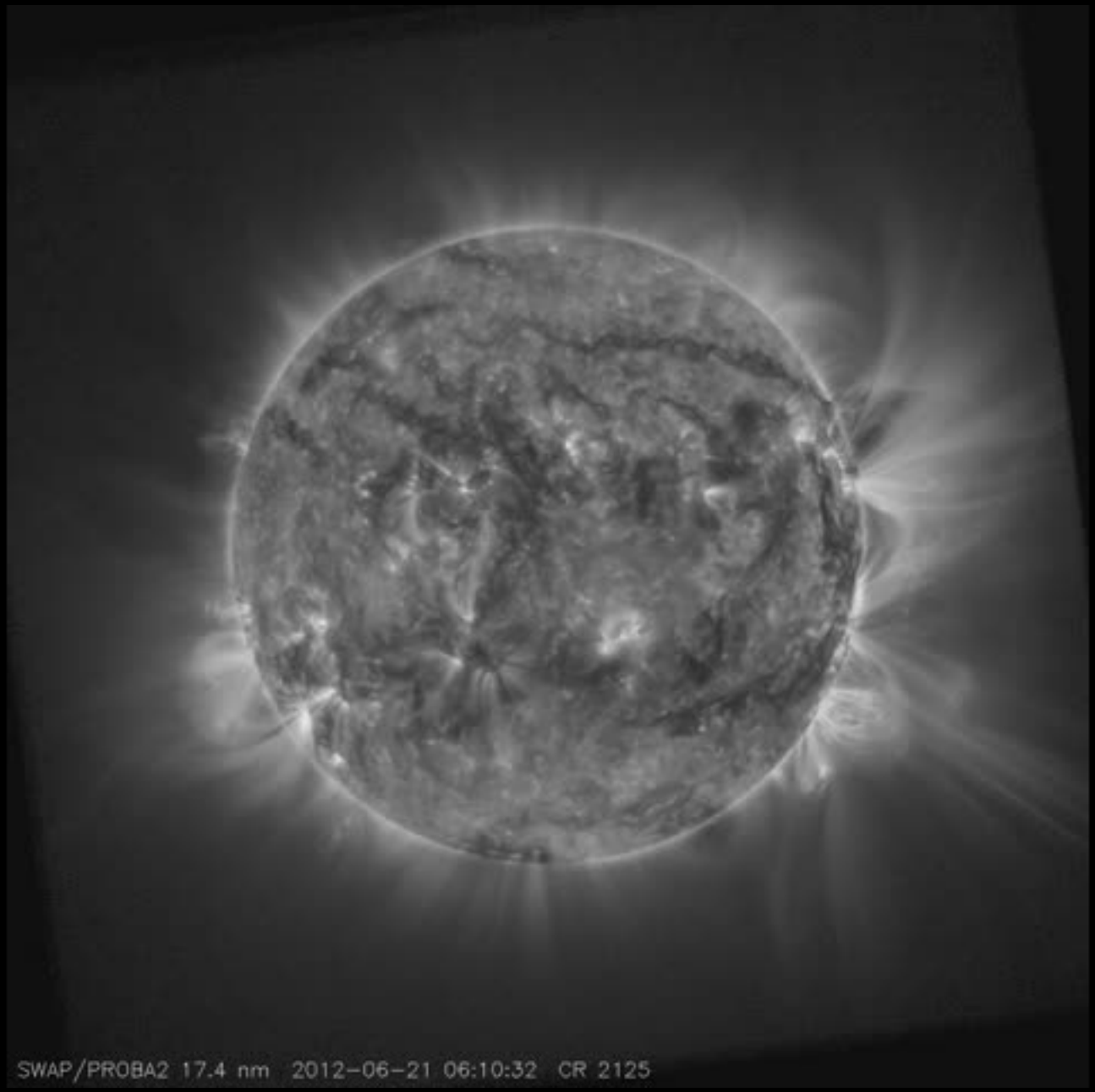
SWAP/PROBA2 17.4 nm 2012-06-21 06:10:32 CR 2125

Solar Magnetic cycle 23-24

http://sohowww.estec.esa.nl/

(EIT, LASCO & MDI Data (satellite SoHO))

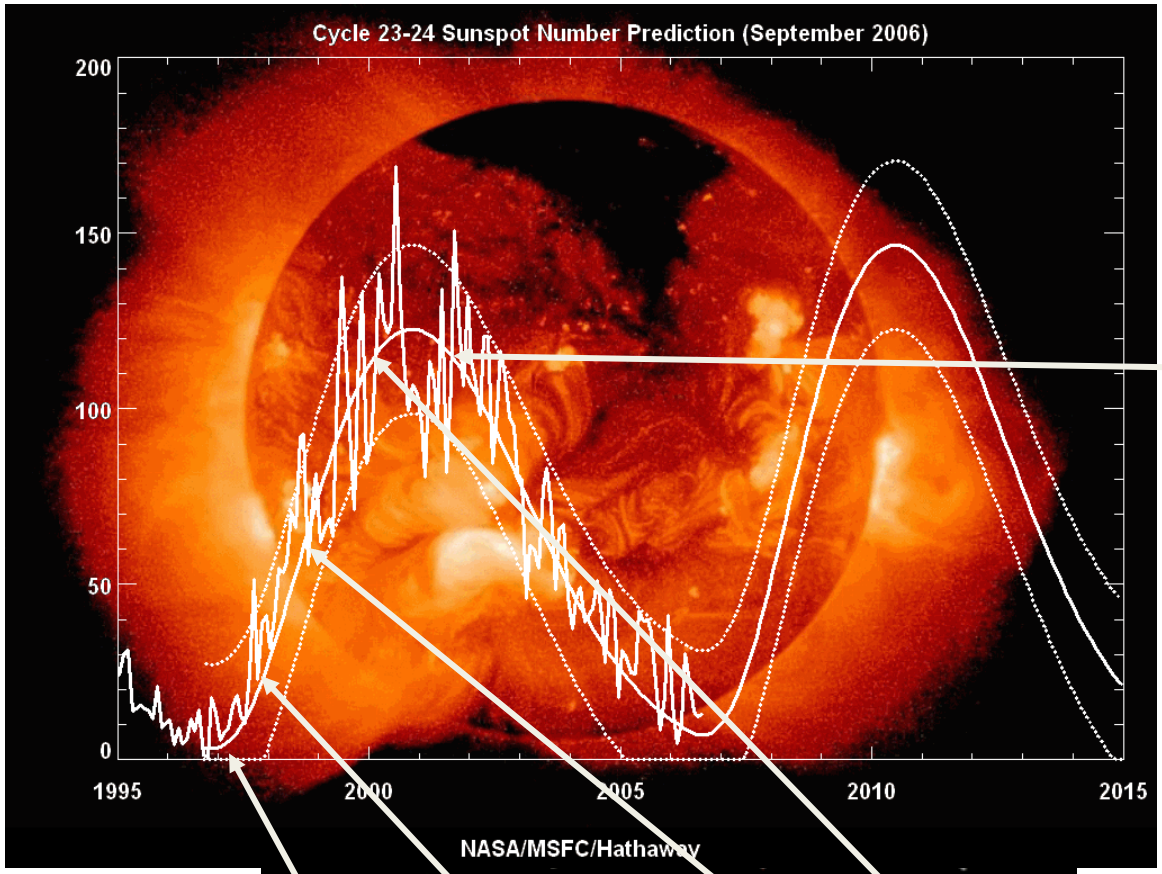

Source: NASA

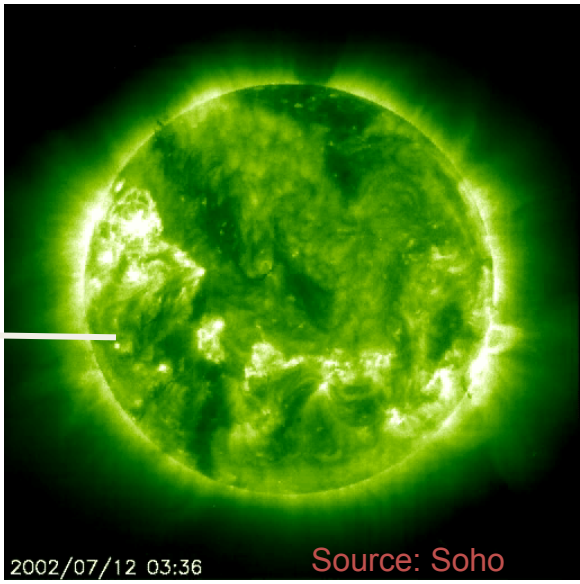

Source: Soho

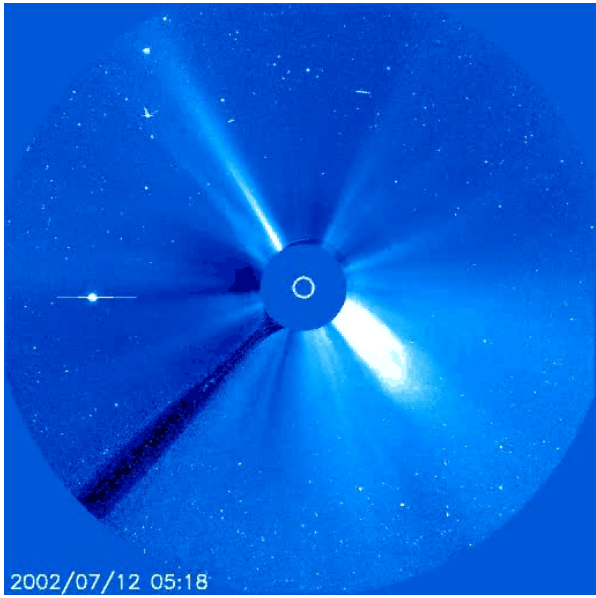

Le Soleil est gros, temps Ohmique long (10 Gans), mais B varie -> dynamo

Granulation and Sunspot Dynamics

(Solar Swedish Telescope- Hinode)

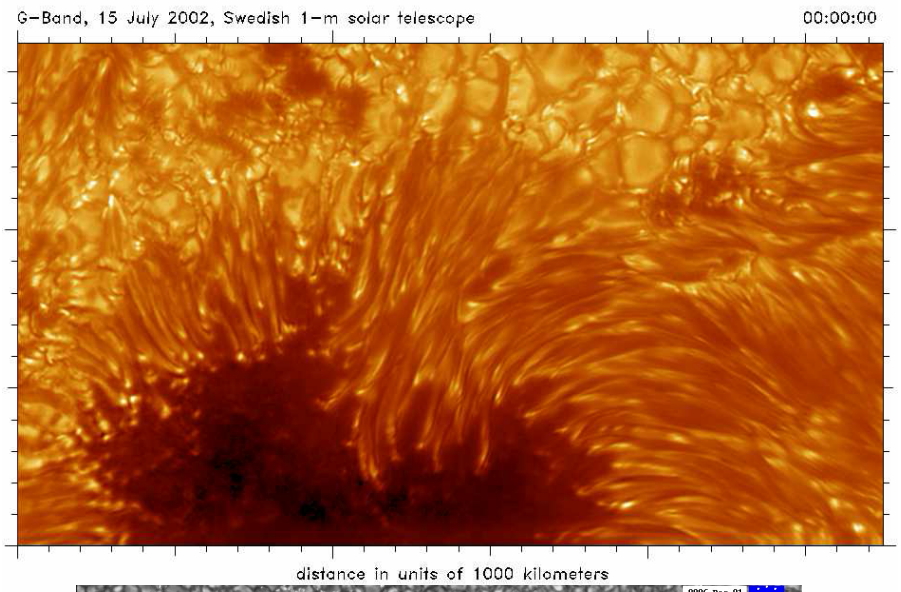

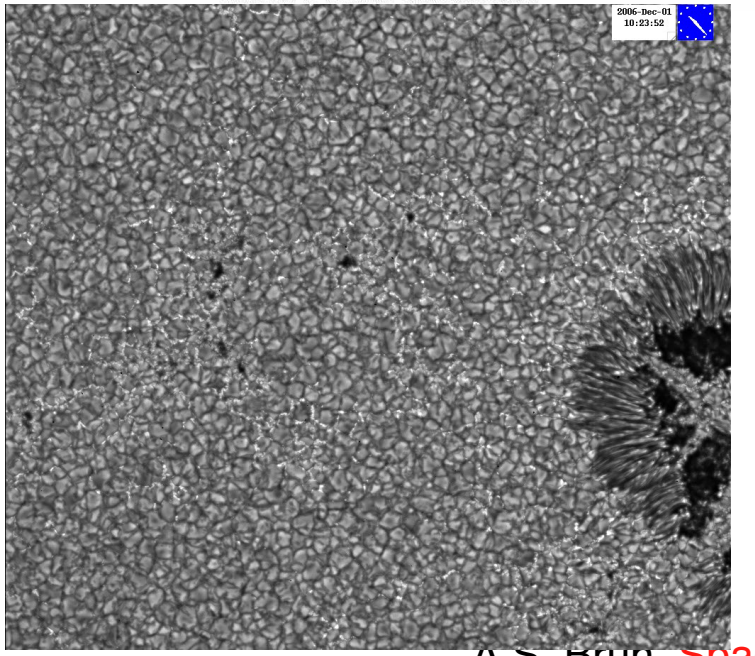

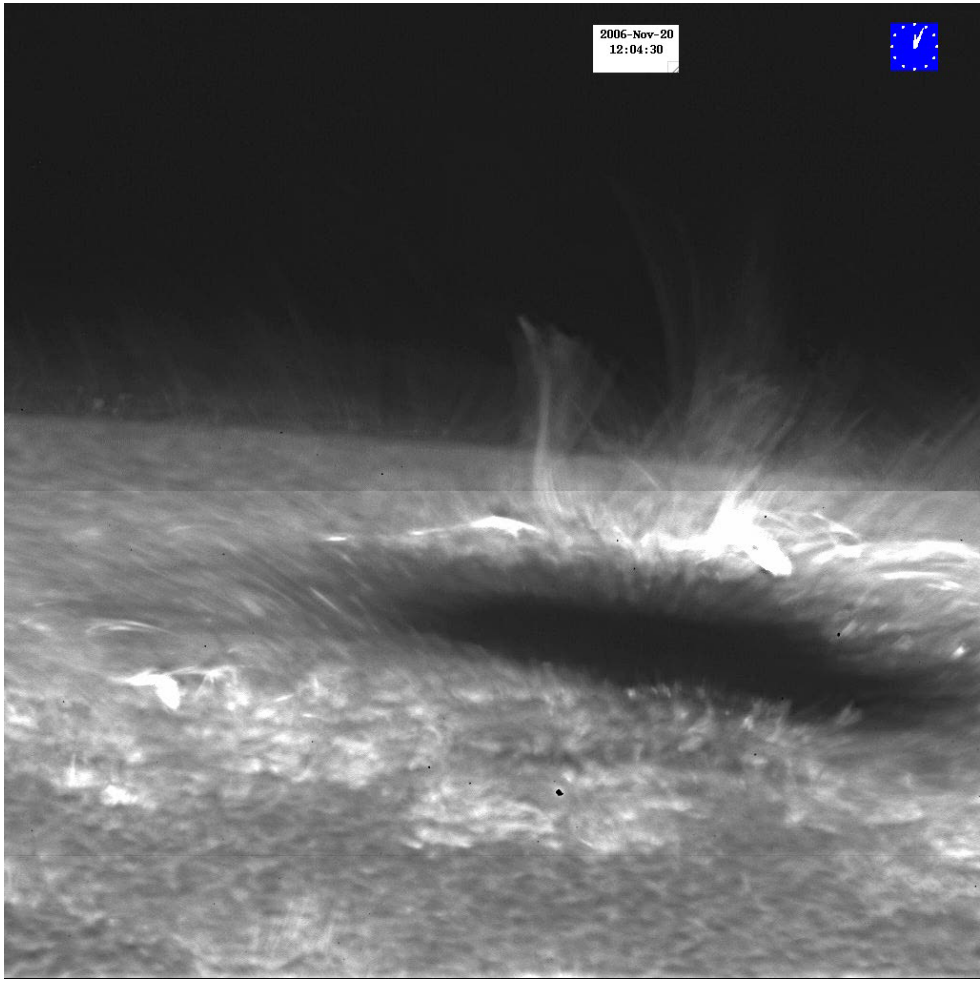

Eruptive event falling back: unguided case

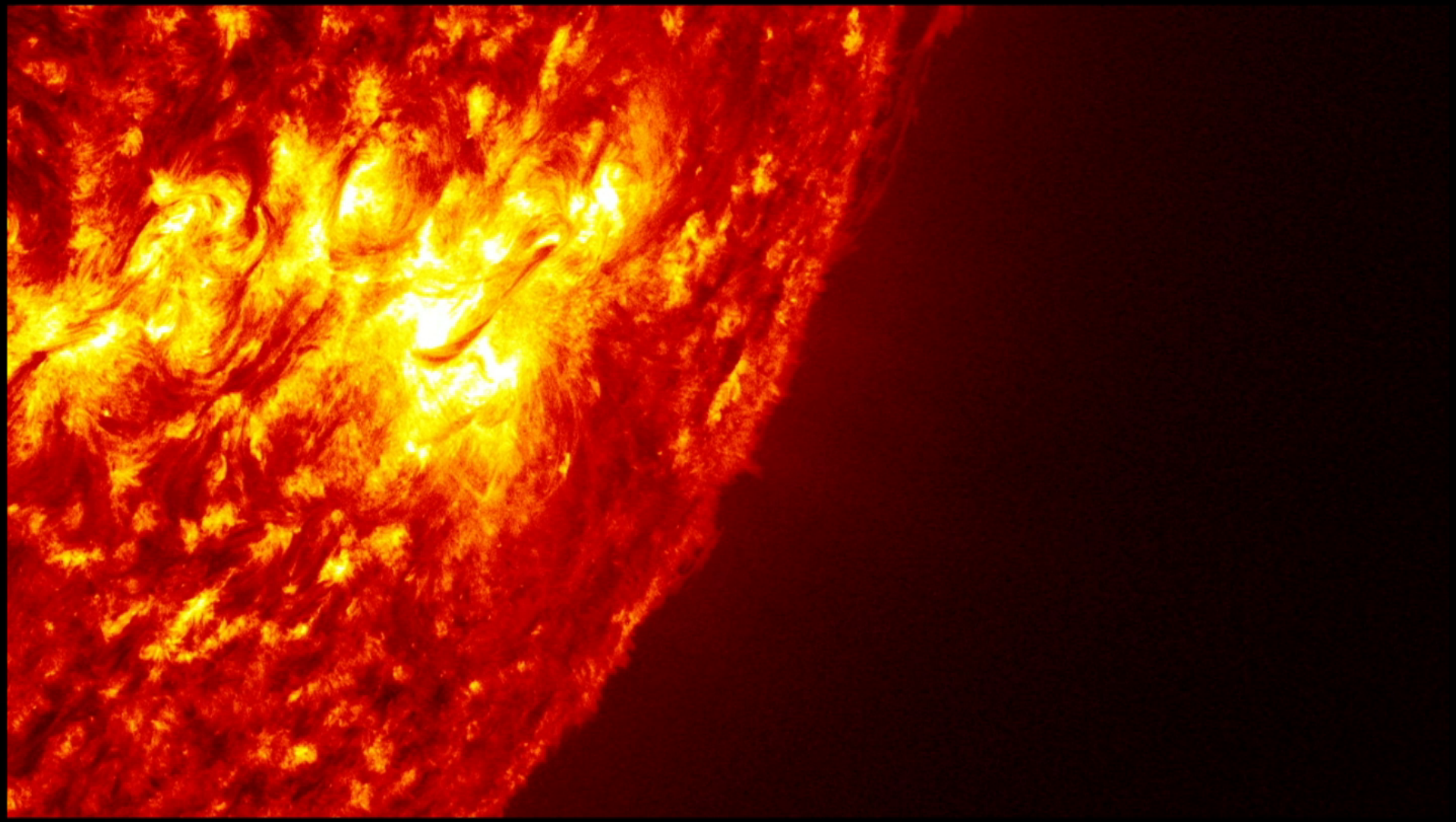

Eruptive event falling back: guided case

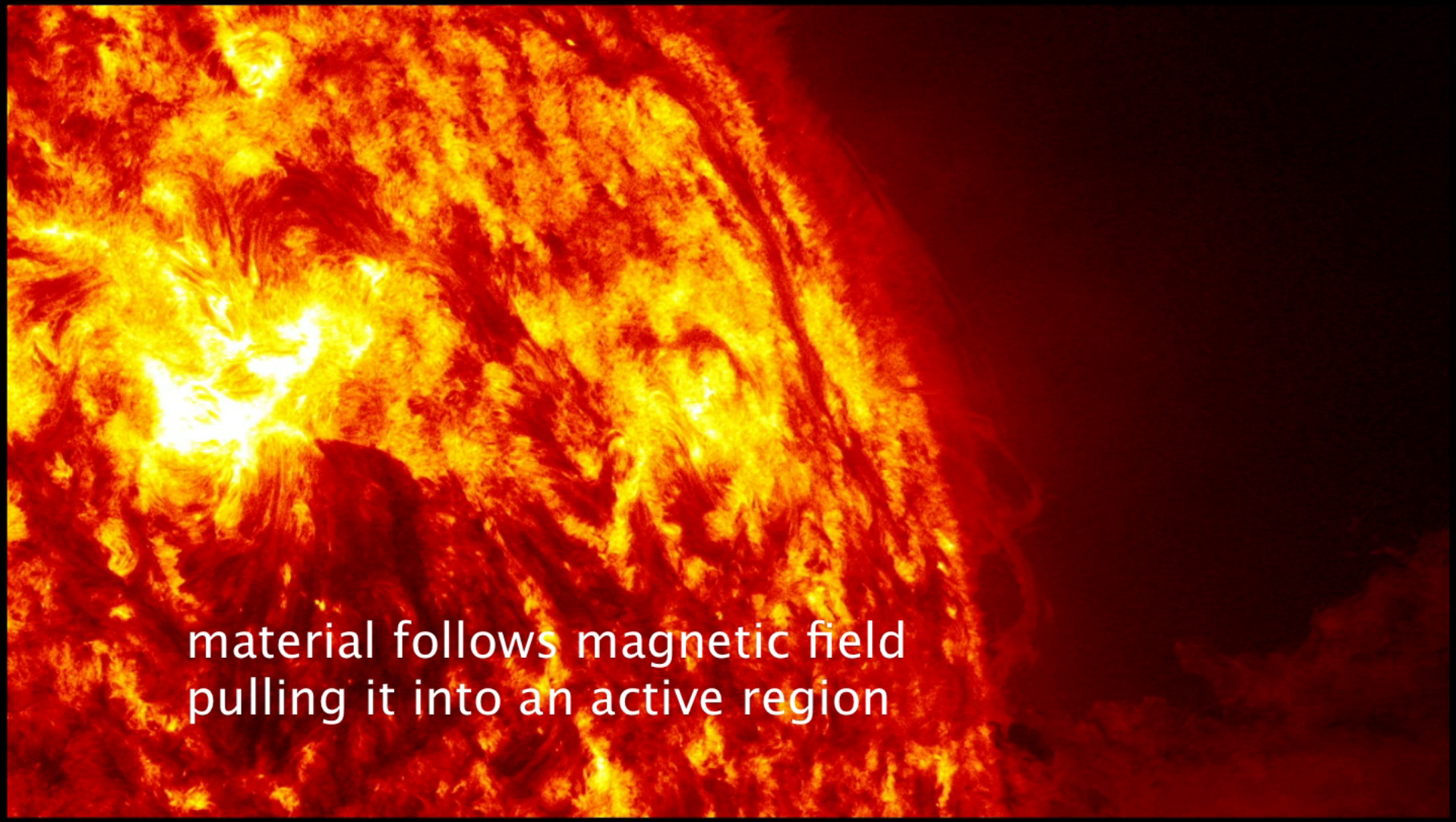

Soft and hard X-ray emission (Rhessi + Trace)

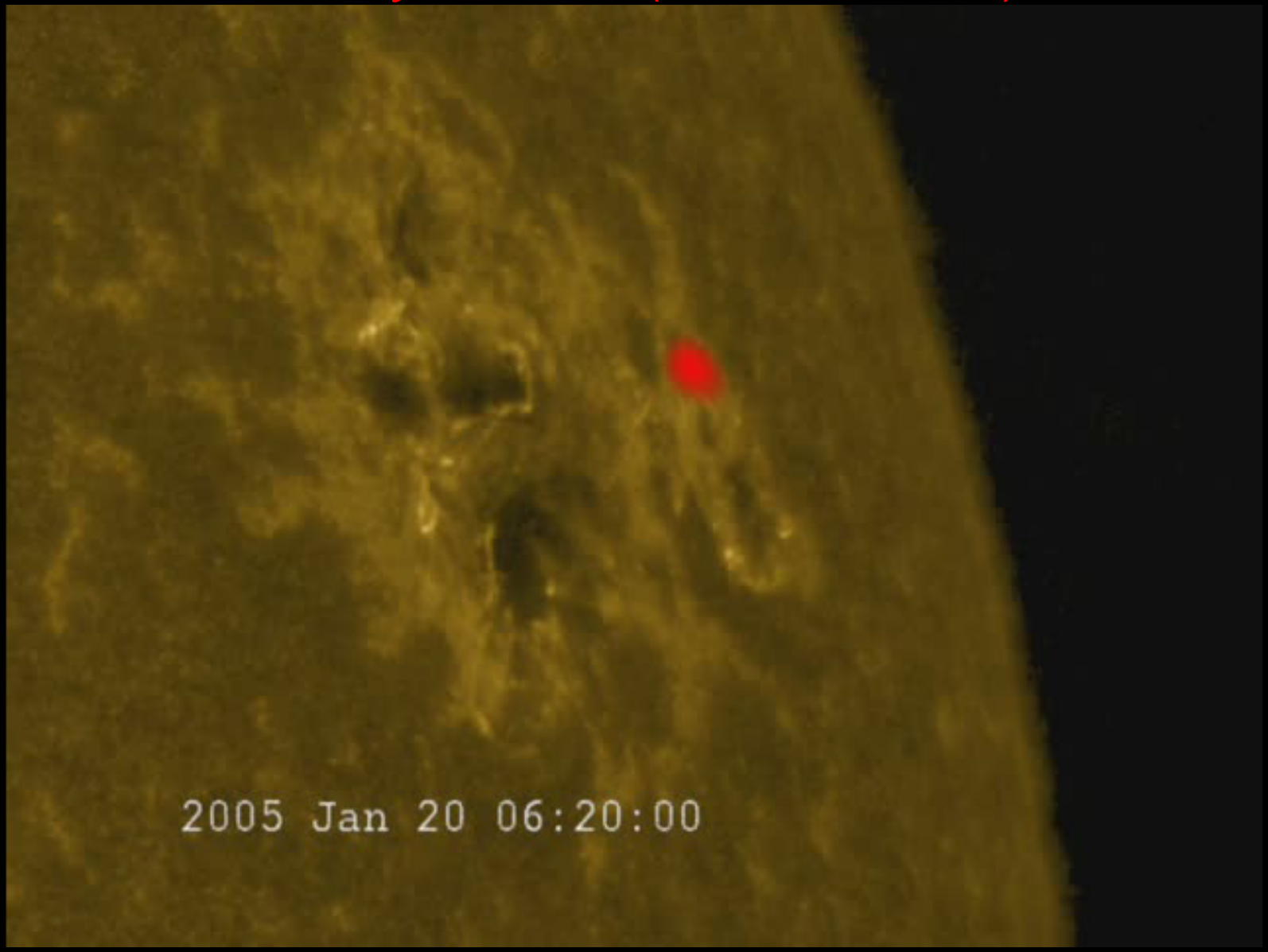

Flare Classification Schemes

After Bhatnagar & Livingston 2005

Hα classification			Radio flux at 5000 MHz in s.f.u.	Soft X-ray class	
Importance Class	Area (Sq. Deg.)	Area 10^{-6} solar disk		Importance class	Peak flux in 1-8 Å w/m^2
S	2.0	200	5	A	10^{-8} to 10^{-7}
1	2.0–5.1	200–500	30	B	10^{-7} to 10^{-6}
2	5.2–12.4	500–1200	300	C	10^{-6} to 10^{-5}
3	12.5–24.7	1200–2400	3000	M	10^{-5} to 10^{-4}
4	>24.7	>2400	3000	X	$>10^{-4}$

Hα sub-classification by brightness: F – faint, N – normal, B – bright

1 s.f.u. = 10^4 jansky = 10^{-2} W m^{-2} Hz^{-1}

Solar Cycle and Rotation

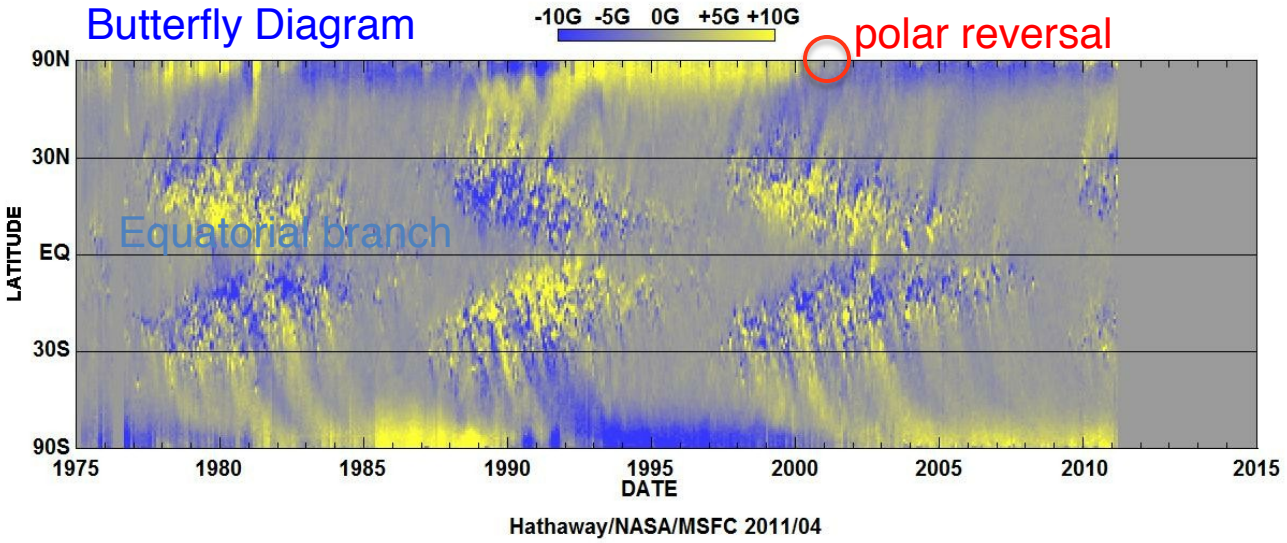

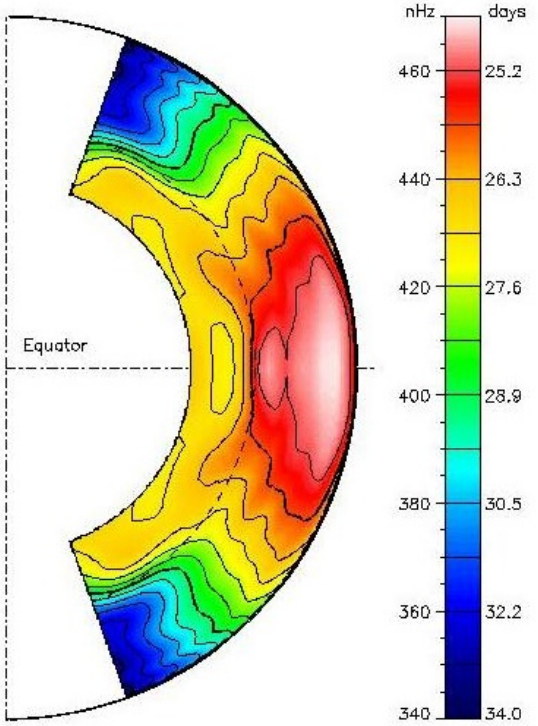

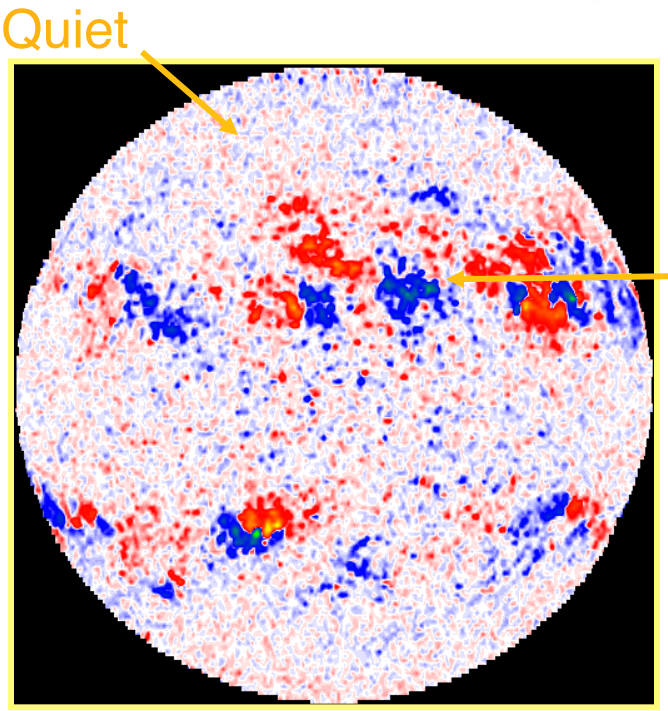

Small vs Large Scale Dynamos

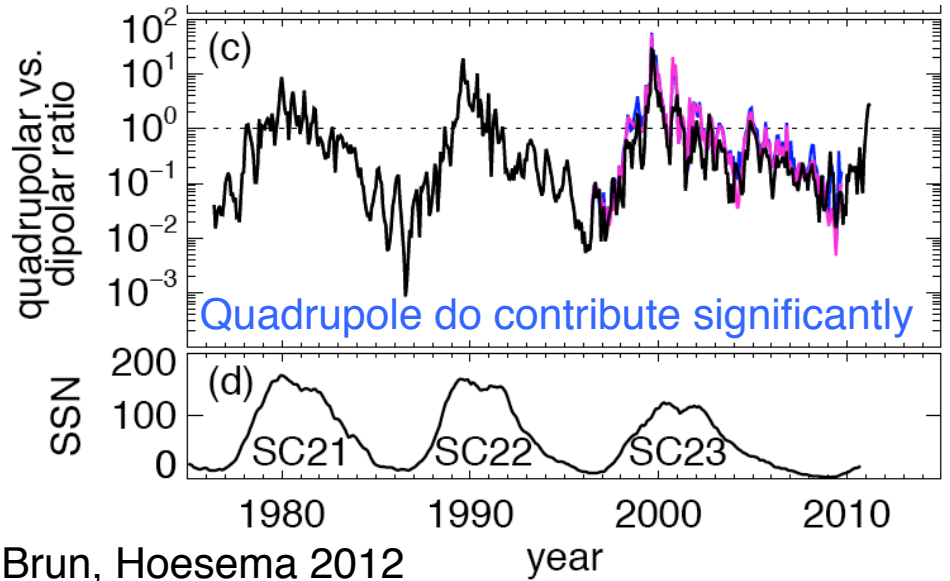

A.S. Brun, Space Sc Derosa, Brun, Hoesema 2012

Meridional Circulation

More & more evidence for multi cellular MC

Zhao et al. 2013

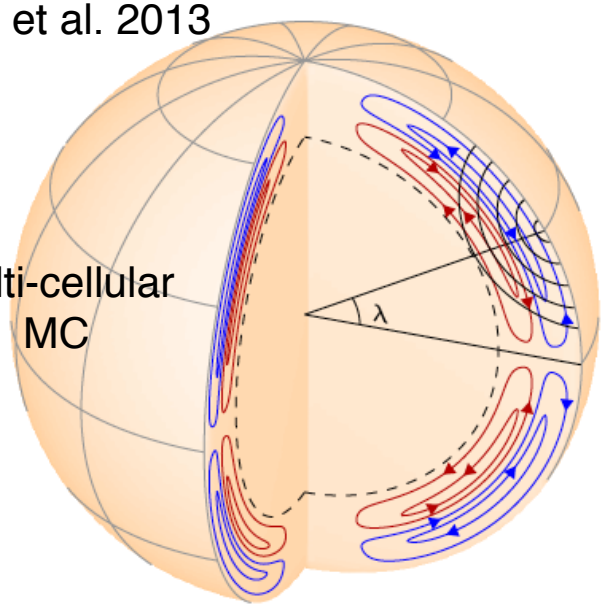

Multi-cellular MC

Influence of B (active region) on MC

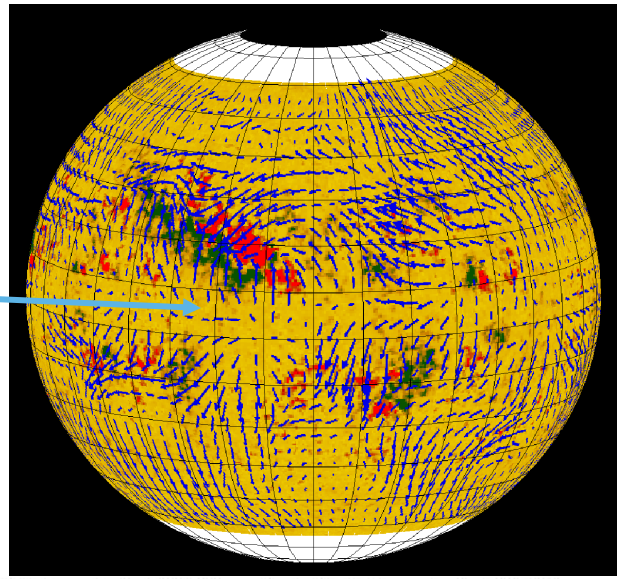

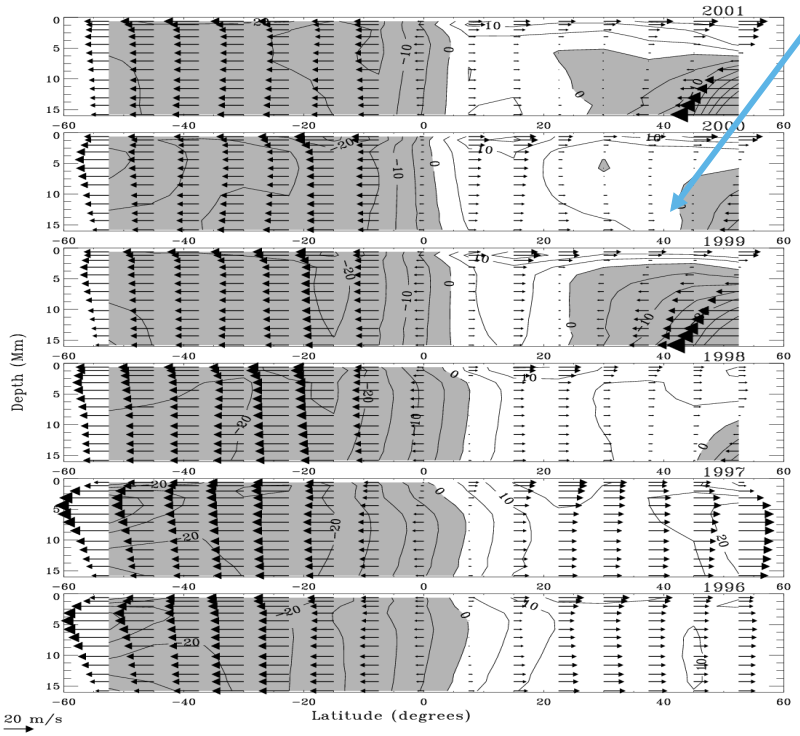

(Haber et al. 2002)

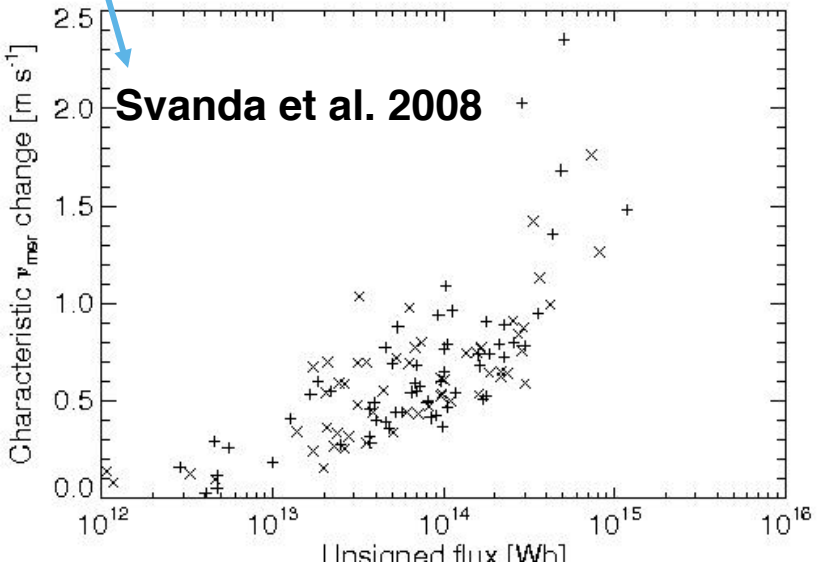

See also Hathaway et al. 1996, Gizon 2004, Zhao & Kosovichev 2004, etc…

Échelles Spatio-Temporelles dans la Zone Convective Solaire

Plasma= gaz chaud (ionisé)
4eme etat de la matière

L' Ordre dans
le Chaos!

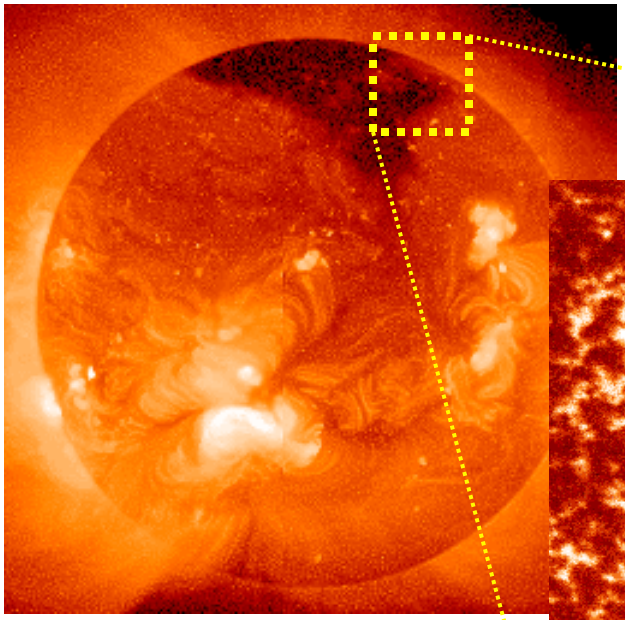

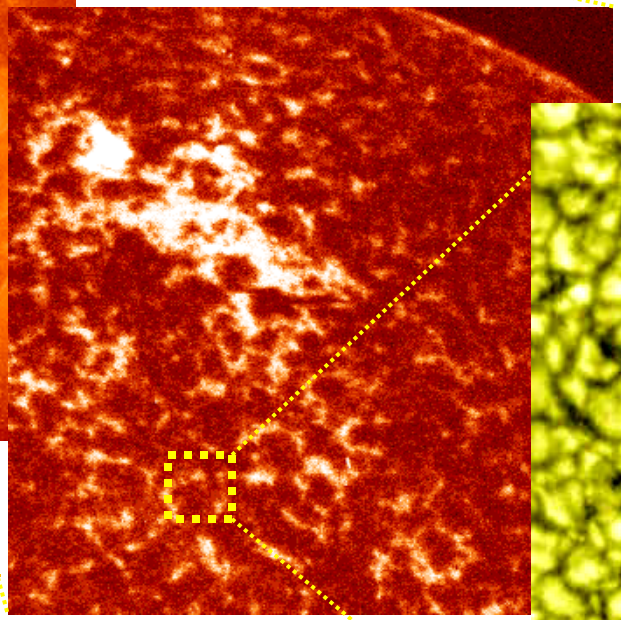

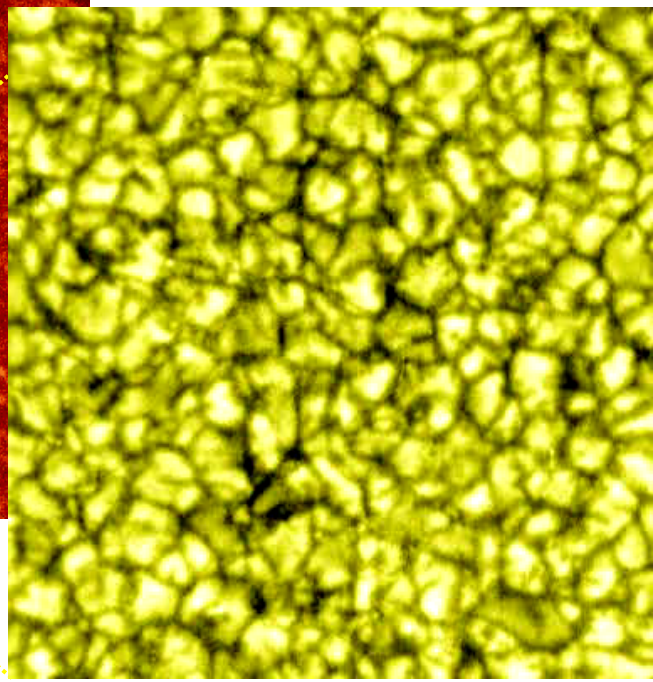

Grosses structures:
Eruptions,
Trous coronaux,
CMEs

Cellules Géantes?
200+ Mm
10-20 jours

Supergranulation:
30-50 Mm
20 heures

Mesogranulation?
7-10 Mm
2 heures

Granulation:
1-2 Mm
5 mins

Petites structures:
Lignes Intergranulaires,
Points magnétiques
brillants, diffusion

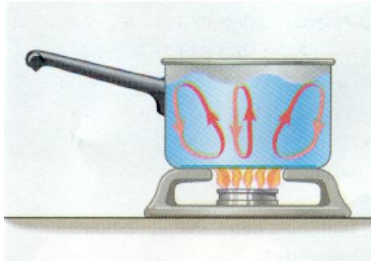

Critères de Stabilité

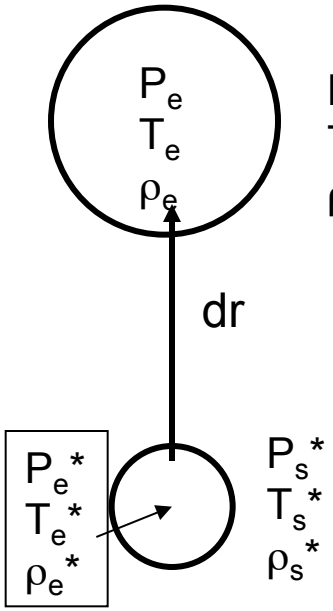

$$\rho_e = \rho_e^* + dr\left(\frac{d\rho}{dr}\right)_e \qquad \rho_s = \rho_s^* + dr\left(\frac{d\rho}{dr}\right)_s$$

$$\rho_e - \rho_s = dr\left[\left(\frac{d\rho}{dr}\right)_e - \left(\frac{d\rho}{dr}\right)_s\right] > 0 \quad \left(\frac{d\rho}{dr}\right)_e - \left(\frac{d\rho}{dr}\right)_s > 0 \ (1)$$

Equation d'etat: $\rho=\rho(P,T,\mu)$

Échelle de pression

$$\frac{d\rho}{\rho} = \alpha\frac{dP}{P} - \delta\frac{dT}{T} + \phi\frac{d\mu}{\mu} \qquad \frac{1}{H_p} = -\frac{d\ln P}{dr}$$

$\rho_e^*=\rho_s^*$

$$\left(\frac{\alpha}{P}\frac{dP}{dr}\right)_e - \left(\frac{\delta}{T}\frac{dT}{dr}\right)_e - \left(\frac{\alpha}{P}\frac{dP}{dr}\right)_s + \left(\frac{\delta}{T}\frac{dT}{dr}\right)_s - \left(\frac{\phi}{\mu}\frac{d\mu}{dr}\right)_s > 0$$

$P_e = P_s$ et $P_e^* = P_s^*$ $\quad$ $d\mu$ nul pour l'élément

Multiplions par Hp:

$$\left(\frac{d\ln T}{d\ln P}\right)_s < \left(\frac{d\ln T}{d\ln P}\right)_e + \frac{\phi}{\delta}\left(\frac{d\ln \mu}{d\ln P}\right)_s$$

Stable

ou $$\nabla < \nabla_e + \frac{\phi}{\delta}\nabla_\mu$$

∇_e et ∇_{ad} sont similaires en ce sens que les deux décrivent la variation de température d'un gaz subissant une variations de pression. ∇_{rad} et ∇_μ par contre décrivent la variation spatiale de T et μ du milieu.

Critères de Stabilité de Schwartzschild et de Ledoux

Considérons une atmosphère dans laquelle l'énergie est transportée par radiation (ou conduction) seulement. Alors $\nabla = \nabla_{rad}$. Testons la stabilité de cette atmosphère et considérons que l'élément se déplace adiabatiquement: $\nabla_e = \nabla_{ad}$

L'atmosphère est stable si:

Critère de Ledoux $\nabla_{rad} < \nabla_{ad} + \frac{\phi}{\delta}\nabla_\mu$

Gaz parfait : P = R ρ T/ μ
=> α=δ=ϕ=1

S'il n'a pas de variation de composition ou d'ionisation:

Critère de Schwarzschild $\nabla_{rad} < \nabla_{ad}$

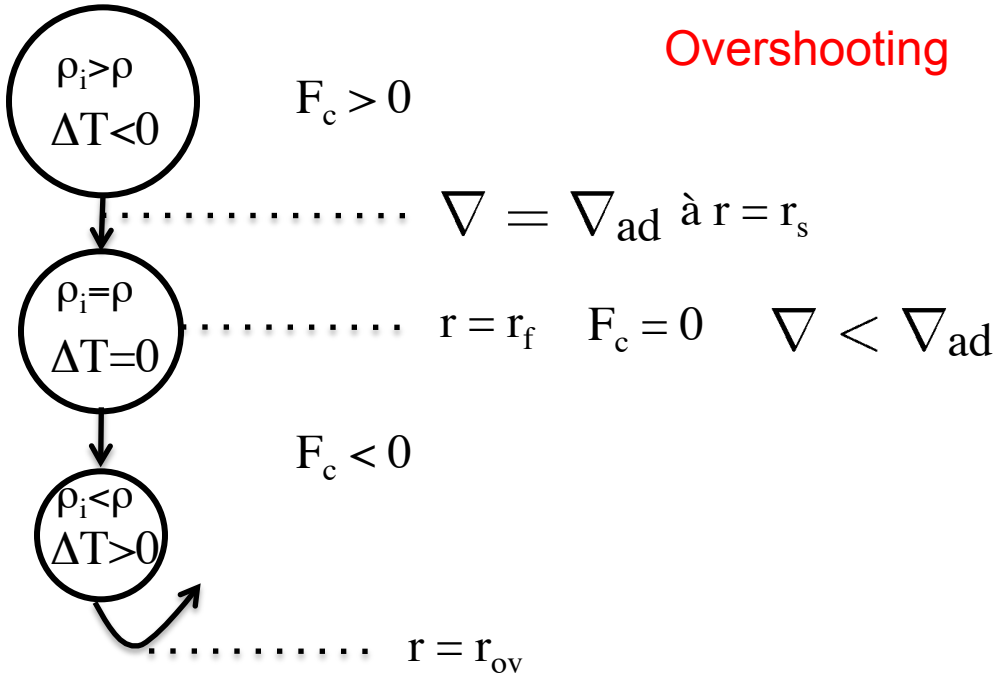

Overshooting

Péclet number: Pe= vL/κ
Pe >> 1 (Soleil) -> change stratification
Pe ~1 , extended overshoot

If a heavy sinking convective parcel penetrates into a subadiabatic layer, when the temperature fluct changes sign, parcel is neutrally buoyant but continues to sink by virtue of inertia until the Buoyancy force reverses the direction of its motion.

Zahn 1991

Critères de Stabilité de Schwartzschild et de Ledoux

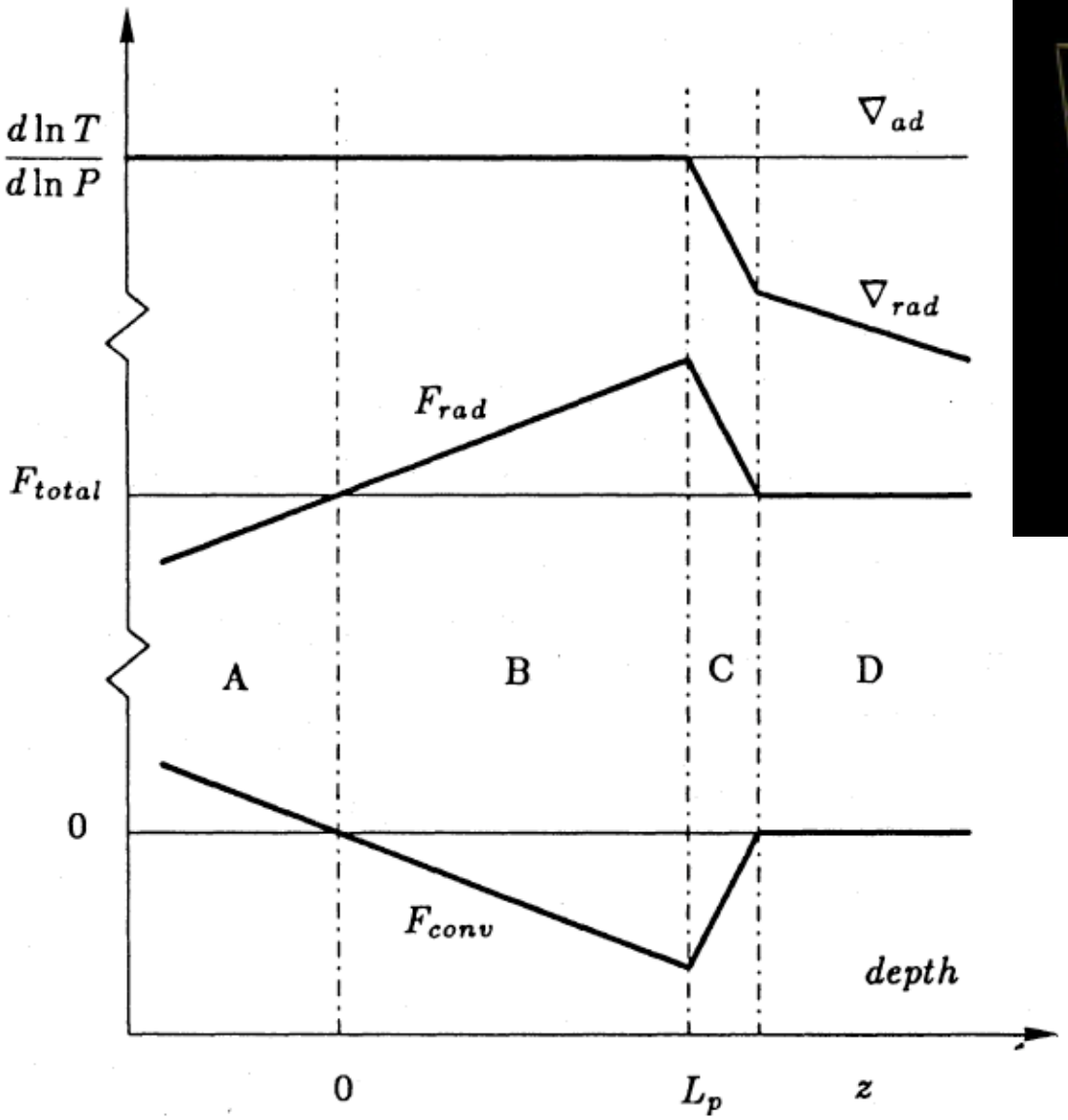

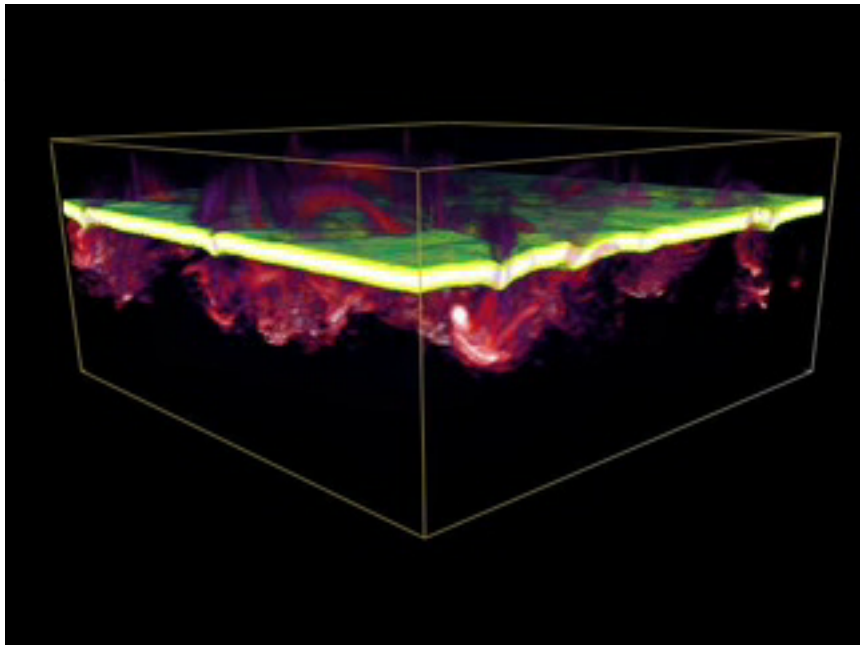

Péclet number: Pe= vL/κ
Pe >> 1 (Soleil) -> change stratification
Pe ~1 , extended overshoot

If a heavy sinking convective parcel penetrates into a subadiabatic layer, when the temperature fluct changes sign, parcel is neutrally buoyant but continues to sink by virtue of inertia until the Buoyancy force reverses the direction of its motion.

Zahn 1991

Deriving an inviscid criteria for convection: Rayleigh number

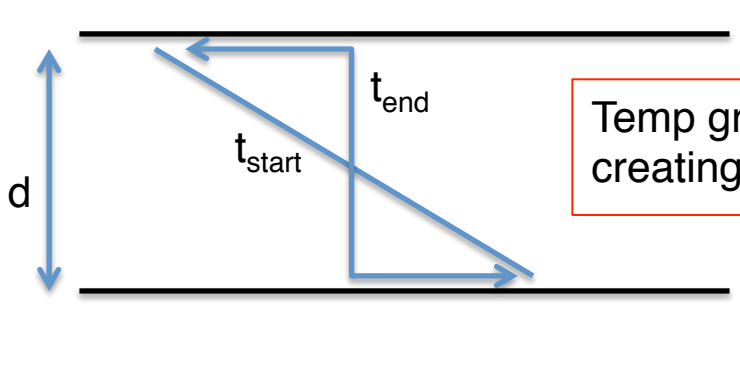

Temp gradient is being homogenized in convection layer creating thermal boundary layers

Bubble is less dense than medium and rise at vertical speed w but as to "fight" against viscous drag:

$\delta\rho\, g = \nu\, \Delta w \sim \nu\, w/d^2 \Rightarrow\ w = \delta\rho\, g\, d^2 / \nu$.

With an ideal gas we can relate density fluctuation to temperature variation ΔT via thermal expansion factor α , e.g. $\delta\rho = \alpha\, \Delta T$

so $w = \alpha\, \Delta T\, g\, d^2 / \nu$

While it rises and since it is hot it radiates away is heat. So in order to retain its buoyancy
Rise time < thermal time $\Leftrightarrow$ $d/w < d^2/\kappa$

$\Rightarrow\ 1 < \alpha\, \Delta T\, g\, d^3 / \nu\, \kappa = Ra$ $\Leftrightarrow$ Rayleigh number Ra must be greater than one
(in this back of the envelope derivation)

Plane Layer Convection

Plane layer conv (cf. Chandrasekhar's book in 1961)

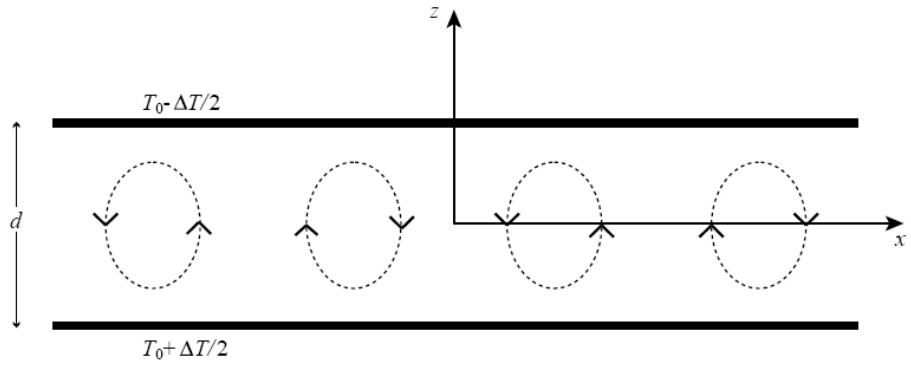

Fig. 17.1: Rayleigh-Bernard convection. A fluid is confined between two horizontal surfaces separated by a vertical distance d. When the temperature difference between the two plates ΔT is increased sufficiently, the fluid will start to convect heat vertically. The reference effective pressure P_0' and reference temperature T_0 are the values of P' and T measured at the midplane $z = 0$.

Rayleigh Number:

$$Ra = \frac{g\alpha\Delta T d^3}{\kappa\nu}$$

Si Ra est suffisament grand alors la convection se déclenche. La différence Avec le critère de Schwatzschild vient du fait qu' ici on prend en compte l' effet des diffusivités

Conditions aux limites stress-free top & bottom: $Ra_c = 658$

stress-free top & no slip bottom: $Ra_c = 1100$

no slip top & bottom : $Ra_c = 1708$

With a vertical magnetic field pervading the system:
BC's stress free top & bottom for V, radial field BC's for B: Ra_c depends on Hartman number, i.e Ha >> 1, alors $Ra_c = \pi^2(Ha)^2$

$$Ha = \left(\frac{\sigma B_0^2 d^2}{\rho\nu}\right)$$

Convective Motions (radial velocity Vr)

Resolution~ 4000^3, Re=VrmsD/ν~5000, Pr=0.25

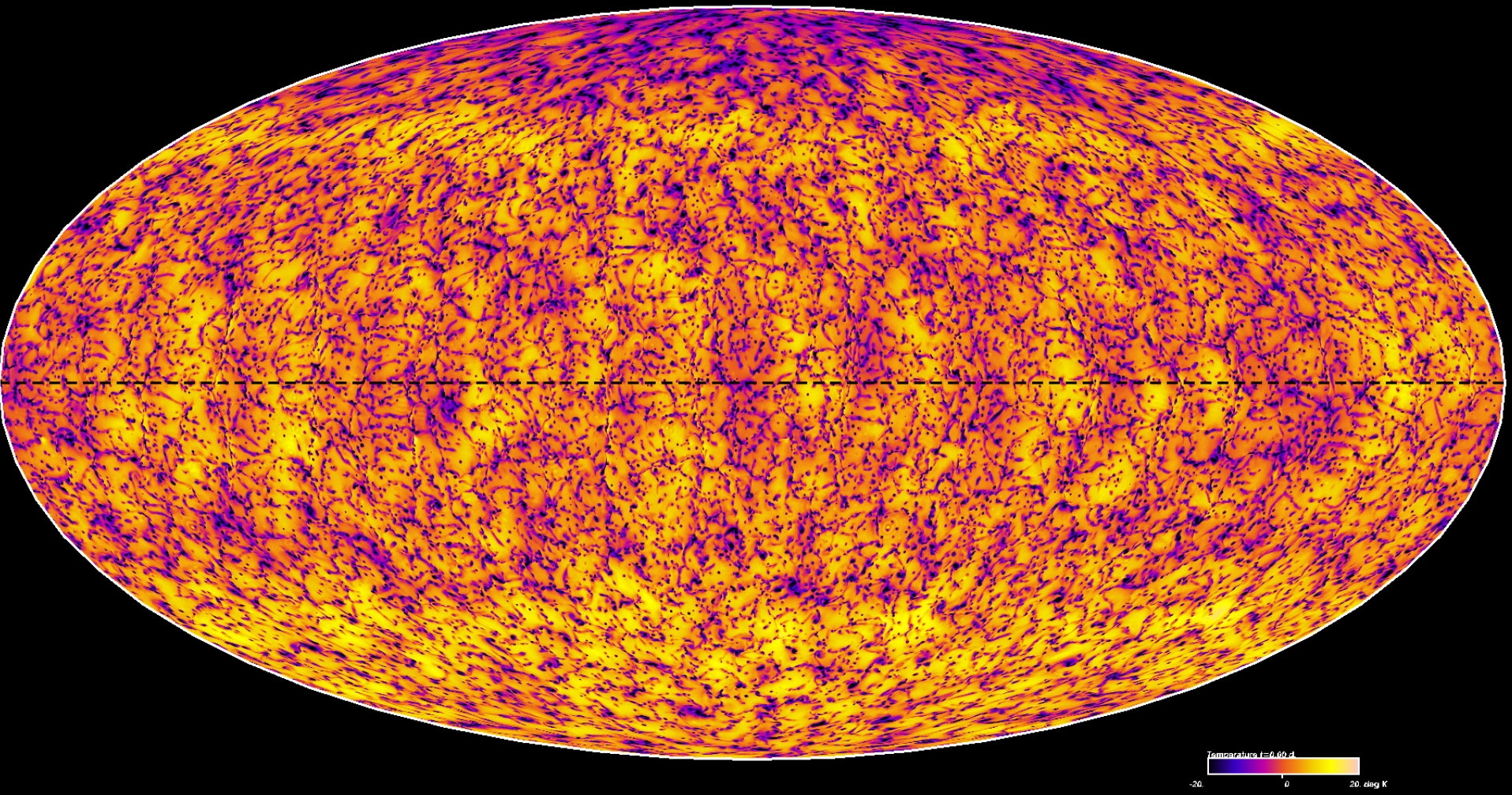

Simulation a 10000 cpus (Curie) ***Brun 2015***

Space-Inn School, 28/10/15

depth=0.98 R

Mean Angular Rotation Profile Ω

(Brun & Toomre 2002, ApJ 570, 865)

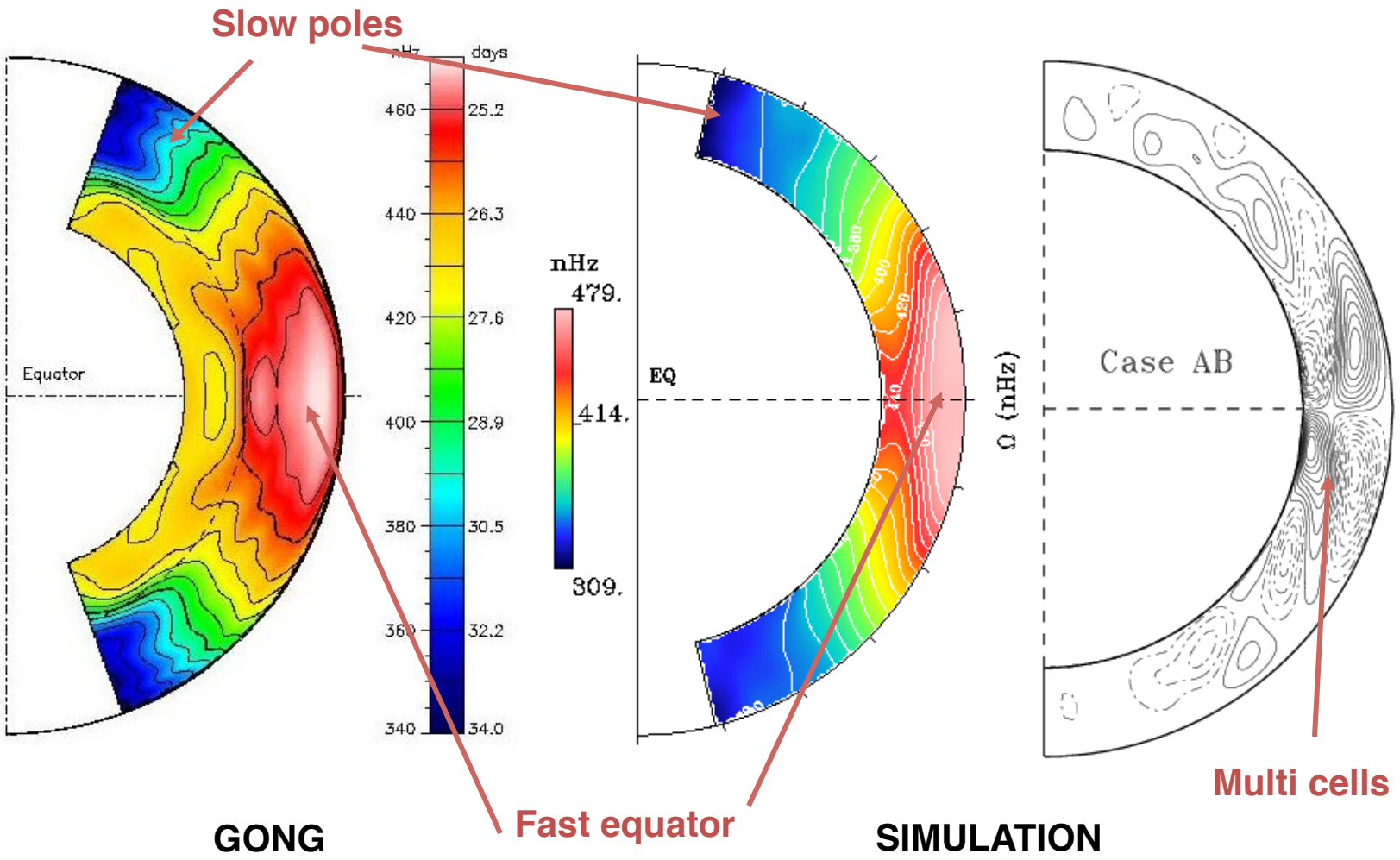

Taylor-Proudman Theorem & Thermal Wind

The curl of the momentum equation gives the equation for vorticity $\omega = \vec{\nabla} \times \vec{v}$:

$$\frac{\partial \vec{\omega}}{\partial t} + \vec{v}.\vec{\nabla}\vec{\omega} - \vec{\omega}.\vec{\nabla}\vec{v} = \nu\vec{\nabla}^2\vec{\omega} + \frac{1}{\rho^2}\vec{\nabla}\rho \wedge \vec{\nabla}p \qquad \text{(a)}$$

Taylor-Proudman Theorem:

In a stationary state, the φ component of (a) can be simplified to:

$$2\Omega \frac{\partial \hat{v}_\varphi}{\partial z} = 0 \quad \Rightarrow v\varphi \text{ is cst along z}$$

the differential rotation is cylindrical (Taylor columns) and the flows quasi 2-D.

Thermal Wind:

The presence of cross gradient between p and ρ (baroclinic effects) can break this constraint (as well as Reynolds & viscous stresses and magnetic field) :

$$2\Omega \frac{\partial \hat{v}_\varphi}{\partial z} = -\frac{1}{\hat{\rho}^2}\vec{\nabla}\hat{\rho} \wedge \vec{\nabla}\hat{p}\Big|_\varphi = \frac{1}{\hat{\rho}C_p}\left[\vec{\nabla}\hat{S} \wedge -\hat{\rho}\vec{g}\right]_\varphi = \frac{g}{rC_p}\frac{\partial \hat{S}}{\partial \theta}$$

Thermal BC's Influence on Ω

No imposed S_{bot}

$S(r_{bot}, \theta) = a_2 Y_2^0 + a_4 Y_4^0$

Best Case

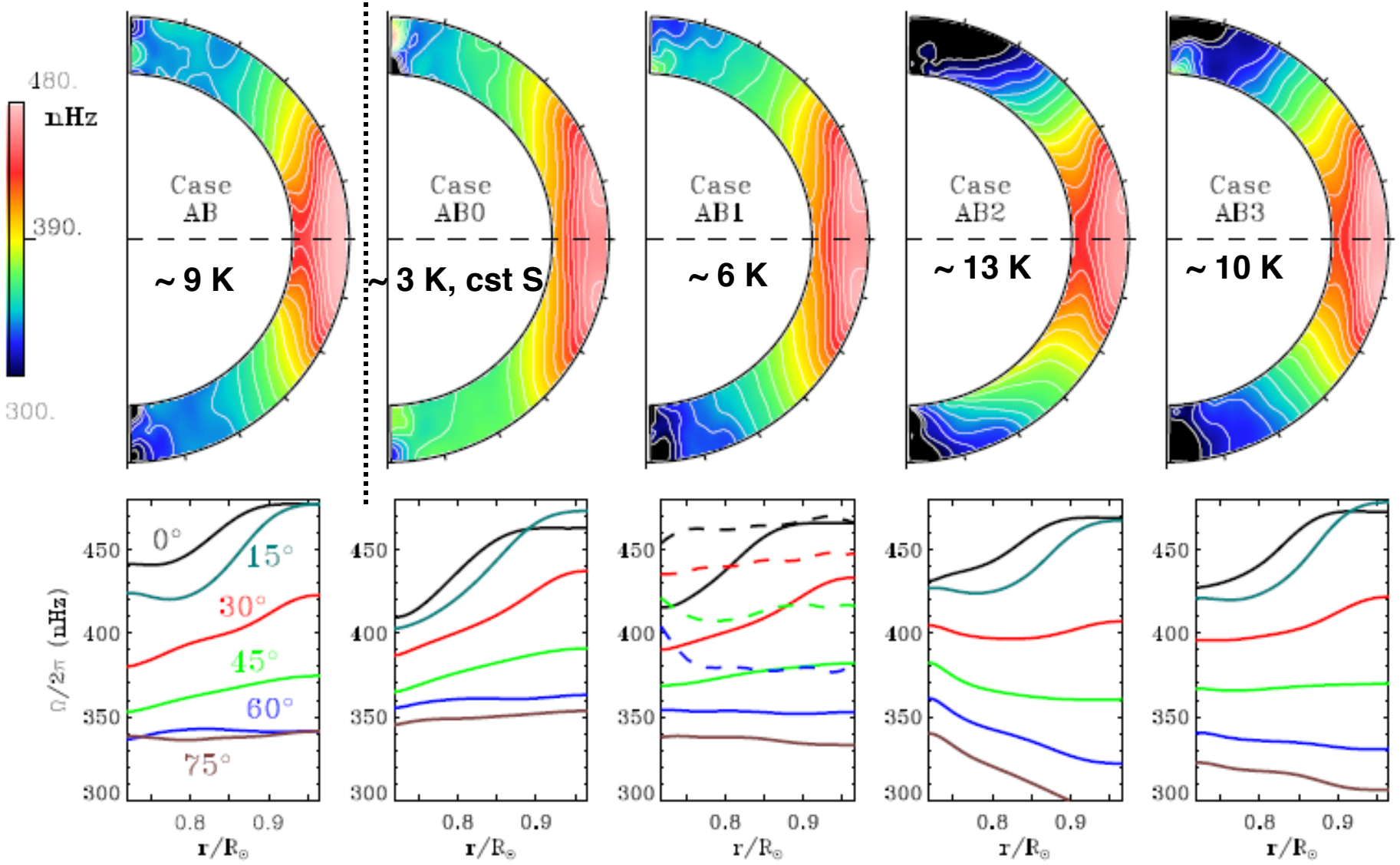

Miesch, Brun & Toomre 2006 ApJ, 641, 618 ; see also Rempel 2005

Latitudinal Heat Flux Balance

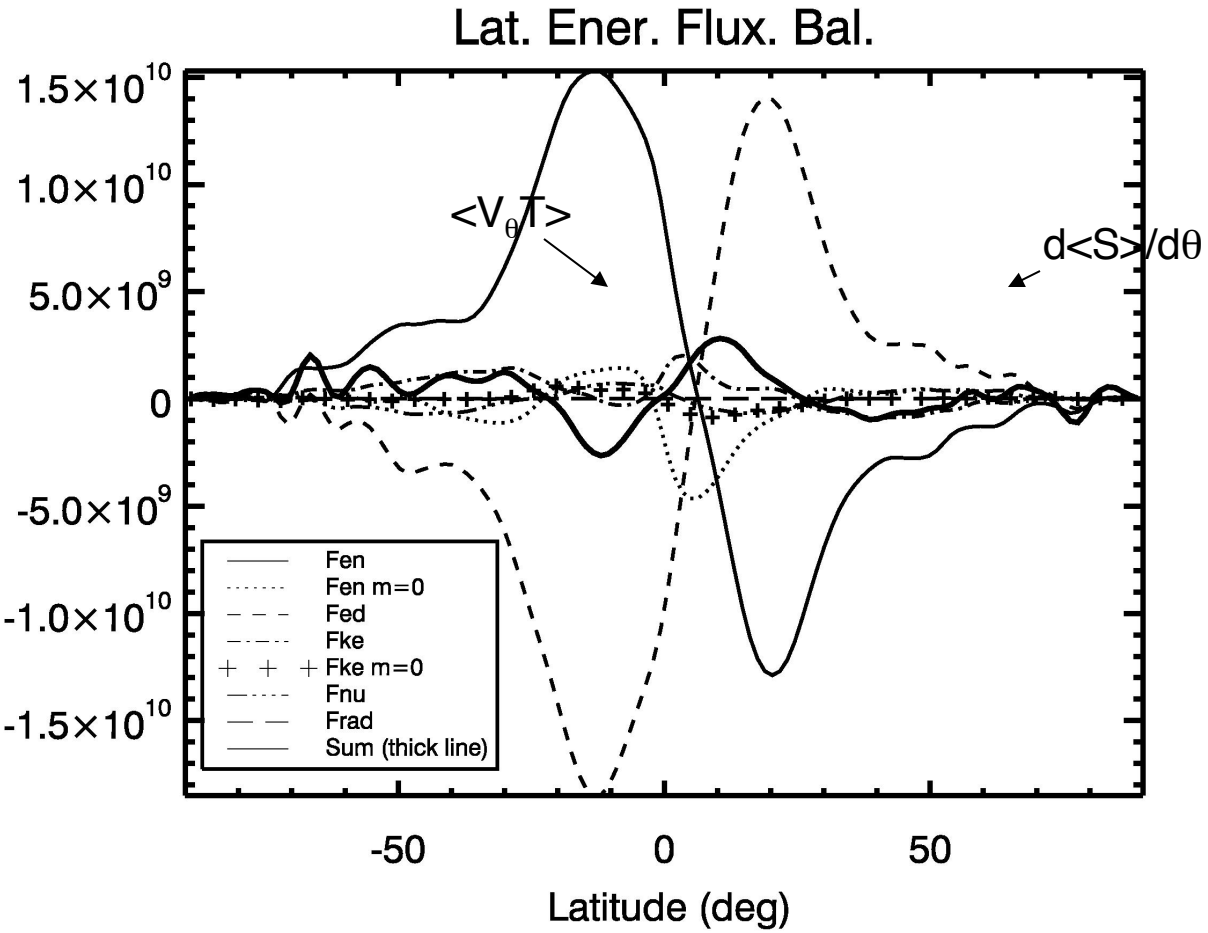

$$F_\theta = -(\mathbf{v}\cdot\mathcal{D})_\theta - \frac{\kappa\bar{\rho}\bar{T}}{r}\frac{\partial S}{\partial\theta} - \frac{\kappa\bar{\rho}C_p}{r}\frac{\partial T}{\partial\theta} + v_\theta\frac{1}{2}\bar{\rho}v^2 + \bar{\rho}C_p v_\theta T$$

Brun & Toomre ApJ 2002, Brun & Rempel 2009

Adding coupling to a stably stratified interior

Coupling Convection to Radiation

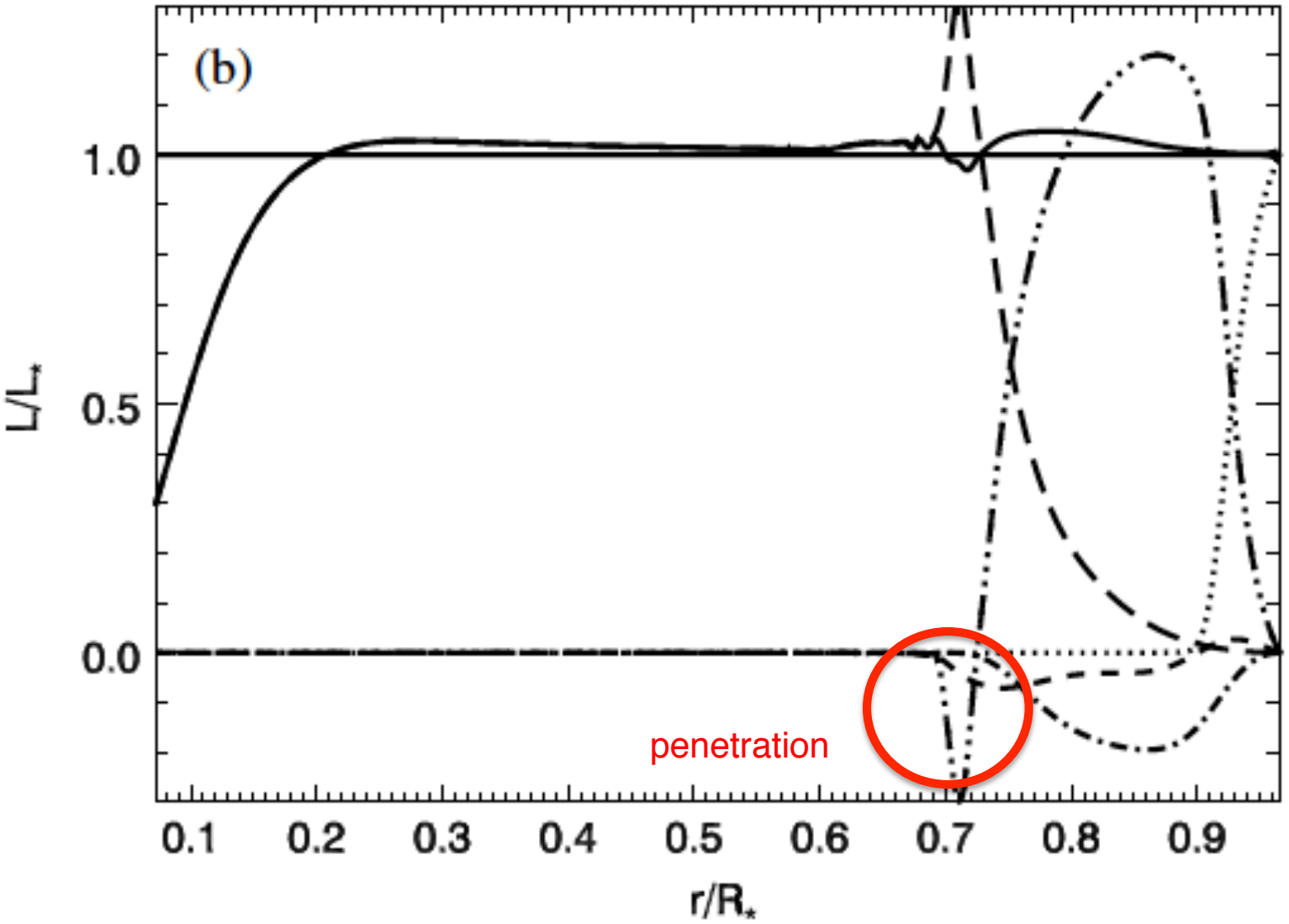

Omega Profile & Thermal Perturbations

Omega

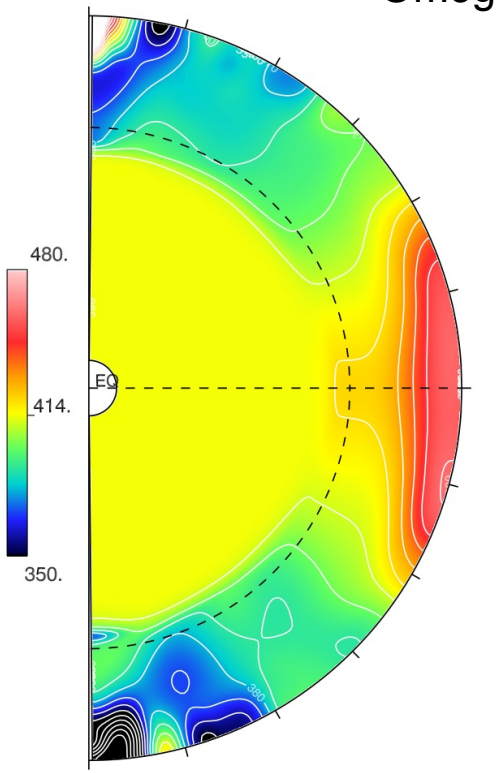

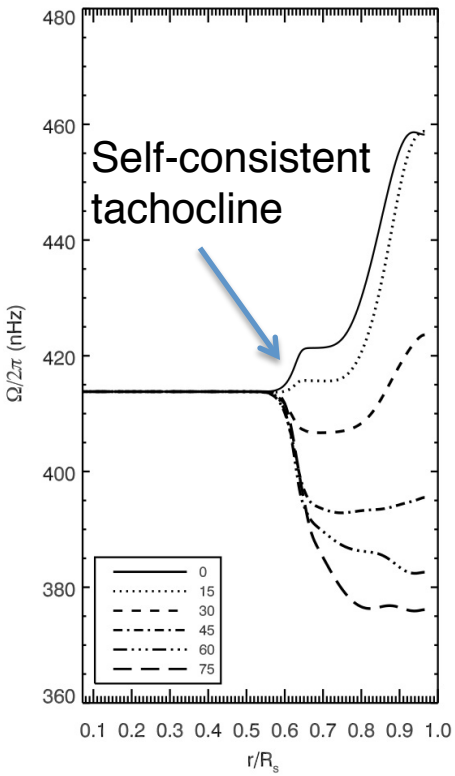

Self-consistent tachocline

Warm poles, cool equator

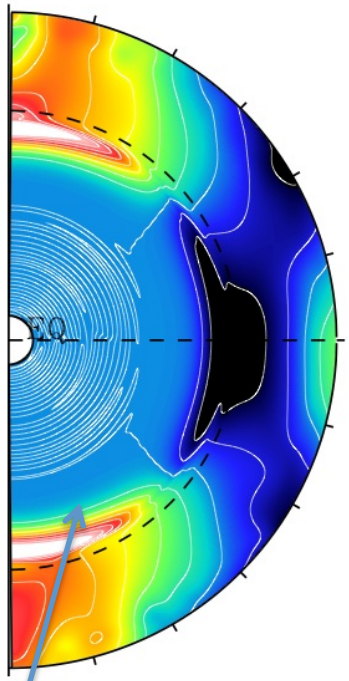

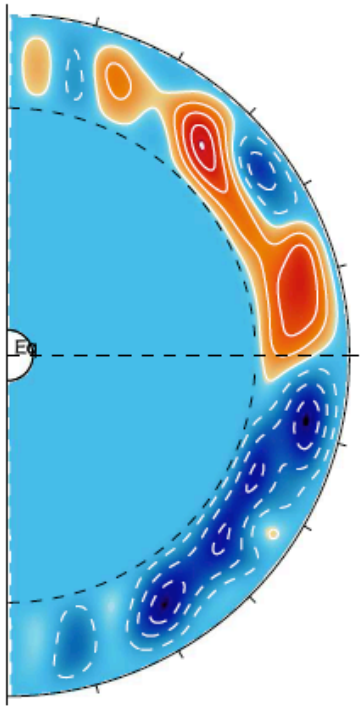

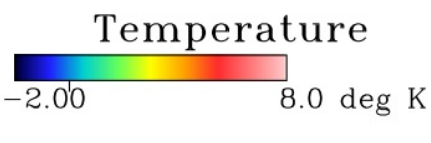

3 orders of mag drop at BCZ
0.02 overshoot

LARGER fluctuations at bcz

Internal Waves

3D view

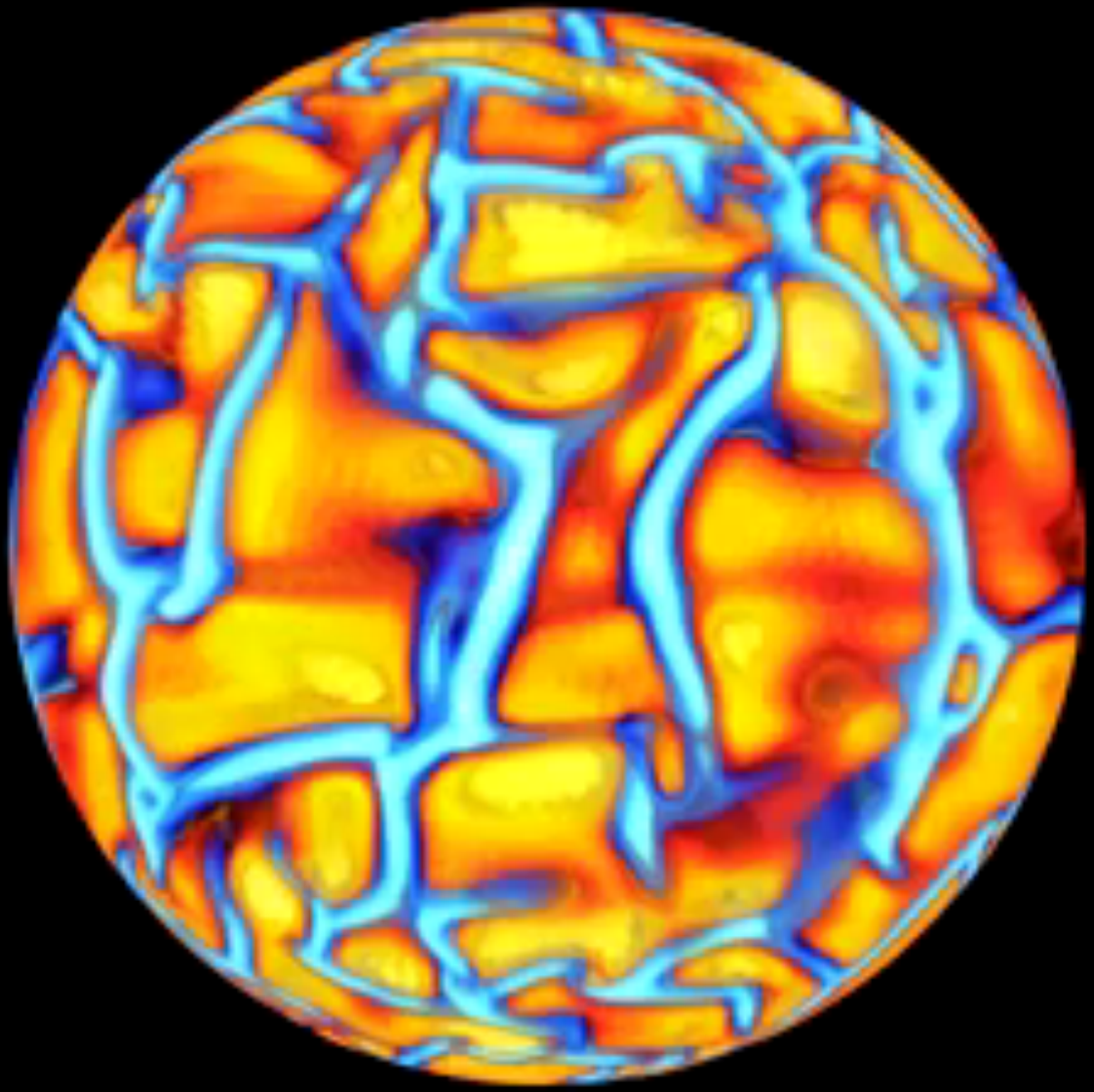

Alvan et al. 2014, A&A

Vr/sqrt(<Vr(r)^2>)

Higher Resolution

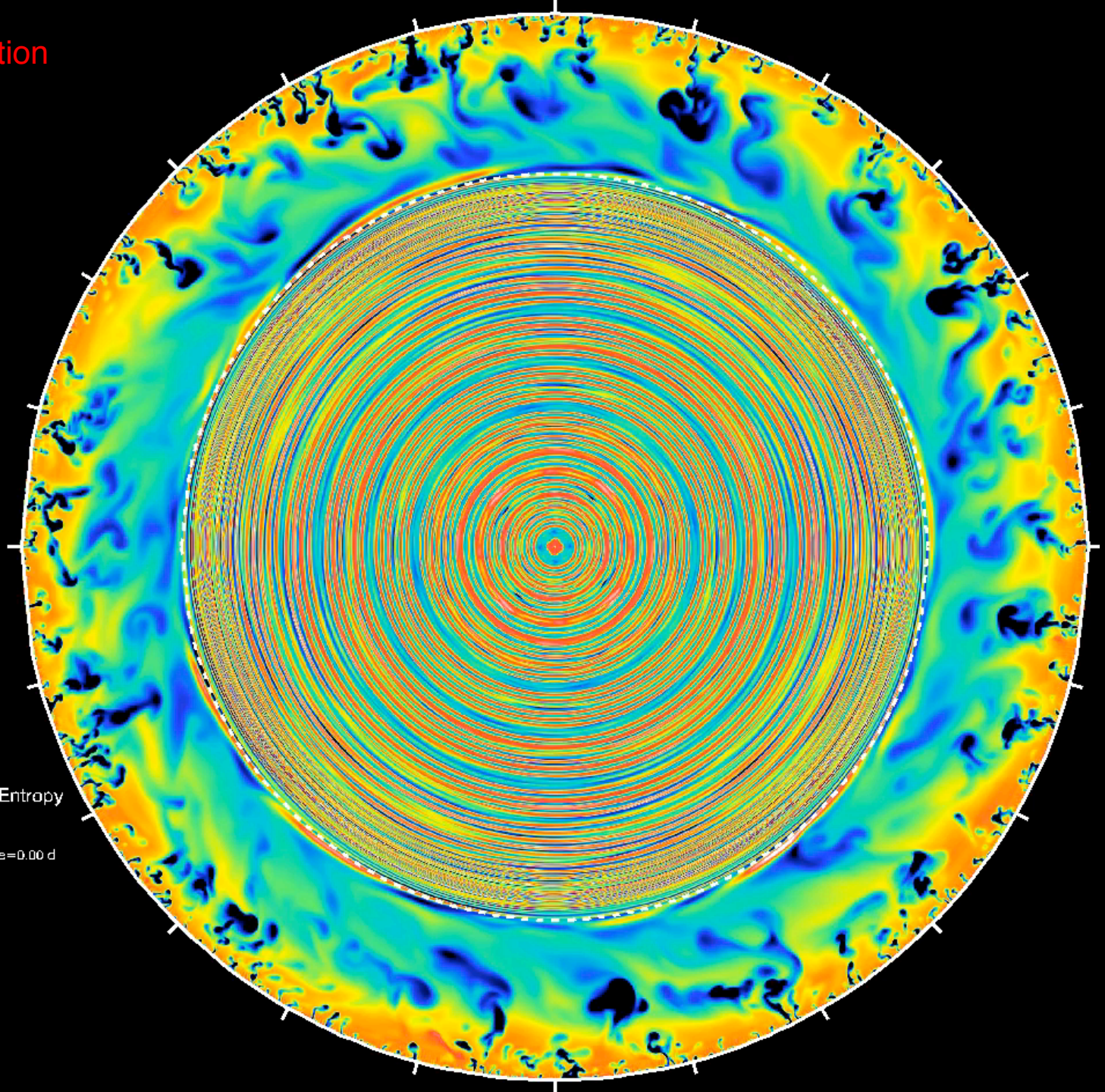

Magnetic Field Generation & Dynamo

Magnetic Convection

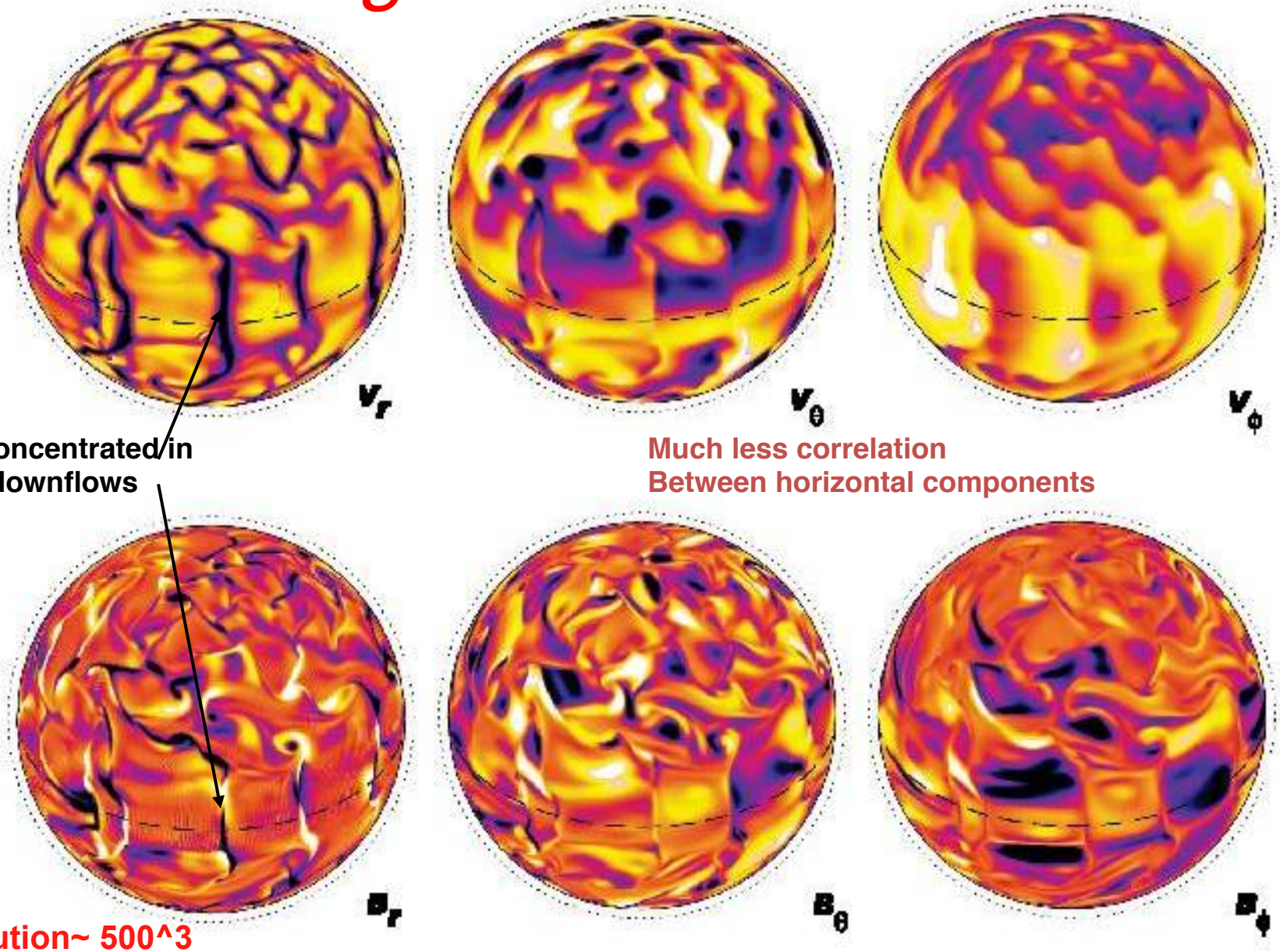

Br concentrated in the downflows

Much less correlation Between horizontal components

Resolution~ 500^3

Re=VrmsD/n~150,P=0.25, Pm=4 MAGNETIC CASE M3 (Brun, Miesch, Toomre 2004, ApJ, 614)

Dynamo Action –Magnetic Energy

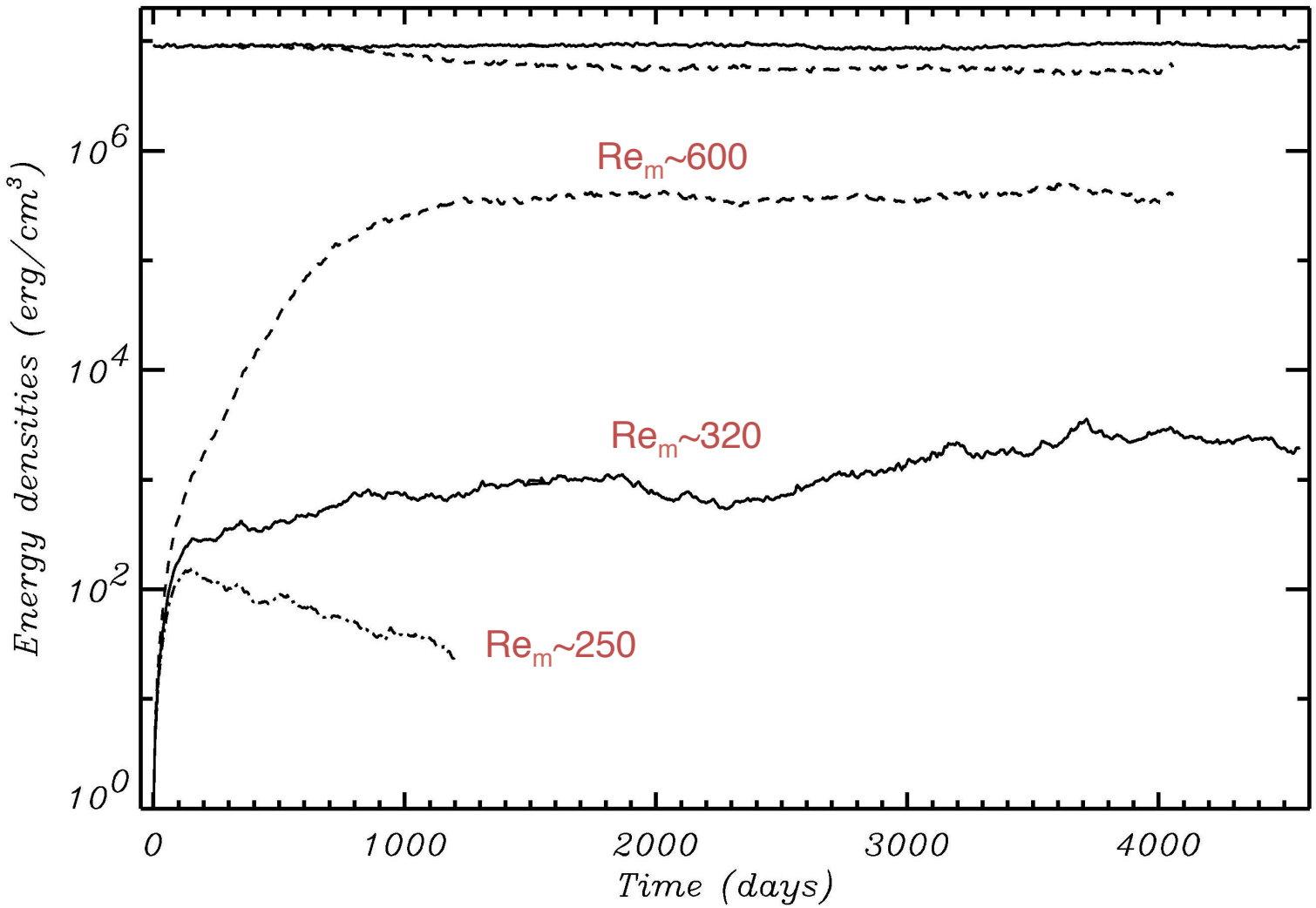

Starting from a small seed field B the magnetic energy reach a level of ~8% of KE while keeping a solar like differential rotation

Dynamo Threshold around Re$_m$=VrmsD/η~300

Magnetic field in a solar-like star dynamo

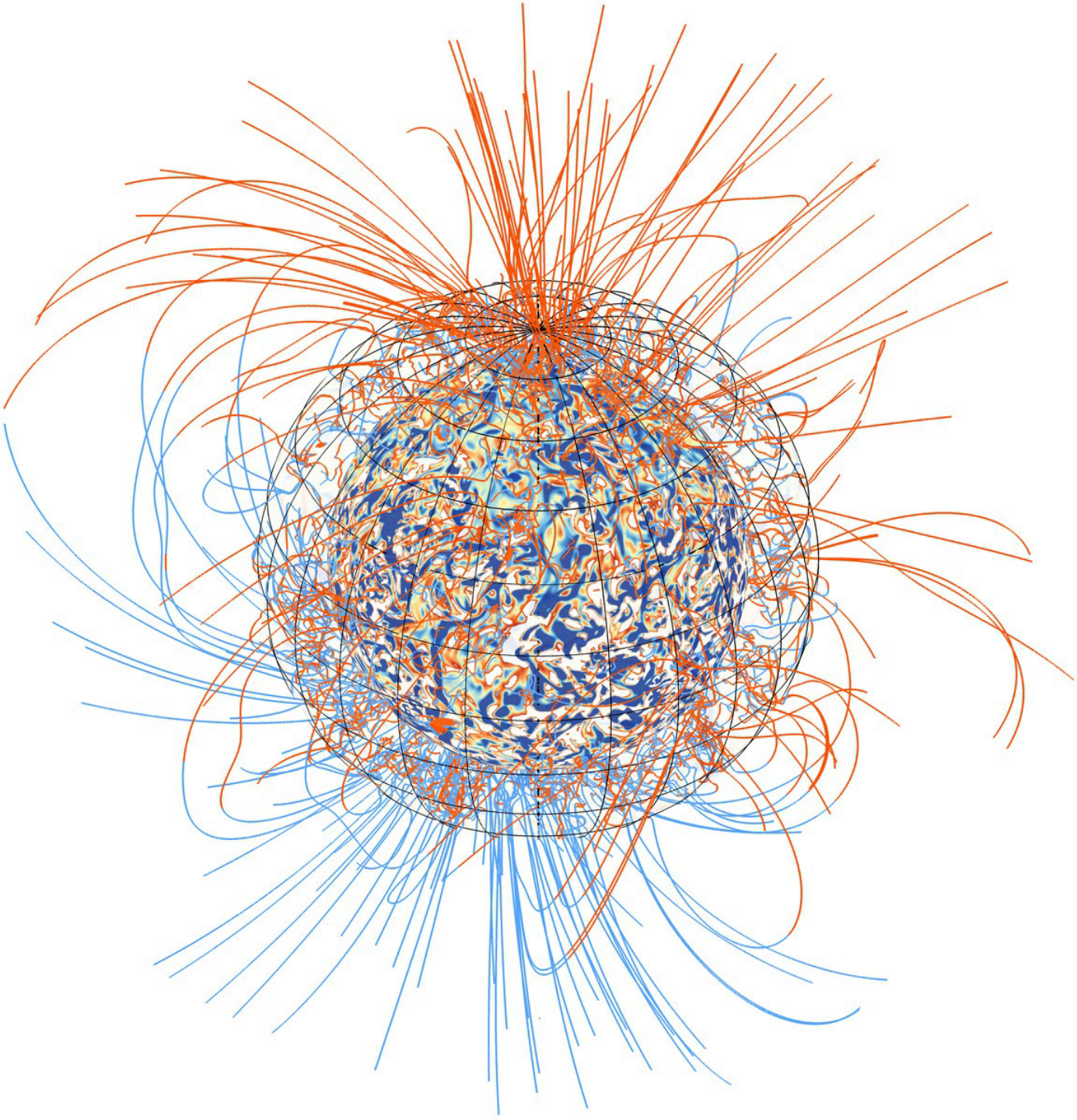

Mean Angular Velocity Ω

Ω quenching!

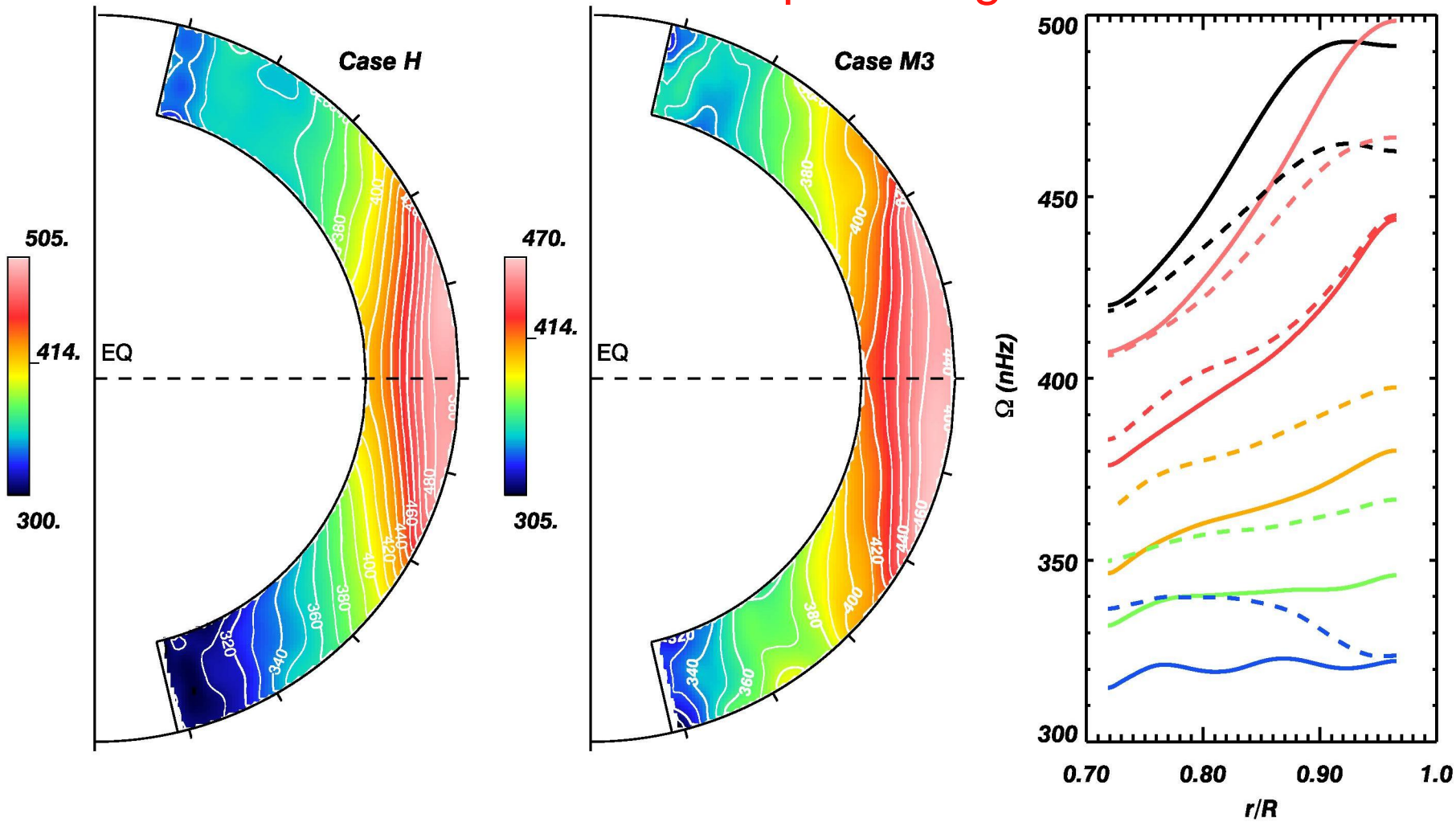

Initial state of differential rotation

Evolved state of differential rotation under the influence of the **Lorentz force**

Angular Momentum Balance in Presence of B

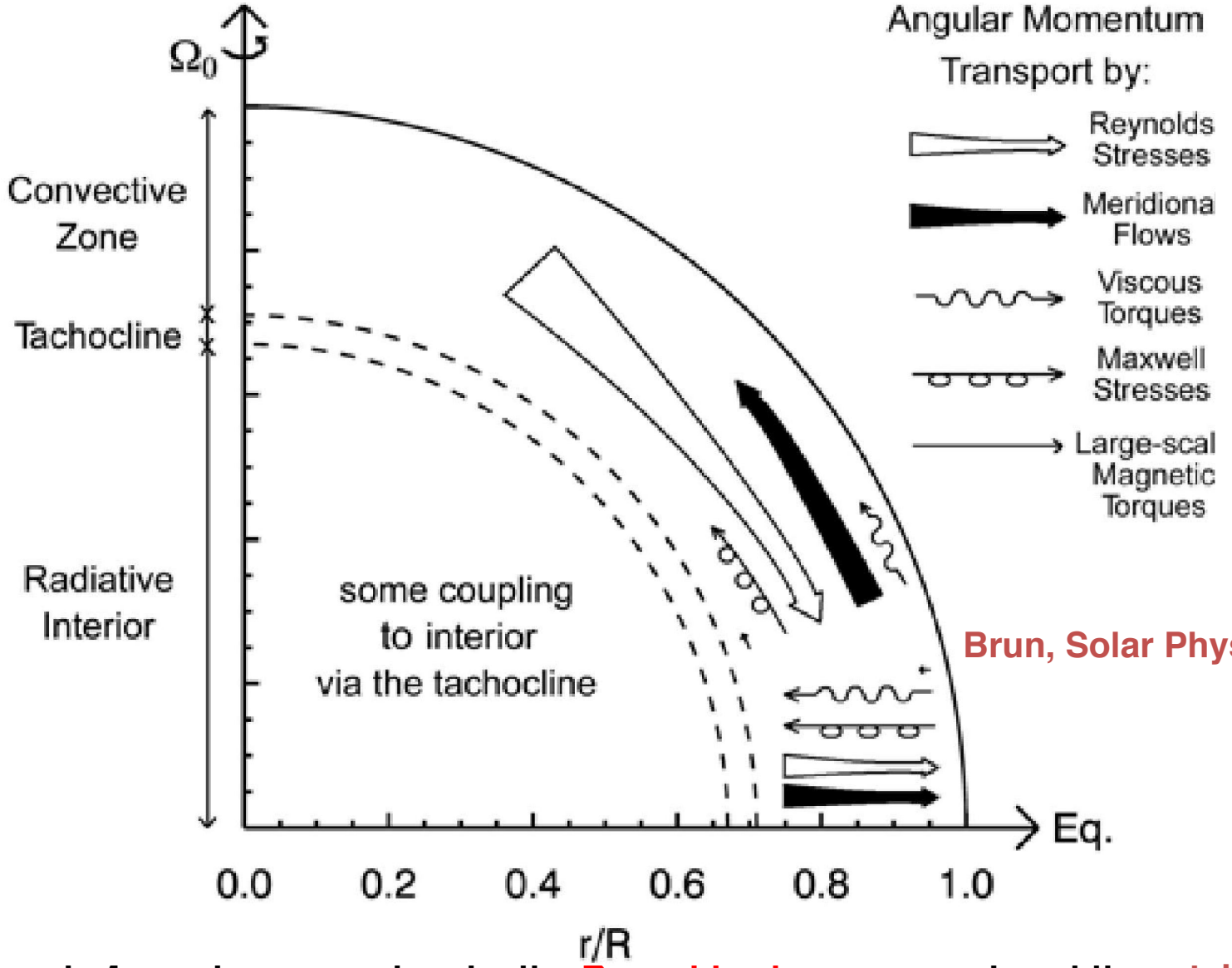

Brun, Solar Physics, 2004

The transport of angular momentum by the Reynolds stresses remains at the origin of the equatorial acceleration. The Maxwell stresses seeks to speed up the poles.

Br

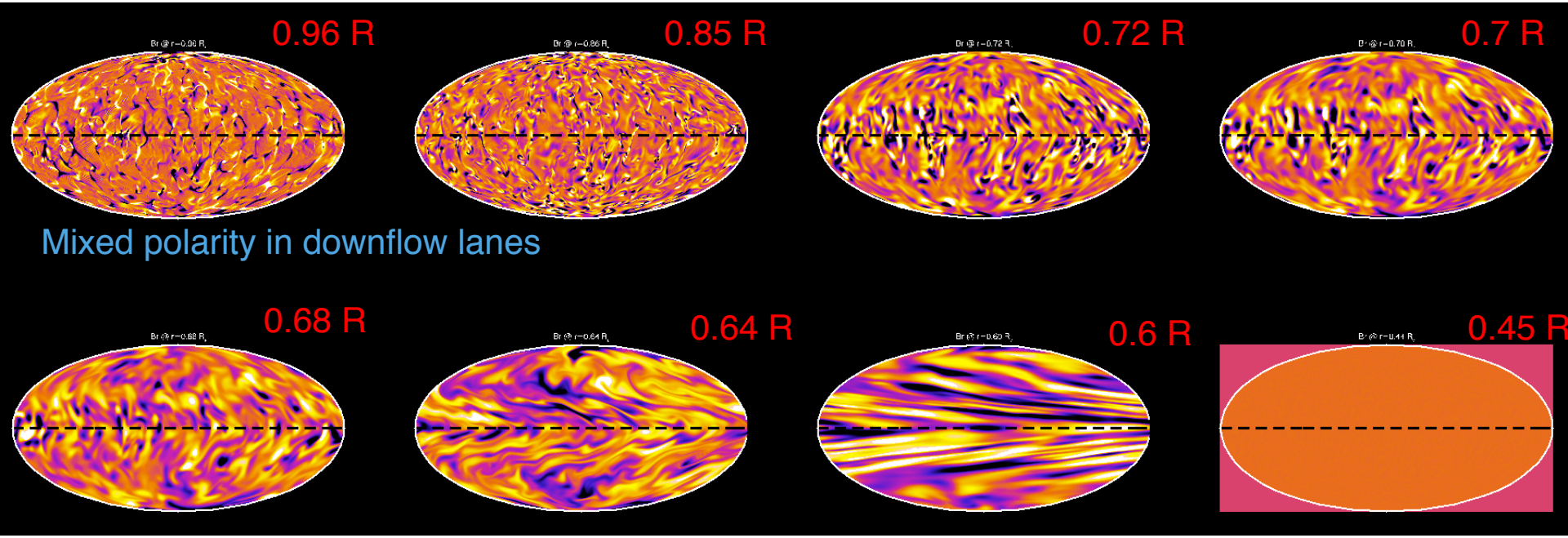
0.96 R
0.85 R
0.72 R
0.7 R
Mixed polarity in downflow lanes
0.68 R
0.64 R
0.6 R
0.45 R

Bphi

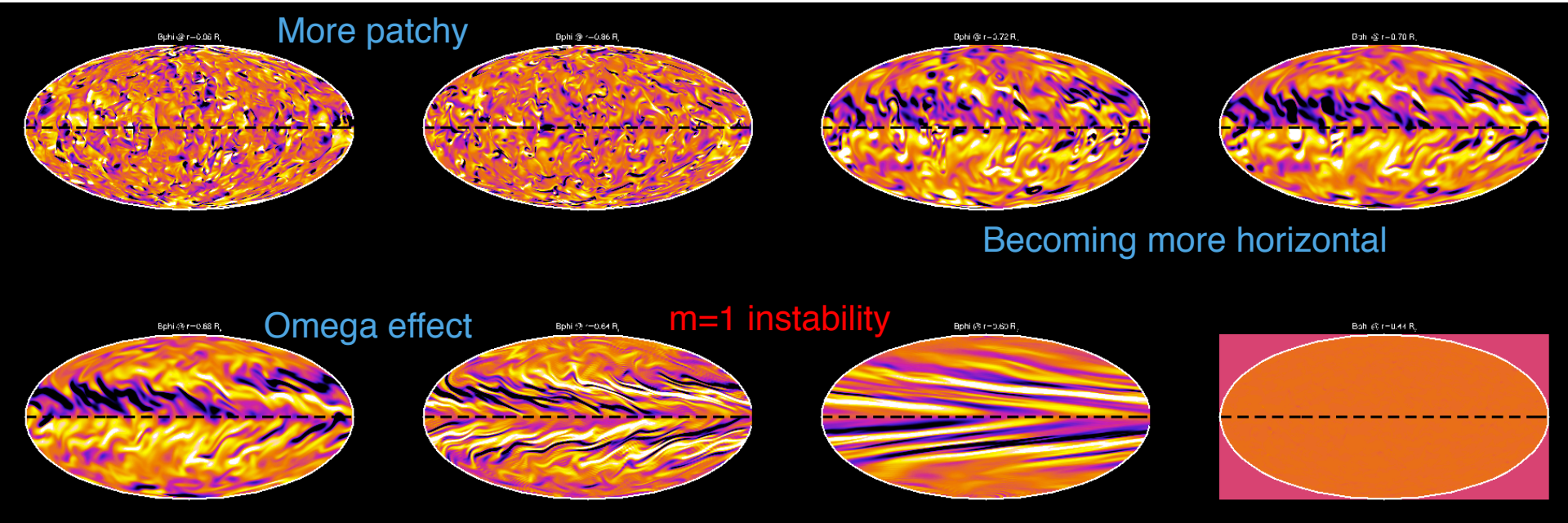
More patchy
Becoming more horizontal
Omega effect
m=1 instability

Getting Cycle
in similar Models

Ghizaru et al. 2010

Model has been run
for several centuries

30 yr period

Cf Talk by J.F Cossette

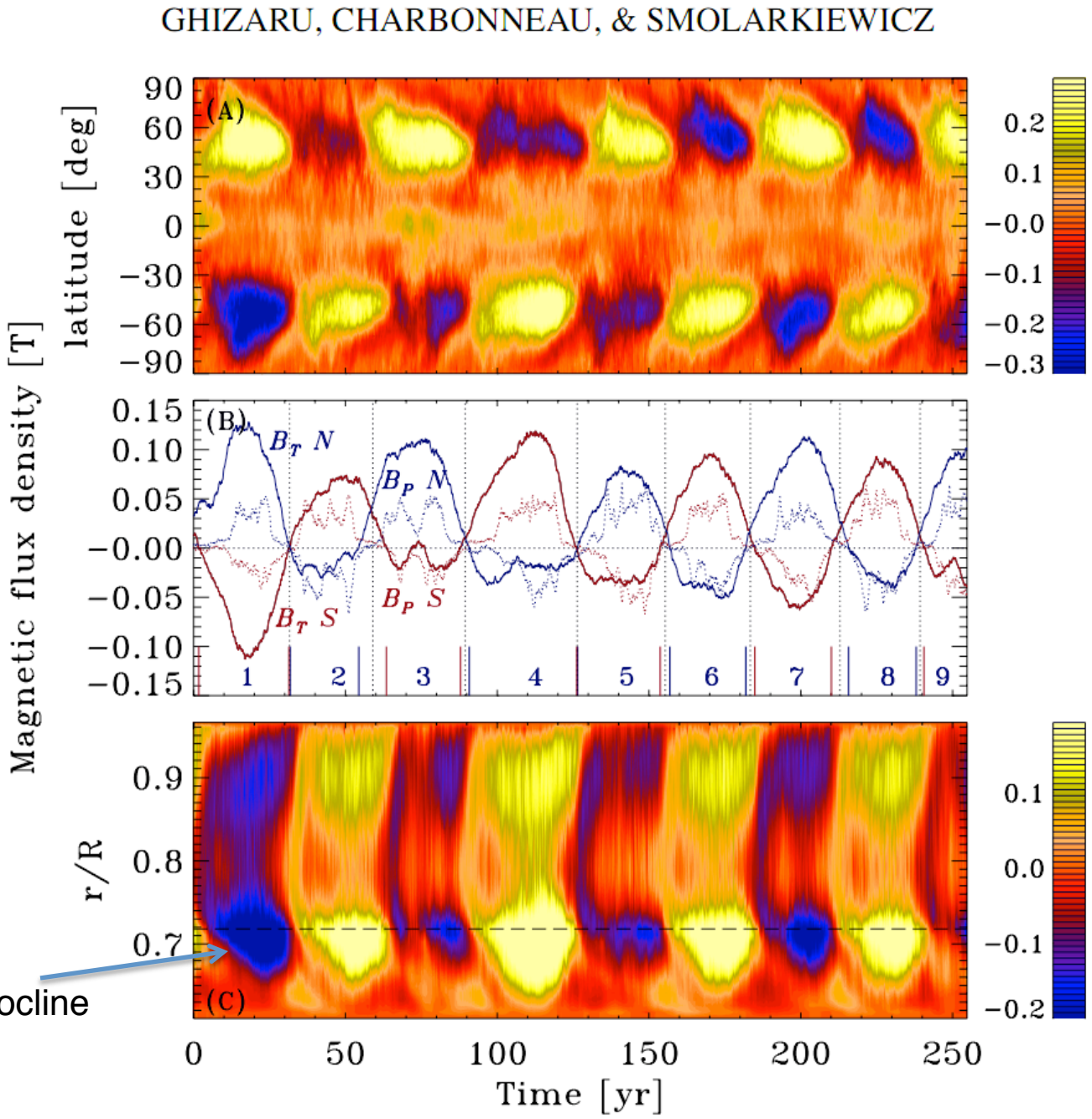

Turbulent pumping and
shearing in imposed tachocline

Effect of Stratification on Dynamo Wave Propagation

Kapyla et al. 2013, arXiv:1301.2595

Caveat:
Relative High Rotation (4 times solar)

$\Delta\rho = 5$

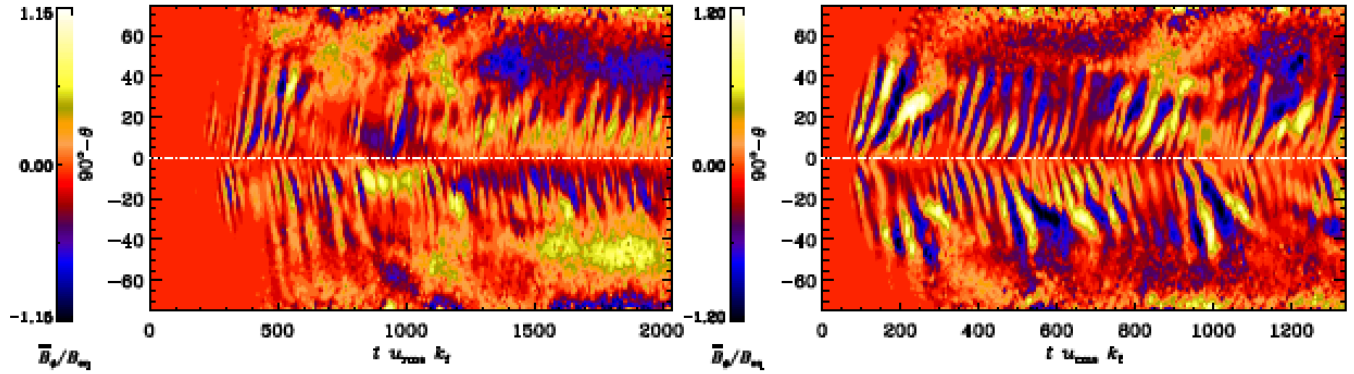

Fig. 4.— Same as Figure 3 but for Runs B1 (top) and B2 (bottom).

$\Delta\rho = 30$

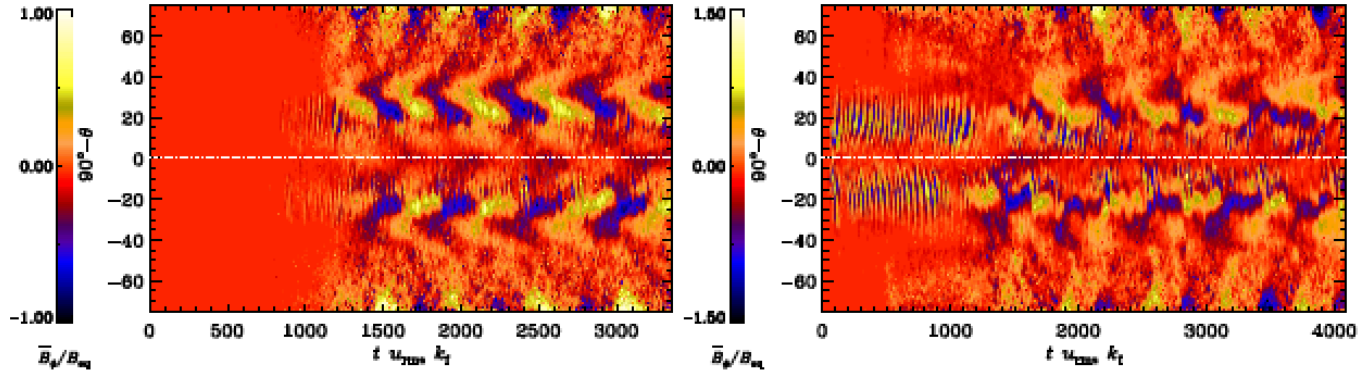

Fig. 5.— Same as Figure 3 but for Runs C1 (top panel) and C2 (bottom). Note the difference in cycle frequency between early times when the frequency is similar to that of Run B2 (Figure 4) and late times.

See Talks by:
Axel, Maarit and Petri

Higher stratification: Modify locations of Omega and alpha effects

A Theoretical View of the Sun's Interior Dynamics

0: convection turbulente (panaches)
1: génération/auto induction de champ mag (effet alpha) ou
1': inclinaison des regions actives,source de Bpol
2: pompage turbulent de B ou
2': transport par circulation méridienne
3: organisation par cisaillement tachocline (effet omega)
3': cisaillement de surface, Sub surface weather
4: instabilité de Parker des structures toroidales (m=1 ou 2)
5: émergence + rotation de structures vrillées, 6: recyclage ou
7: apparation à la surface sur forme bi-polaire
8: ones internes extractant du moment cinetique
9: interactions entre champ dynamo et champ interne (fossile?)
10:instabilité de Tayler du champ interne,
Il y a t il un effet dynamo dans la RZ?

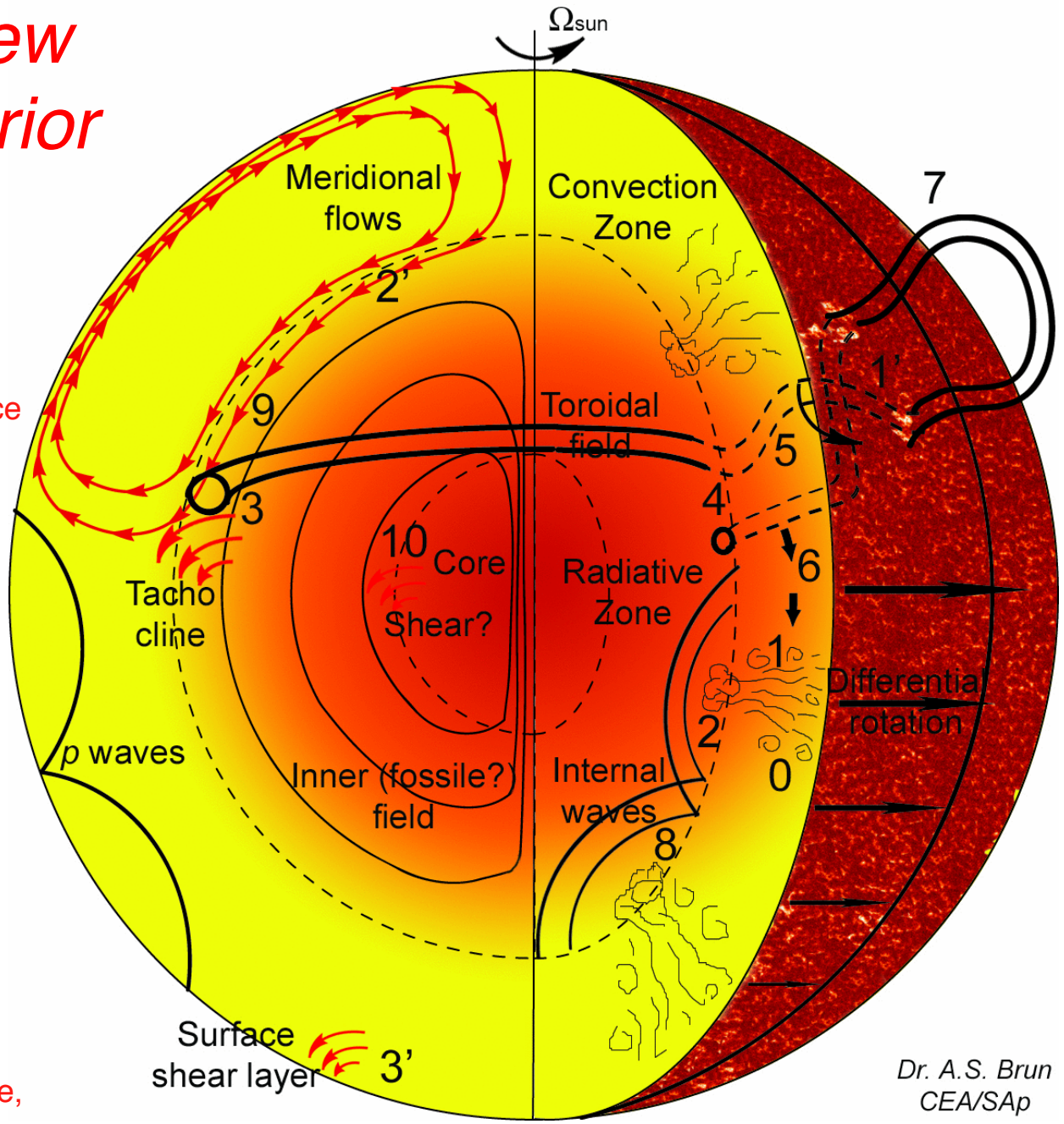

From the Sun to the Stars

A.S. Brun, Space-Inn School, 28/10/15

Solar Type Stars (late F, G and early K-type)

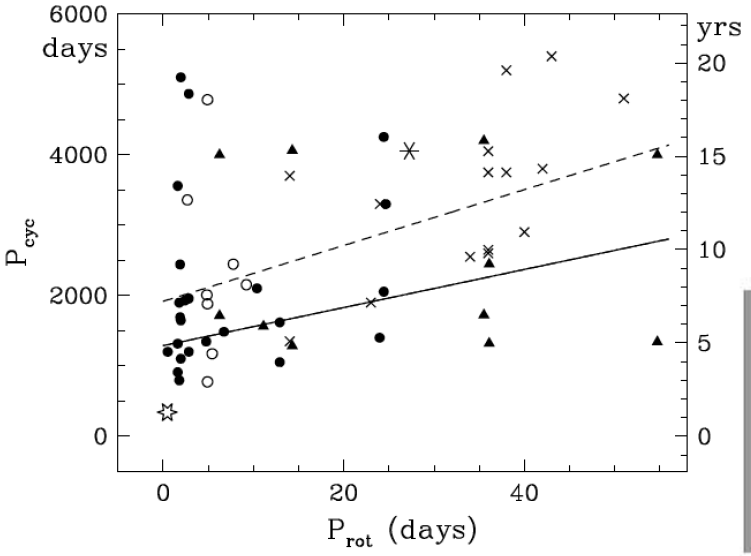

Fig. 6. The rotational period-cycle period diagram, with symbols as Fig. 5. The dashed line is the fit to all results including the ones from t literature, and the solid line is the relation for the shortest cycle lengt determined by us.

Olah et al. 2009

In stars activity depends on rotation & convective overturning time via Rossby nb $Ro=P_{rot}/\tau$

$<R'_{HK}> = Ro^{-1}$, $P_{cyc}=P_{rot}^{1.25+/-0.5}$

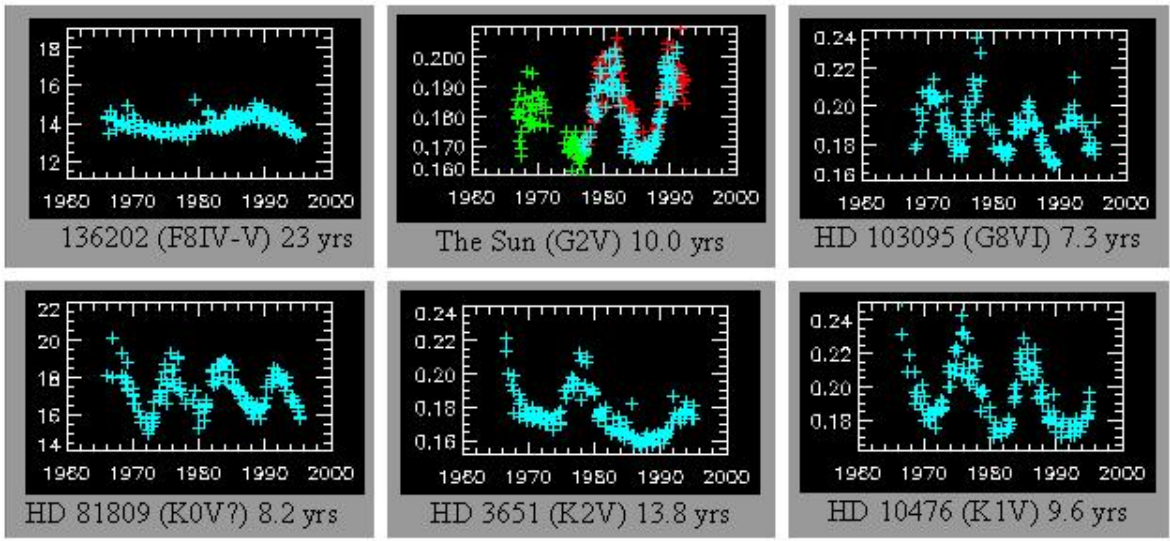

CaII H & K lines , $<R'_{HK}>$

Over 111 stars in HK project (F2-M2):

31 flat or linear signal

29 irregular variables

51 + Sun possess magnetic cycle

=> Much more coming in Asteroseismology Era

see also Noyes et al. 1984, Wilson 1978, Baliunas et al. 1995

Solar Analogs

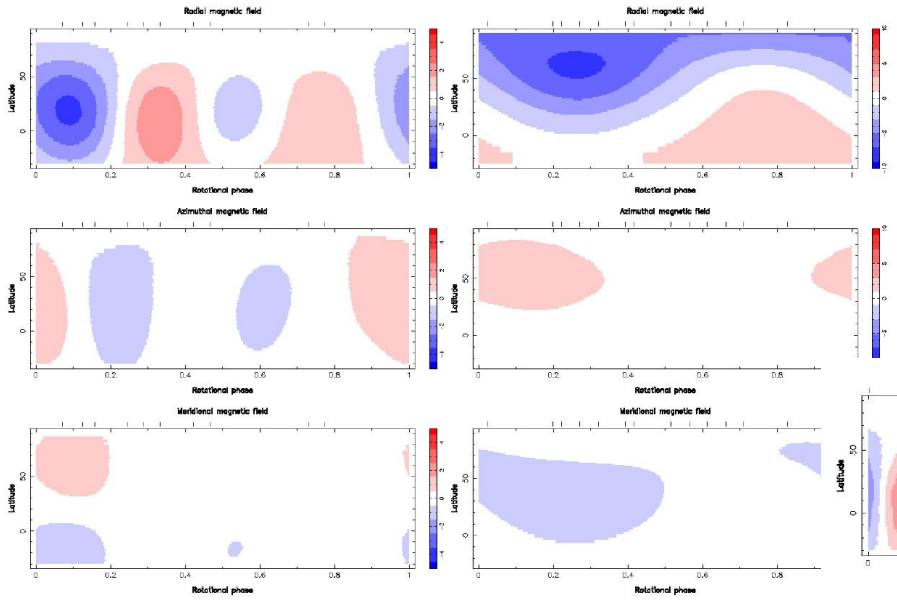

Figure 4. Magnetic maps of HD 146233 and HD 76151 (left and right panel, respectively). Each chart illustrates the onto one axis of the spherical coordinate frame. The magnetic field strength is expressed in Gauss. Vertical ticks above the the observed rotational phases. Note that color scales are not the same for every star.

Faster the solar analogs rotate more toroidal Field contribution they possess.

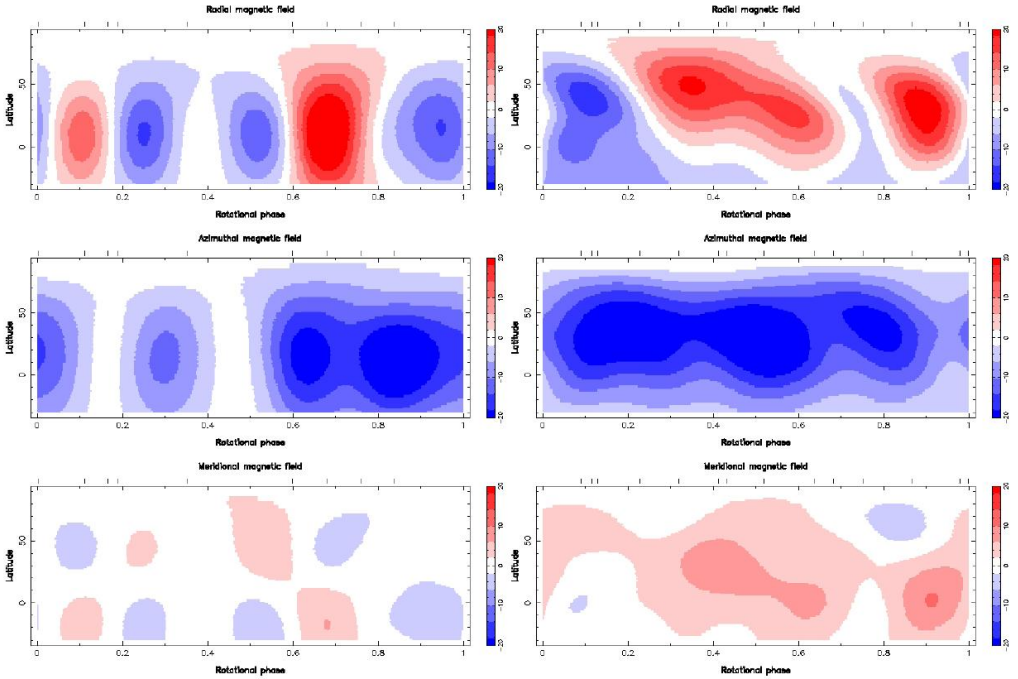

Figure 5. Same as Fig. 4, for HD 73350 (left panel) and HD 190771 (right panel).

Petit et al. 2008, MNRAS

ESPADON/NARVAL

2D Mean Field models: Babcock-Leighton

Standard model: 1 cell per hemisphere

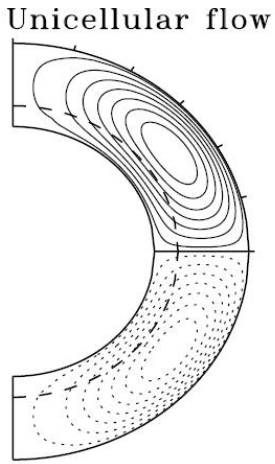

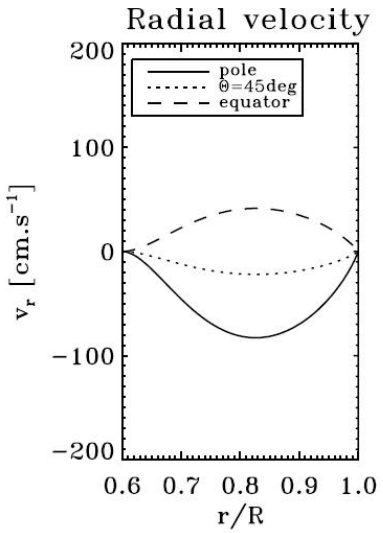

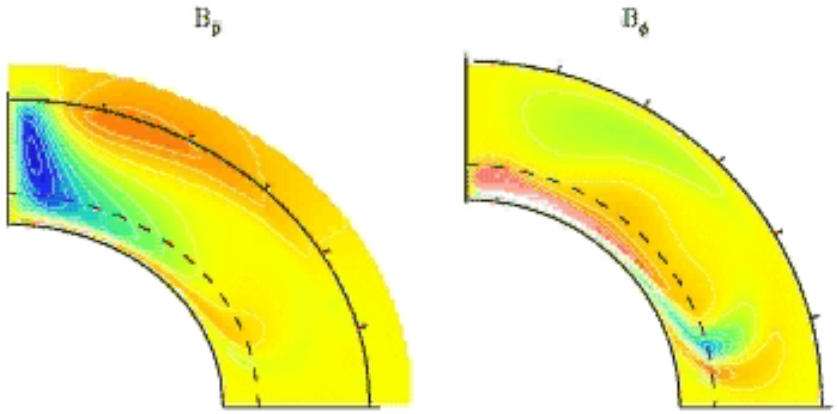

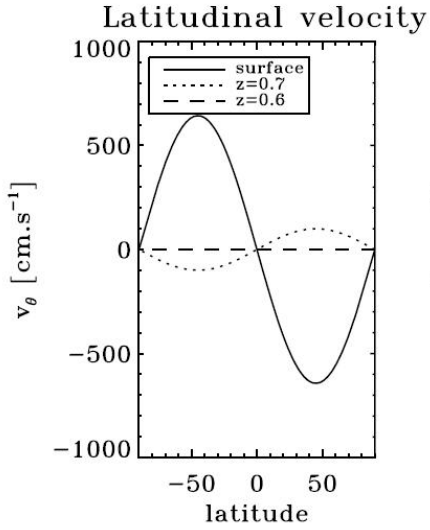

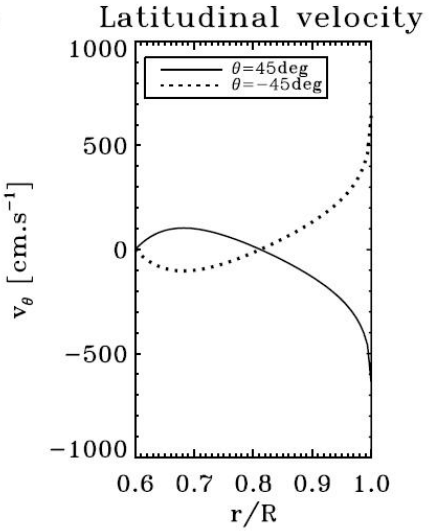

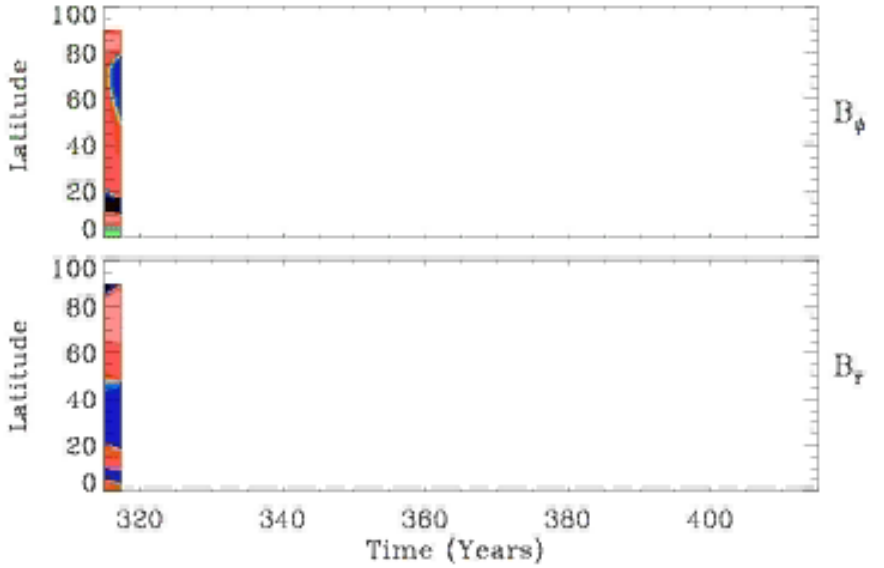

Jouve & Brun, 2007 A&A, 474, 239

Check international Benchmark: Jouve et al. 2008, A&A

Few Points We Must Address

- Source of variability (chaos, intermittency,…)
- Can we reproduce the trend $P_{cyc} \sim P_{rot}^{n}$ (n ~1+/-0.2)
- Can we reproduce the increase of the toroidal vs poloidal component
- Which « solar model» is best to explain stellar data?

BL mean field models

$$P_{cyc} = v_0^{-0.91} s_0^{-0.013} \eta^{-0.075} \Omega_0^{-0.014}$$

Strong dependancy on meridional flow amplitude

Our G & K star Models

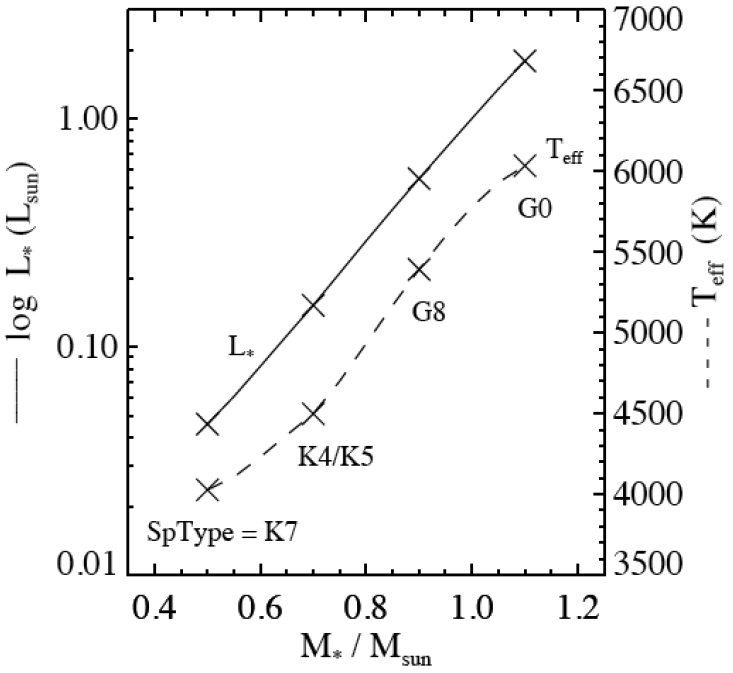

Mass ($M_\odot$)	Radius ($R_\odot$)	L_* ($L_\odot$)	$T_{\rm eff}$ (K)	SpT	$M_{\rm cz}$ ($M_\odot$, M_*)	$R_{\rm cz}$ ($R_\odot$, R_*)
0.5	0.44	0.046	4030	K7	0.18, 0.36	0.25, 0.56
0.7	0.64	0.15	4500	K4/K5	0.079, 0.11	0.42, 0.66
0.9	0.85	0.55	5390	G8	0.042, 0.046	0.59, 0.69
1.1	1.23	1.79	6030	G0	0.011, 0.0100	0.92, 0.75

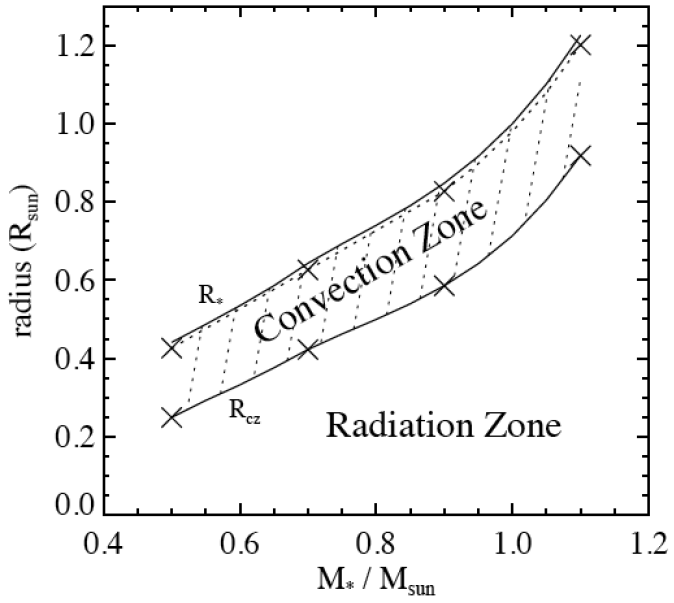

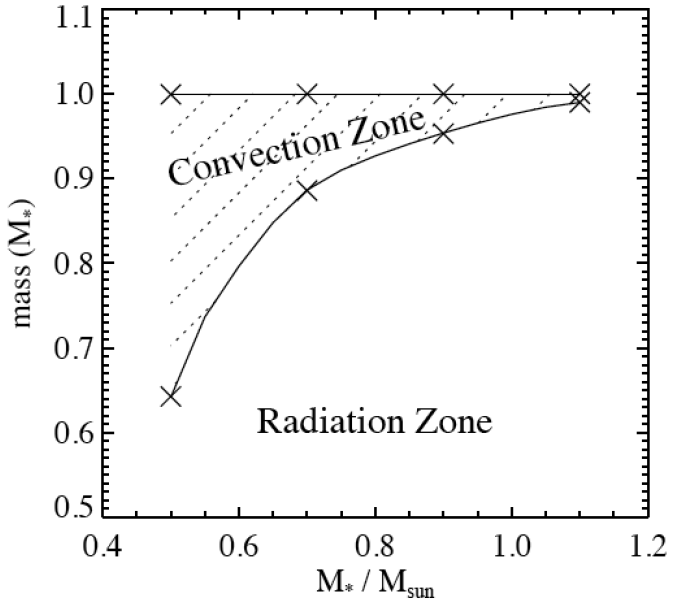

Effect of Rotation on Convection

Matt, DoCao, Brun et al. 2011, 2013

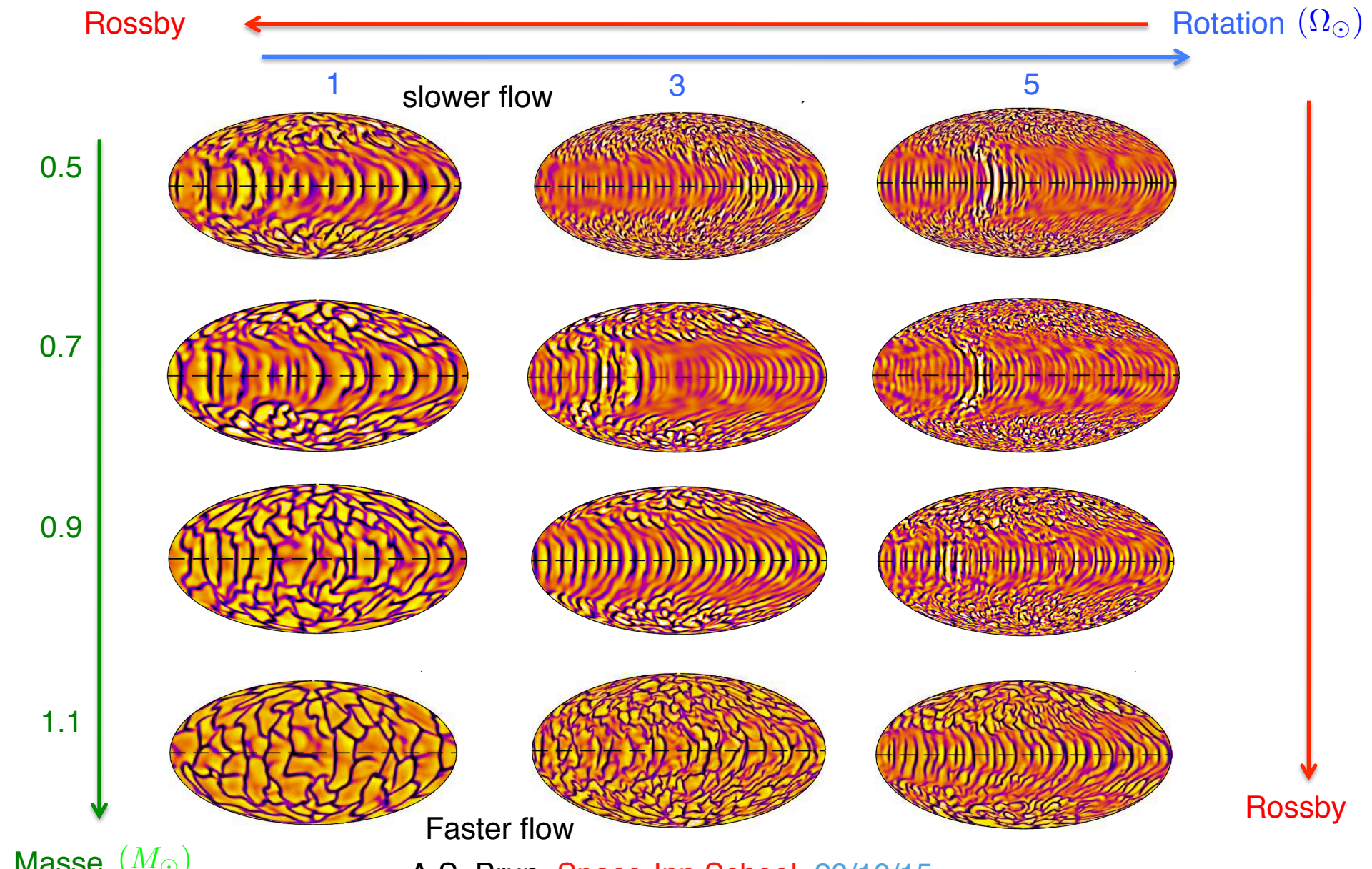

Turbulent Convection in Stars

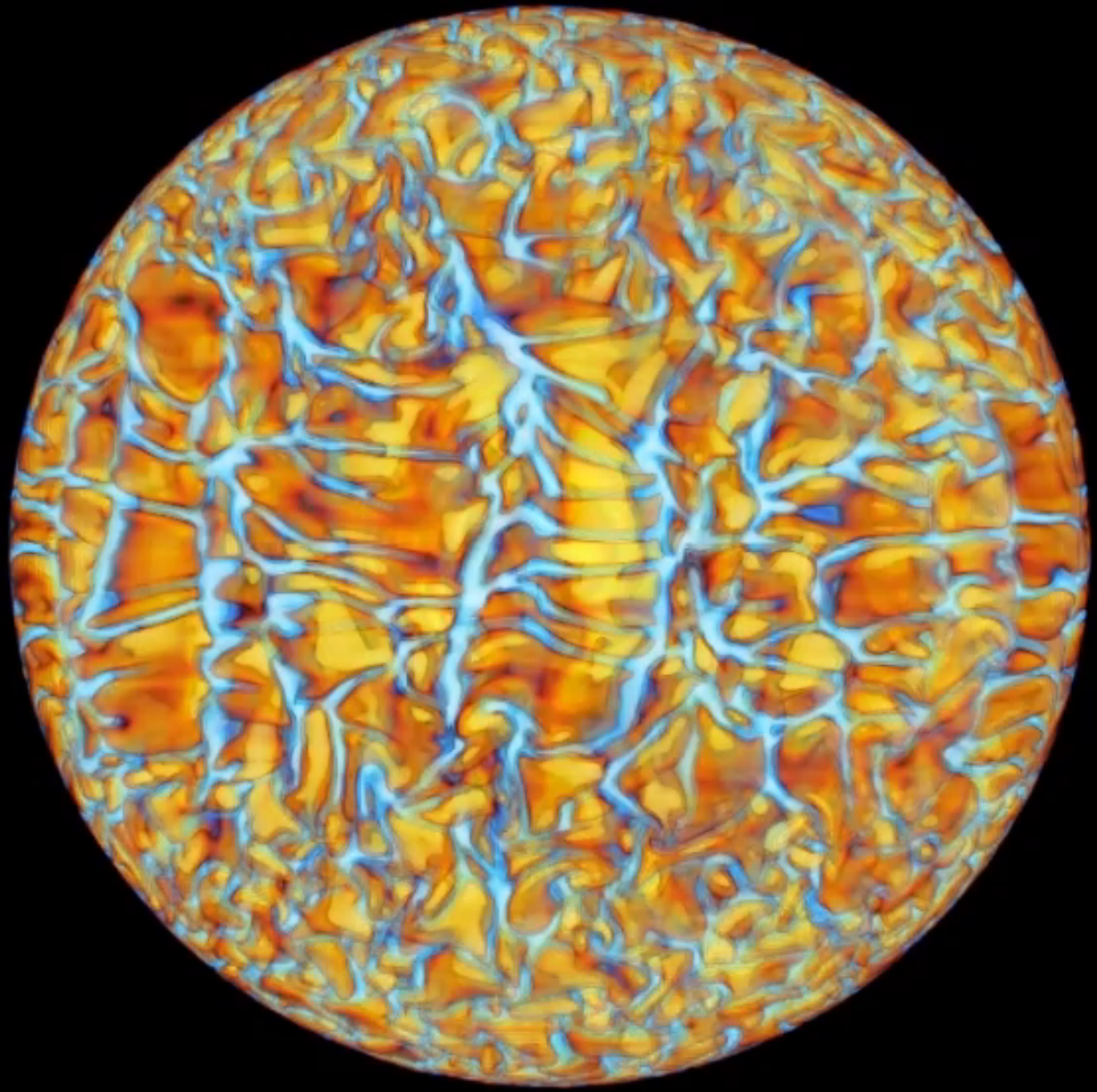

Bessolaz & Brun 2011

Trends in Differential Rotation with Ω & Mass (Teff)

Weak trend with Ω

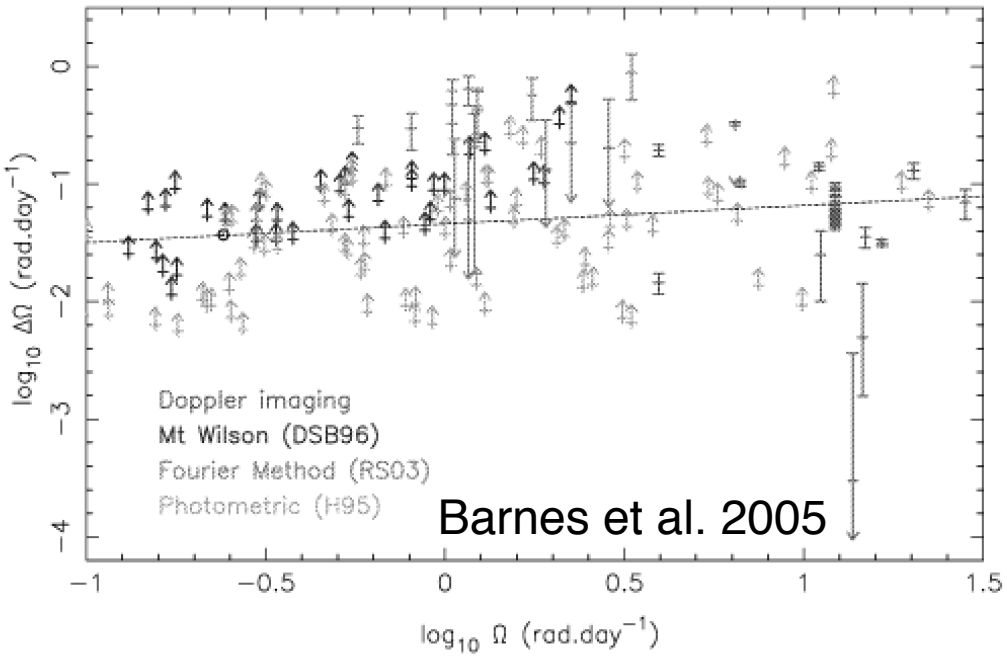

ΔΩ increases with M*

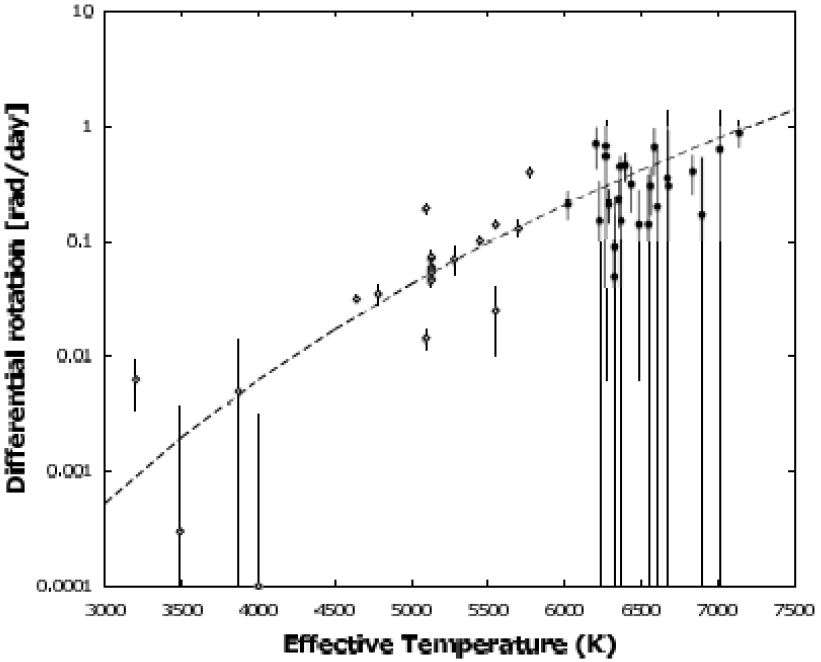

Collier-Cameron 2007

In Donahue et al. 1996: ΔΩ propto $\Omega^{0.7}$

Confirming these observational scaling is key

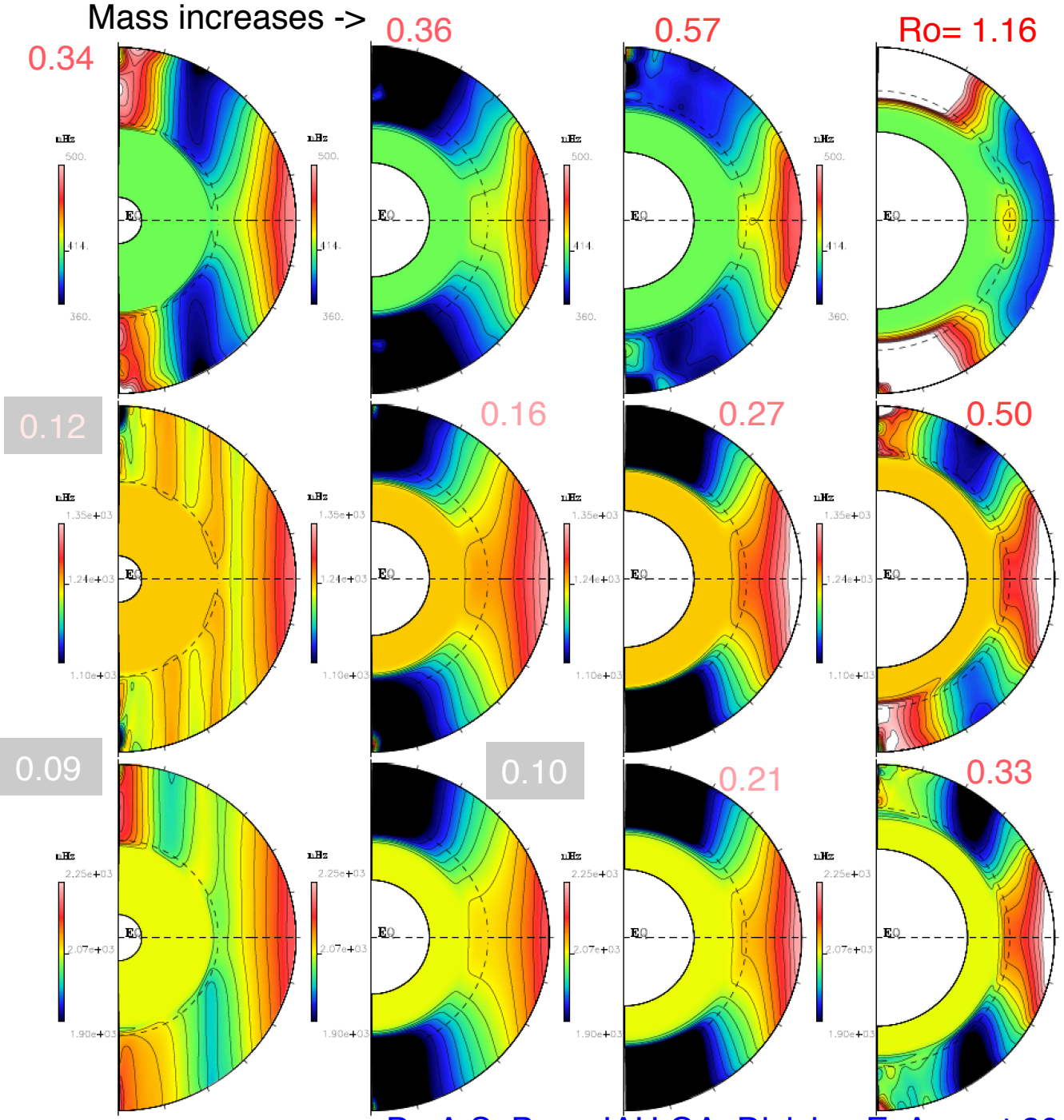
Mass increases ->
0.34
0.36
0.57
Ro= 1.16
0.12
0.16
0.27
0.50
0.09
0.10
0.21
0.33
Differential Rotation
In G & K stars
Ω
Matt et al. 2011,
Brun et al. 2015
Rotation
Increases
Rossby nb
Ro=ω/2Ω*
5 Ω

Scaling Law for $\Delta\Omega$

Matt et al. 2011; Brun et al. 2015

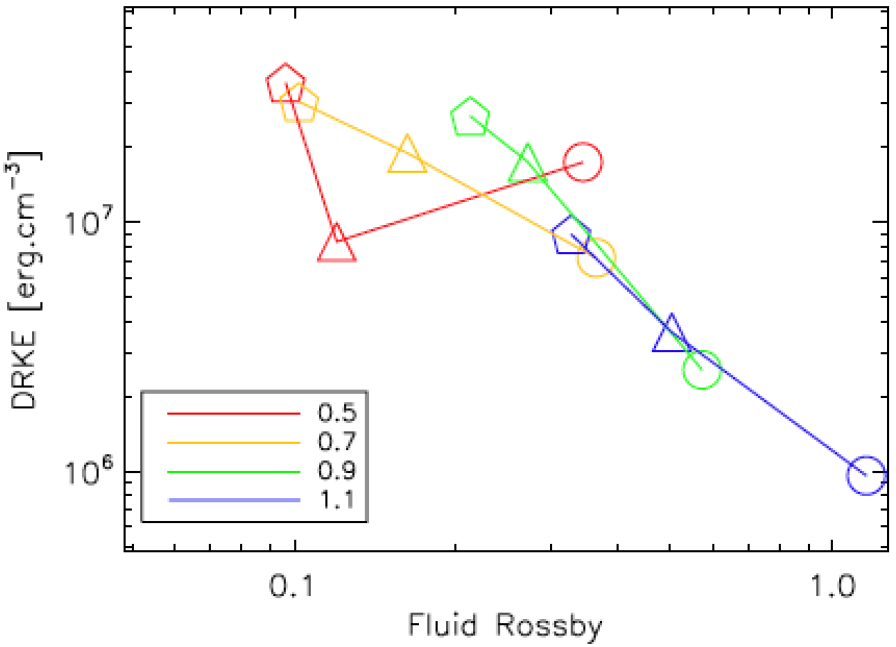

1.2, 1.3 M

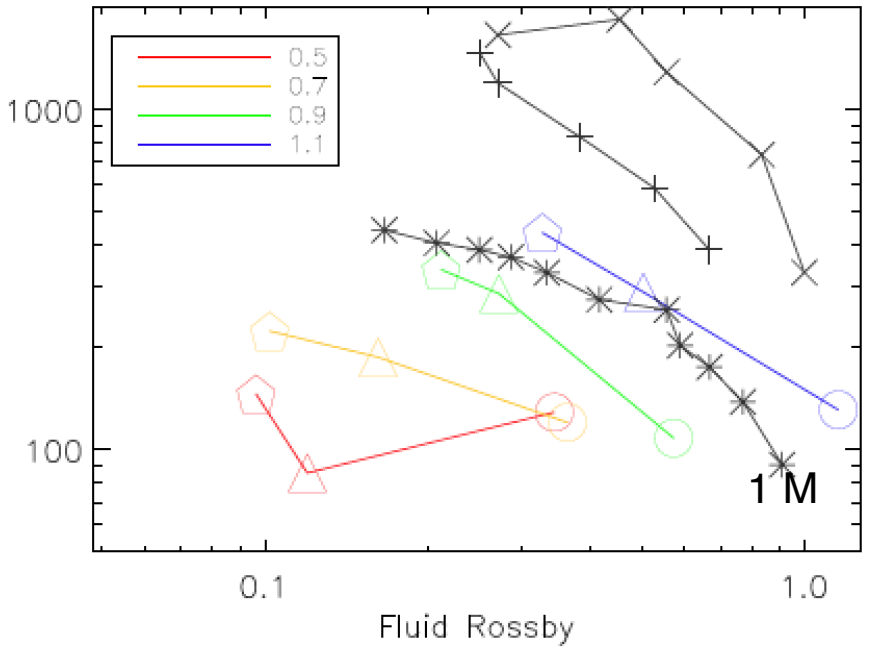

Brown et al. 2008
Augustson et al. 2012

$$\Delta\Omega = 156.0\ \mathrm{nHz} \left(\frac{\mathrm{M}}{\mathrm{M}_\odot}\right)^{1.0} \left(\frac{\Omega_0}{\Omega_\odot}\right)^{0.47}$$

$$= 150.3\ \mathrm{nHz} \left(\frac{\mathrm{M}}{\mathrm{M}_\odot}\right)^{1.85} \mathrm{R}_{\mathrm{of}}^{-0.52}$$

Smaller $\Delta\Omega$ with smaller Mass

Rossby Number vs Stellar Mass and Rotation

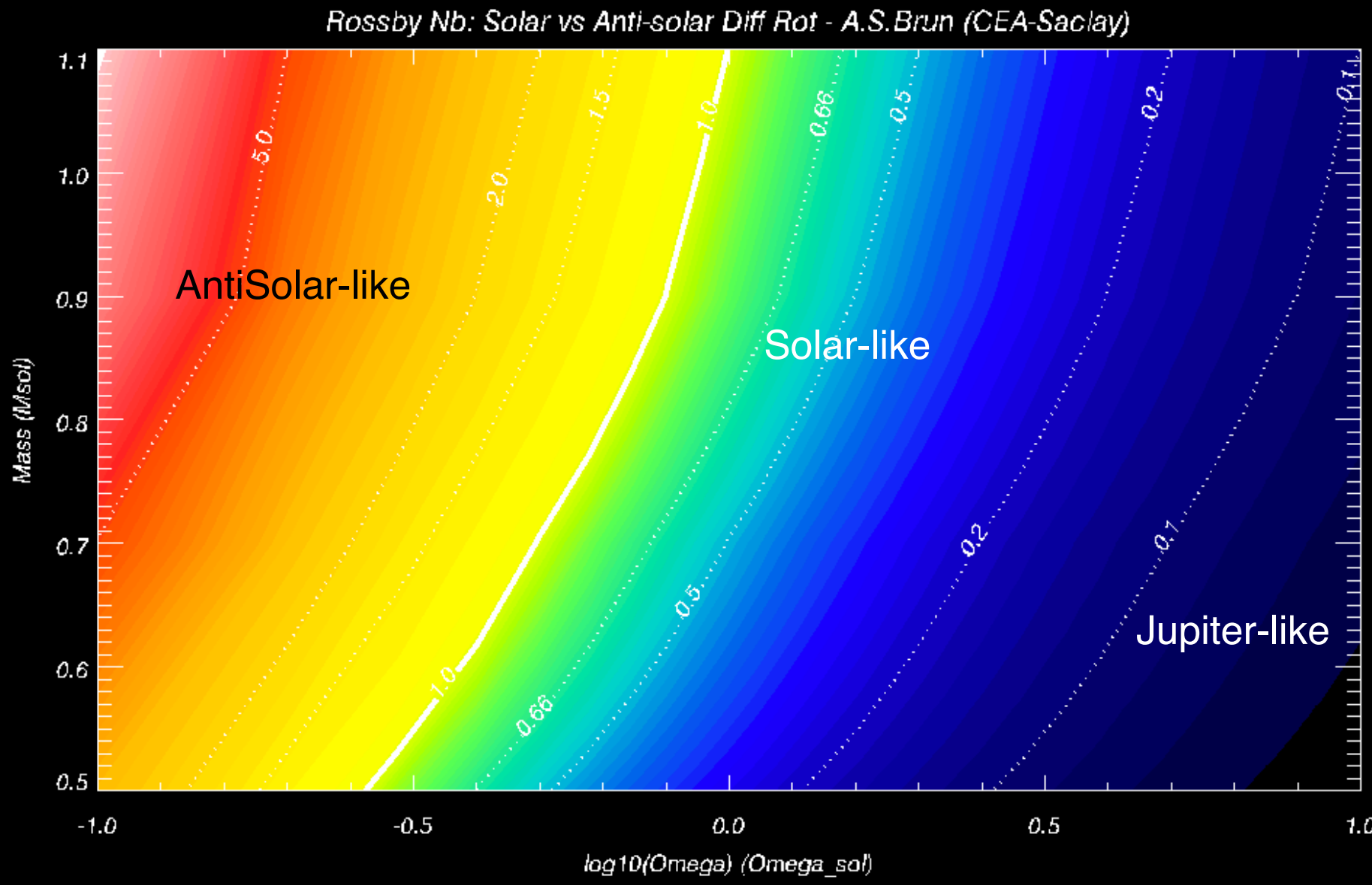

Brun et al. 2014, 2015

Maintenance of Differential Rotation

d KE_tor/dt = Q_reynolds + Q_coriolis – Q_viscous

0.5 M – 1 Ω

integrated DRKE = 1.5901175e+39
integrated d/dt DRKE = 4.6470157e+30
DRKE / d/dt DRKE [days] = 3960.4207

Coriolis term/Lstar = 0.037586119
Reynolds term/Lstar = 0.16090859 16%
viscous loss/Lstar = -0.16390712

0.5 M – 3 Ω

integrated DRKE = 9.0776181e+38
integrated d/dt DRKE = 9.4017225e+30
DRKE / d/dt DRKE [days] = 1117.5082

Coriolis term/Lstar = 0.010619773
Reynolds term/Lstar = 0.23647836 23%
viscous loss/Lstar = -0.18979752

1.1 M – 1 Ω

integrated DRKE = 1.4332822e+39
integrated d/dt DRKE = 7.7483491e+31
DRKE / d/dt DRKE [days] = 214.09611

Coriolis term/Lstar = 0.019980844
Reynolds term/Lstar = 0.018322031 1.8%
viscous loss/Lstar = -0.031056443

More of the energy (Luminosity) of the star goes into maintaining the Differential Rotation as a fct of increasing rotation rate but decreasing mass.

Matt, DoCao Brun 2013
See also Nelson et al. 2013, Rempel 2005, 2006

Profile and Amplitude of Meridional Flow

Matt, Brun et al. 2011, 2013

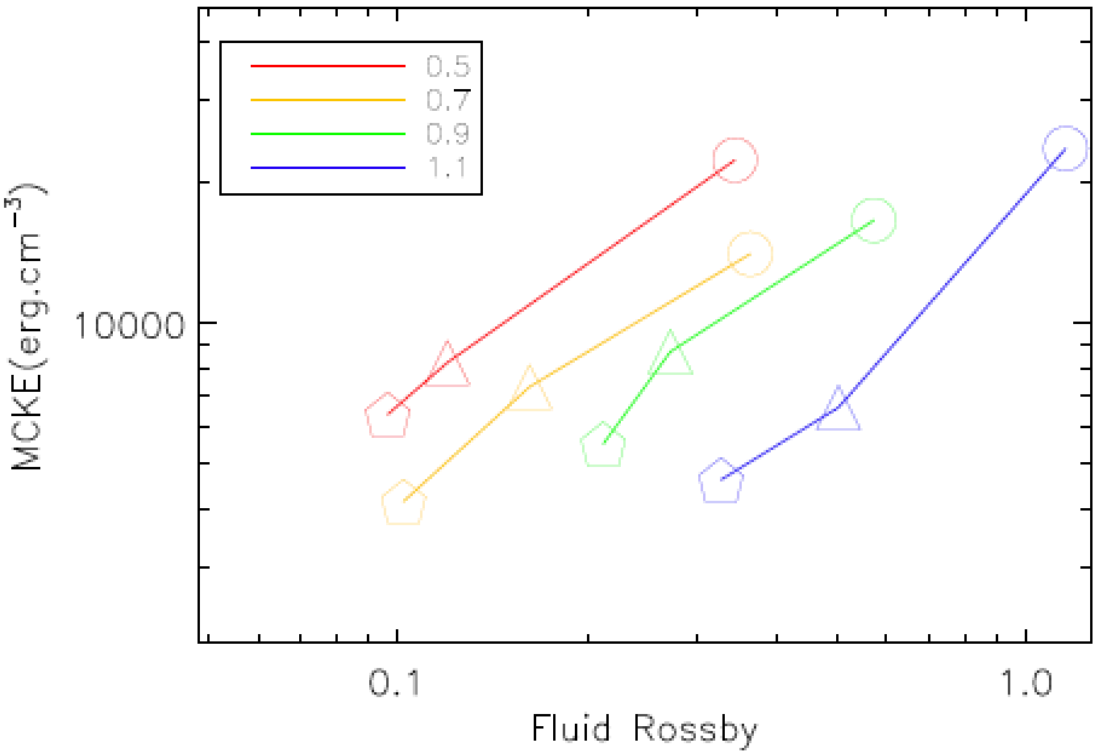

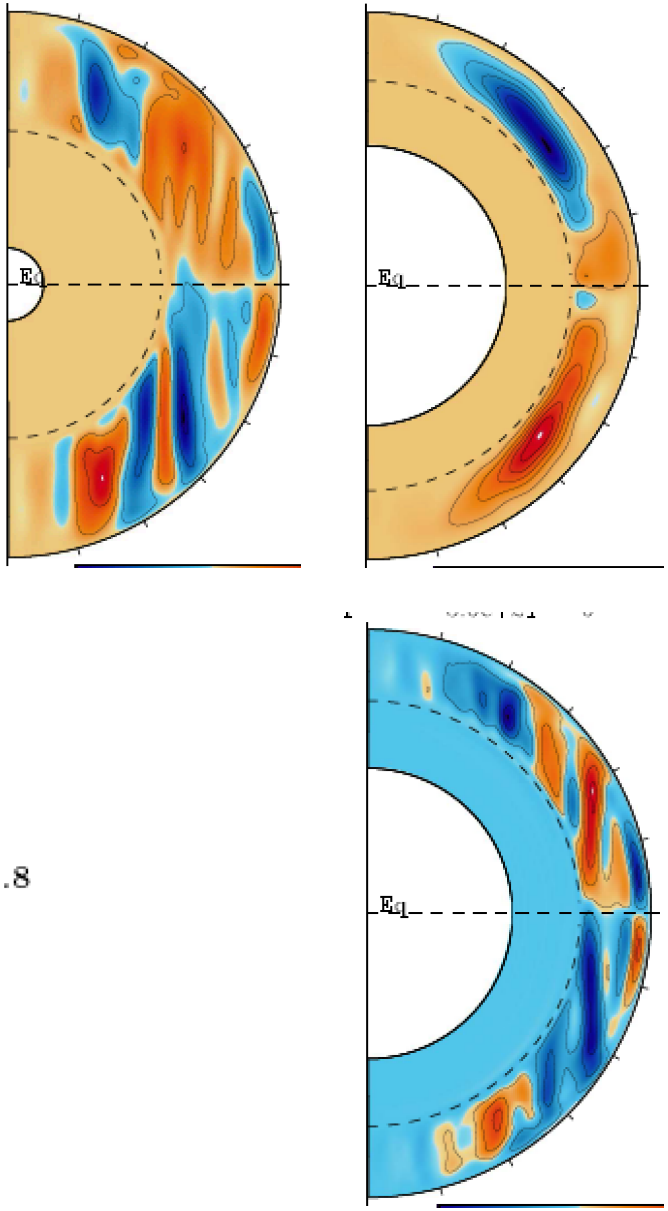

$$\mathrm{MCKE} = 1.8 \times 10^4 \ \mathrm{erg.cm^{-3}} \left(\frac{\mathrm{M}}{\mathrm{M}_\odot}\right)^{-0.14} \left(\frac{\Omega_0}{\Omega_\odot}\right)^{-0.8}$$

$$= 2.1 \times 10^4 \ \mathrm{erg.cm^{-3}} \left(\frac{\mathrm{M}}{\mathrm{M}_\odot}\right)^{-1.8} \mathrm{R}_{\mathrm{of}}^{1.0}$$

Testing Babcock-Leighton Models with Stellar Magnetism Data

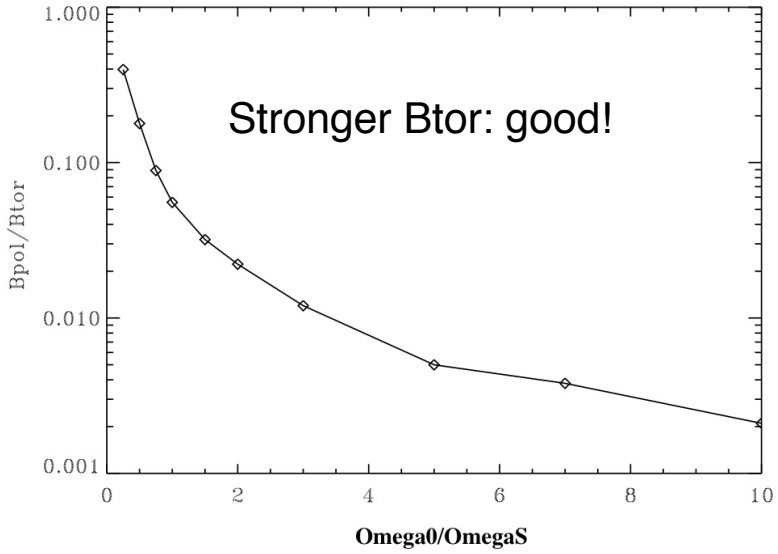

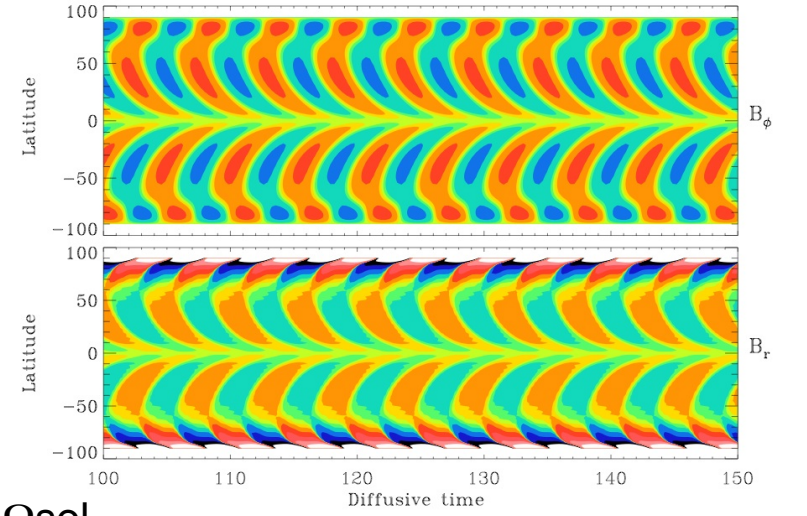

0.5 Ωsol

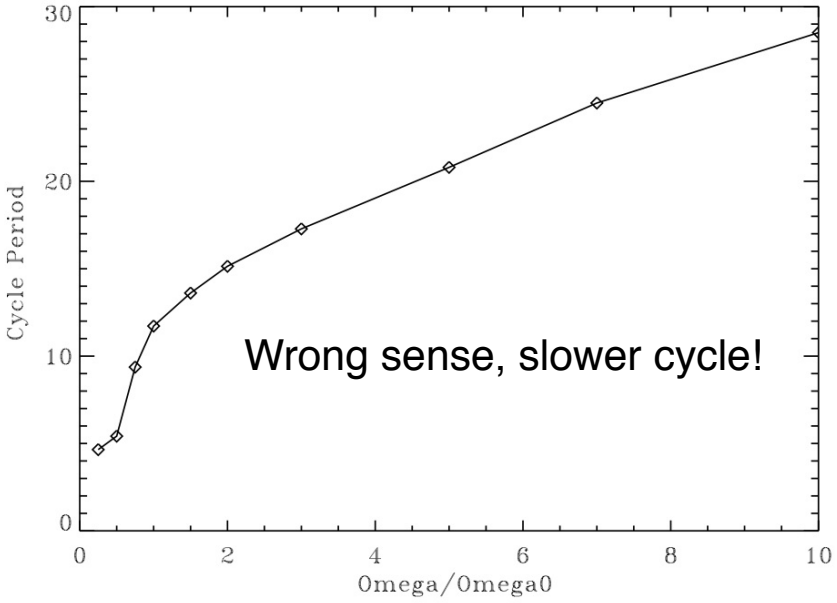

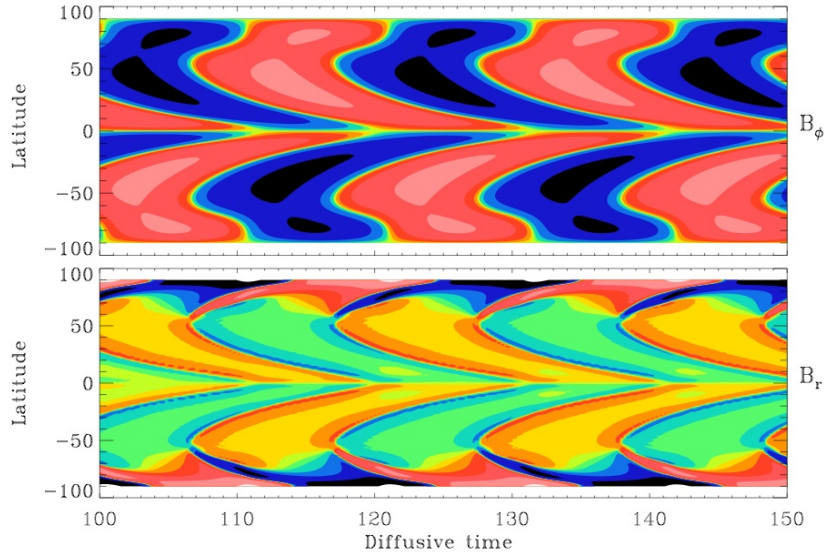

5 Ωsol

Pcyc = 20 yr!

Jouve, Brown, Brun, A&A 2010

Testing Babcock-Leighton Models with Stellar Magnetism Data

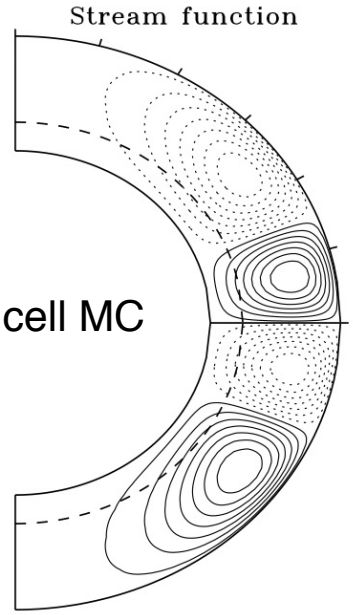

Multi cell MC

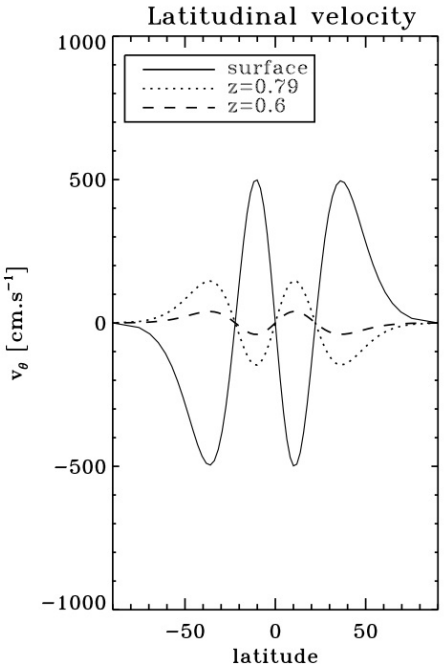

We have seen in the solar case that MC profile greatly influences the cycle and butterfly diagram. Can we reconcile stellar data with more complex MC?

Pcyc = 5.2 yr !!!! success

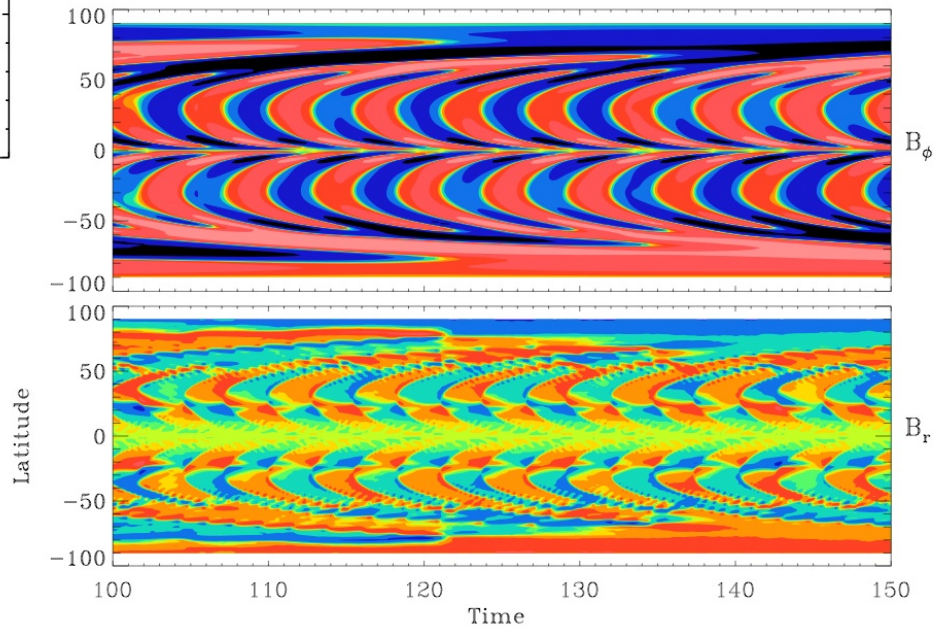

See also talk
C. Dubé

Jouve, Brown, Brun, A&A 2010

5 Ωsol

Alternative solution: Turbulent Pumping (implies a weaker dependancy of Pcyc to MC)
see Guerrero et al. (2008) and DoCao & Brun (2011)

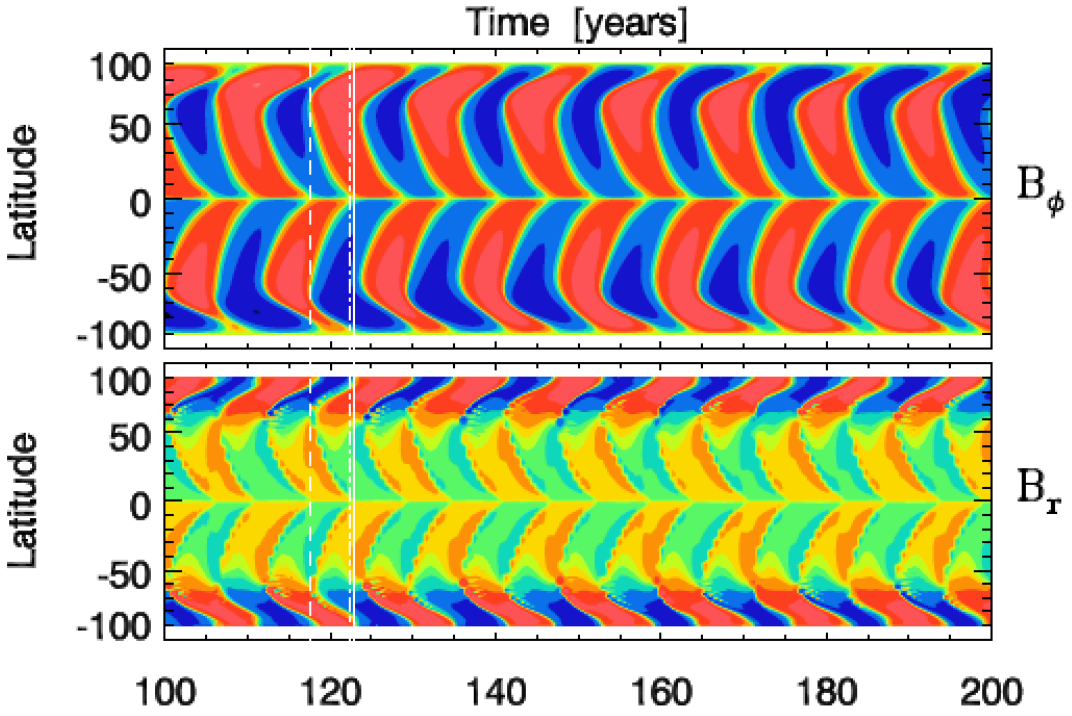

Another Option to make cycle faster:
Turbulent Pumping

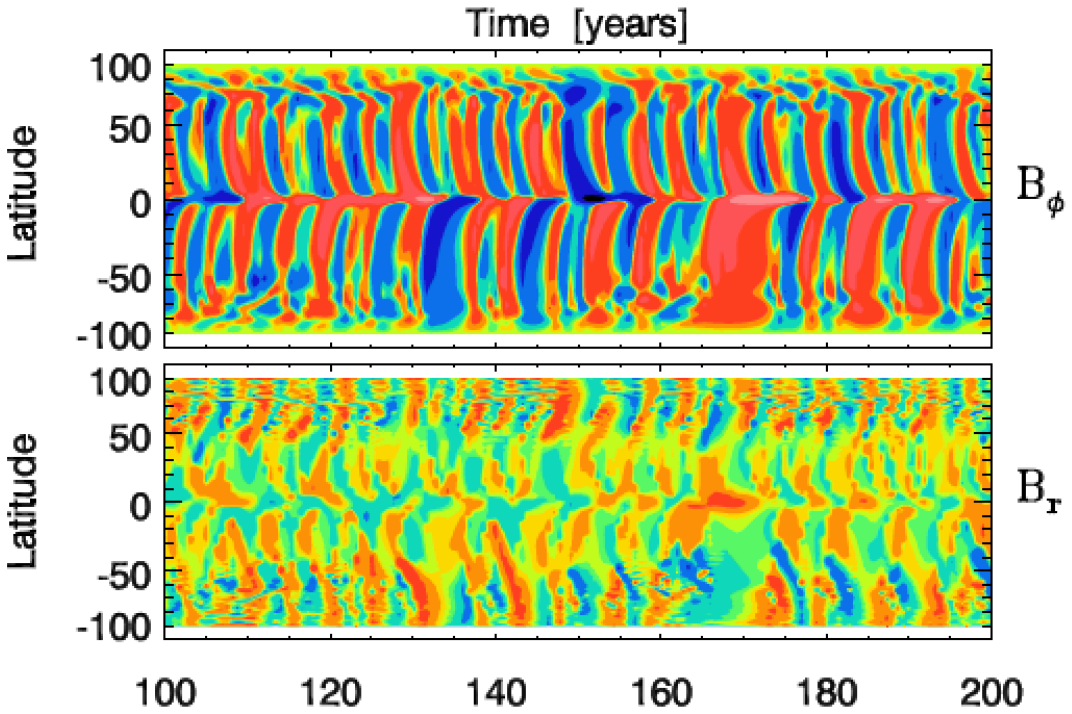

DoCao & Brun 2011

$$P_{\rm cyc} \propto v_0^{-0.40} \gamma_{r0}^{-0.30} \gamma_{\theta 0}^{-0.15}$$

See also Guerrero et al. 2008

Magnetic Wreaths vs Turbulence

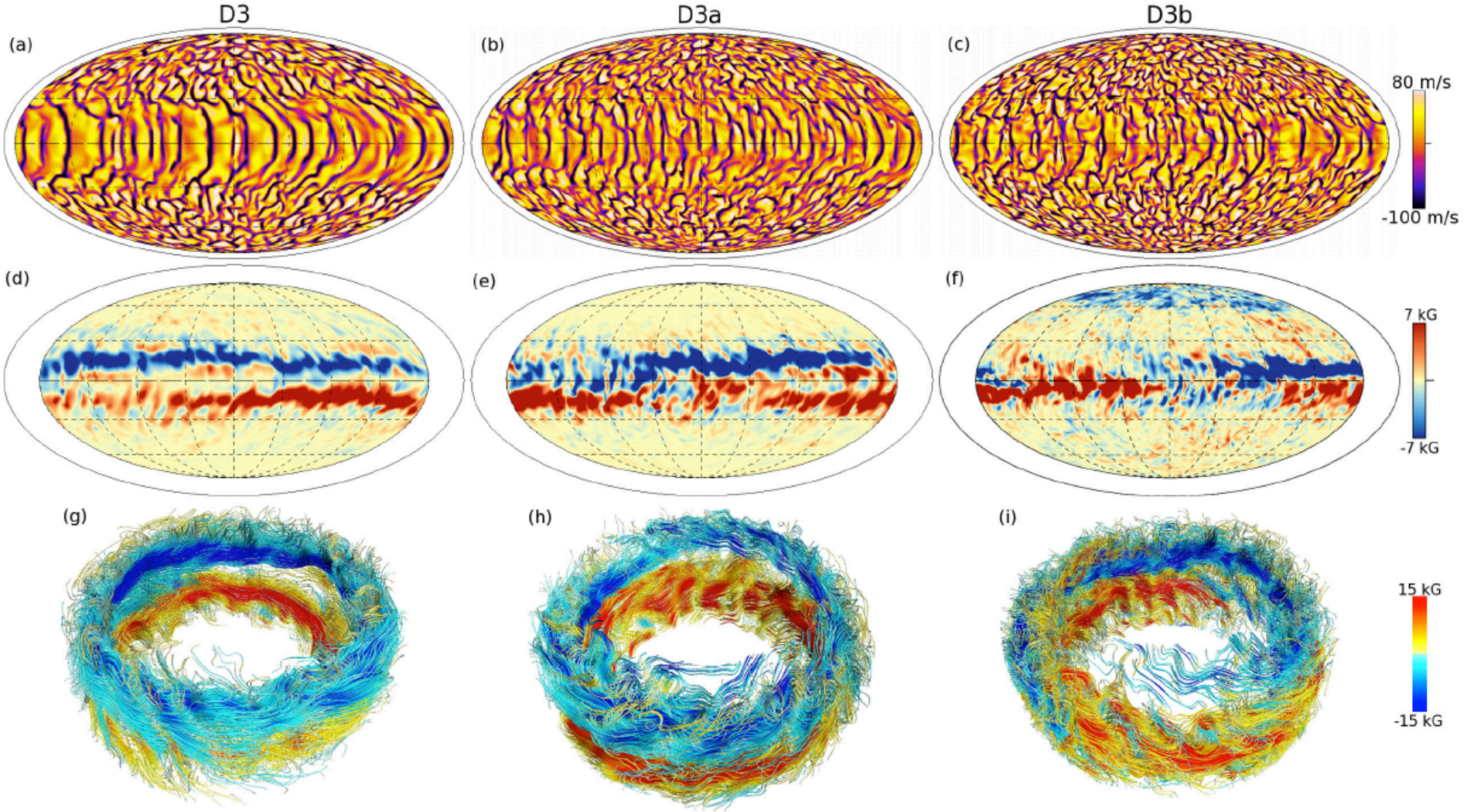

Nelson et al. 2013a

Magnetic Cycles and Torsional Oscillations

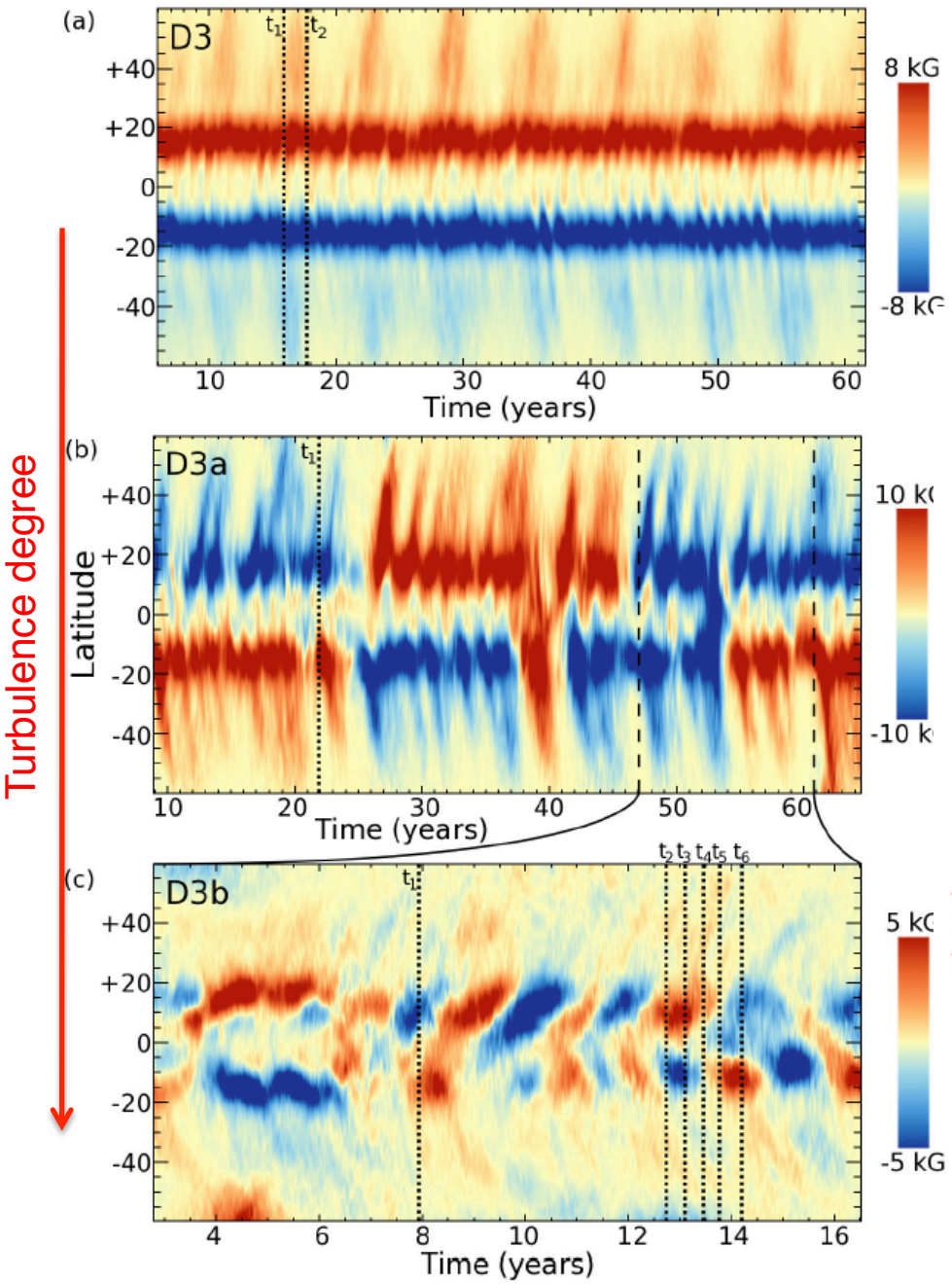

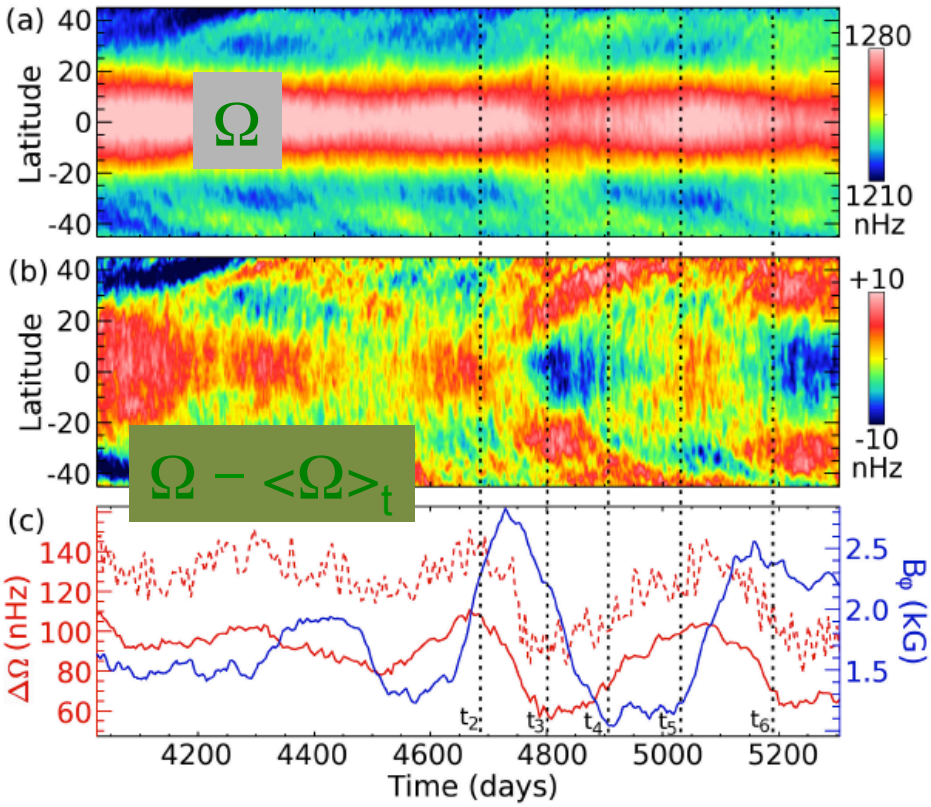

Brown et al. 2011, Nelson et al. 2012

Current best solar-like case: getting cycle and equatorward branch

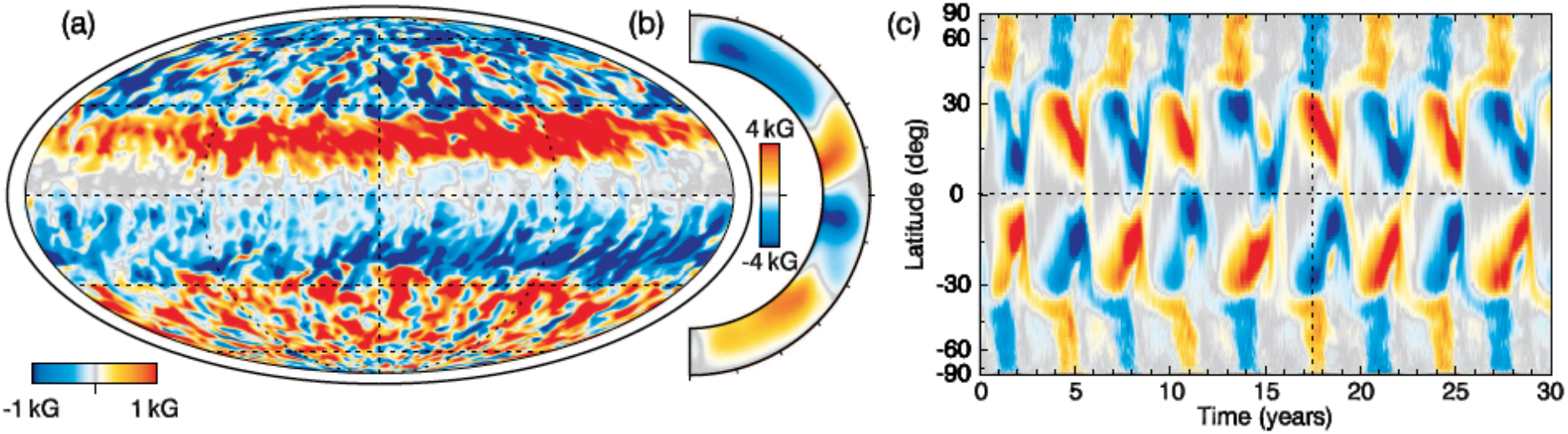

Reducing nu even further nu by using SLD scheme makes the simulation develop a more regular cyclic behavior

Augustson, Brun et al. 2015, ApJ, in press

Origin of Poloidal Field Reversal

$$\Delta\langle A_\varphi\rangle = \langle A_{\varphi,2}\rangle - \langle A_{\varphi,1}\rangle = \{\mathcal{E}'_\varphi\} + [\mathcal{E}_\varphi] + \eta\{J_\varphi\}$$

$$= \int_{t_1}^{t_2} dt\,\hat{\boldsymbol{\varphi}}\cdot\langle \mathbf{v}'\times\mathbf{B}'\rangle + \int_{t_1}^{t_2} dt\,\hat{\boldsymbol{\varphi}}\cdot\big(\langle\mathbf{v}\rangle\times\langle\mathbf{B}\rangle\big) - \int_{t_1}^{t_2} dt\,\eta\langle J_\varphi\rangle .$$

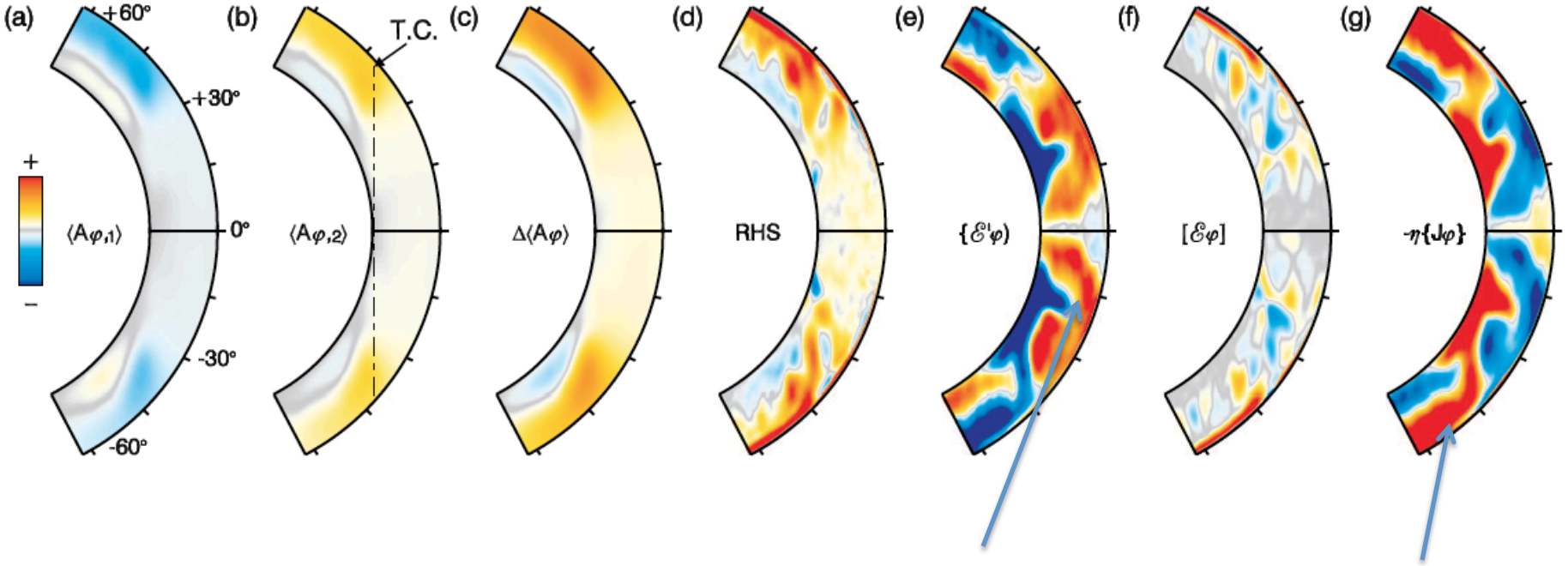

Fluctuating Emf key term

some contribution from diffusion term at high latitudes

Parker-Yoshimura Rule

In kinematic theory the propagation direction of such a wave is given by the Parker-Yoshimura rule (e.g., Parker 1955; Yoshimura 1975) as

$$\mathbf{S} = -\lambda \overline{\alpha} \hat{\varphi} \times \nabla \frac{\Omega}{\Omega_0}, \qquad (19)$$

where $\lambda = r \sin\theta$ and $\overline{\alpha} = -\tau_o \langle \mathbf{v}' \cdot \boldsymbol{\omega}' \rangle / 3$. Thus $\overline{\alpha}$ depends on the convective overturning time τ_o and the kinetic helicity.

uncorrect sign

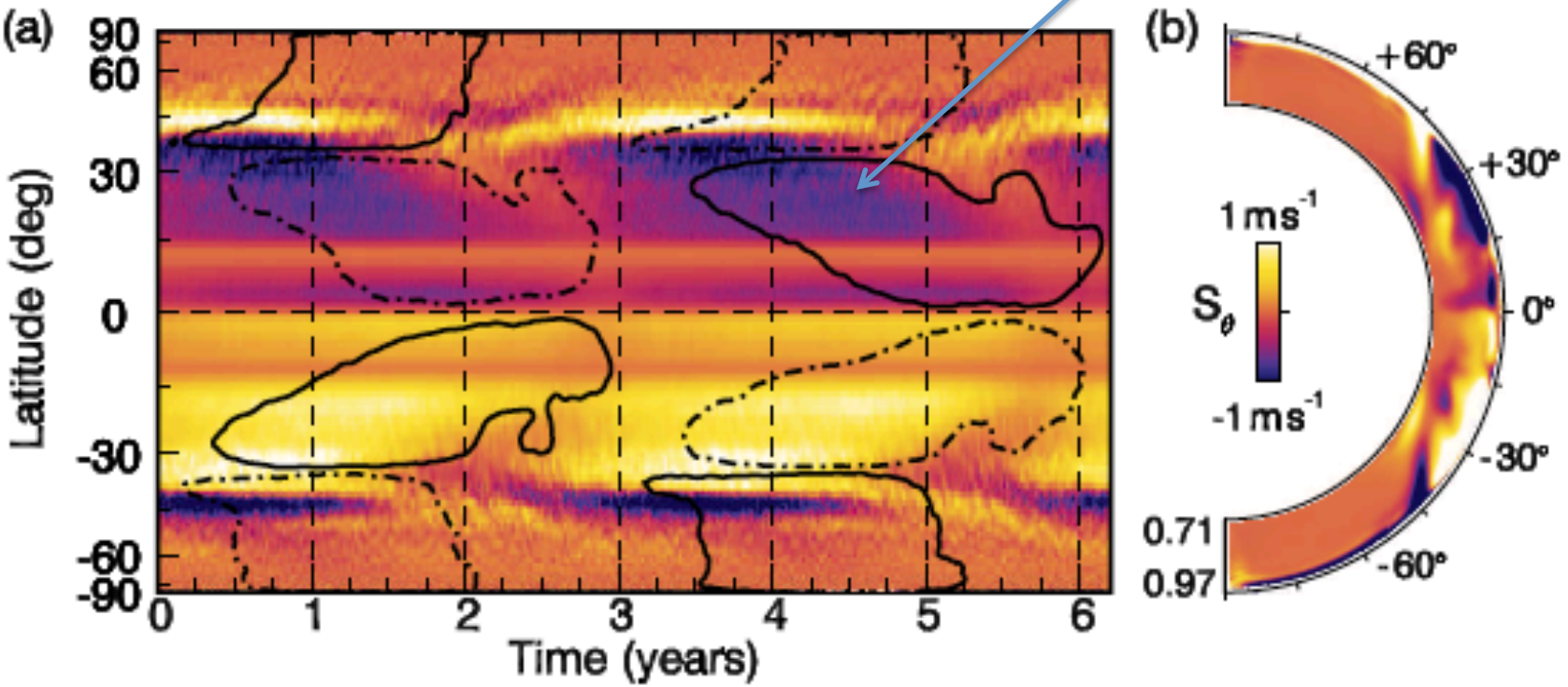

Non-linear dynamo wave

Correct sign

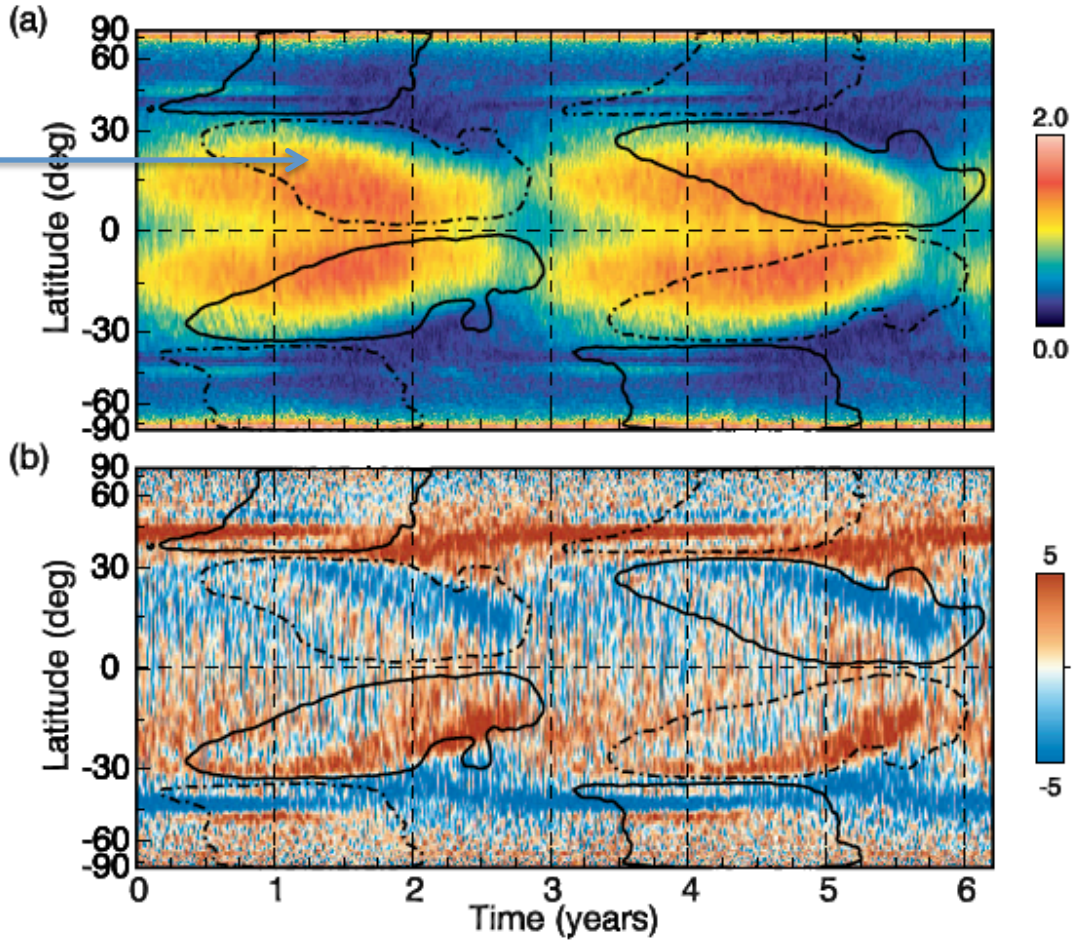

Interaction between Shear and Bphi

Figure 11. Coevolution of the mean toroidal magnetic field $\langle B_\varphi \rangle$ at $0.92\,R_\odot$ over the average magnetic polarity cycle with (a) the magnitude of the mean angular velocity gradient $R_\odot|\nabla\Omega|/\Omega_0$ and (b) latitudinal velocity $\langle v_\theta \rangle$ of the evolving meridional circulation in units of $m\,s^{-1}$. Here $\langle B_\varphi \rangle$ is overlain with positive magnetic field as solid lines and negative field as dashed lines, with the contours corresponding to a 1 kG strength field.

Current best solar-like case
Getting Maunder like minimun

See Kyle Augustson talk

Quadrupole dominates over Dipole during reversal and Grand minimum phase

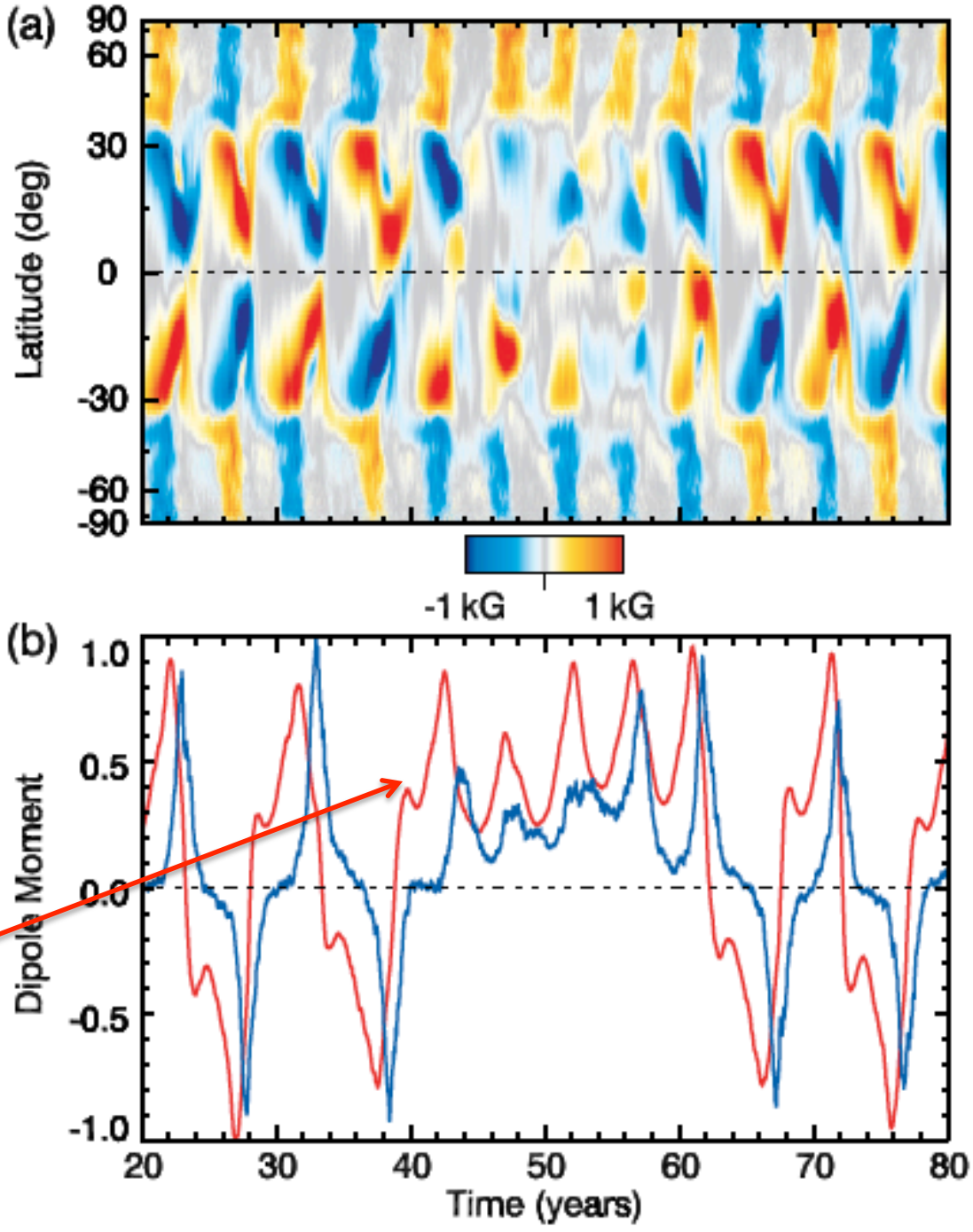

Augustson, Brun et al. 2013, ApJL

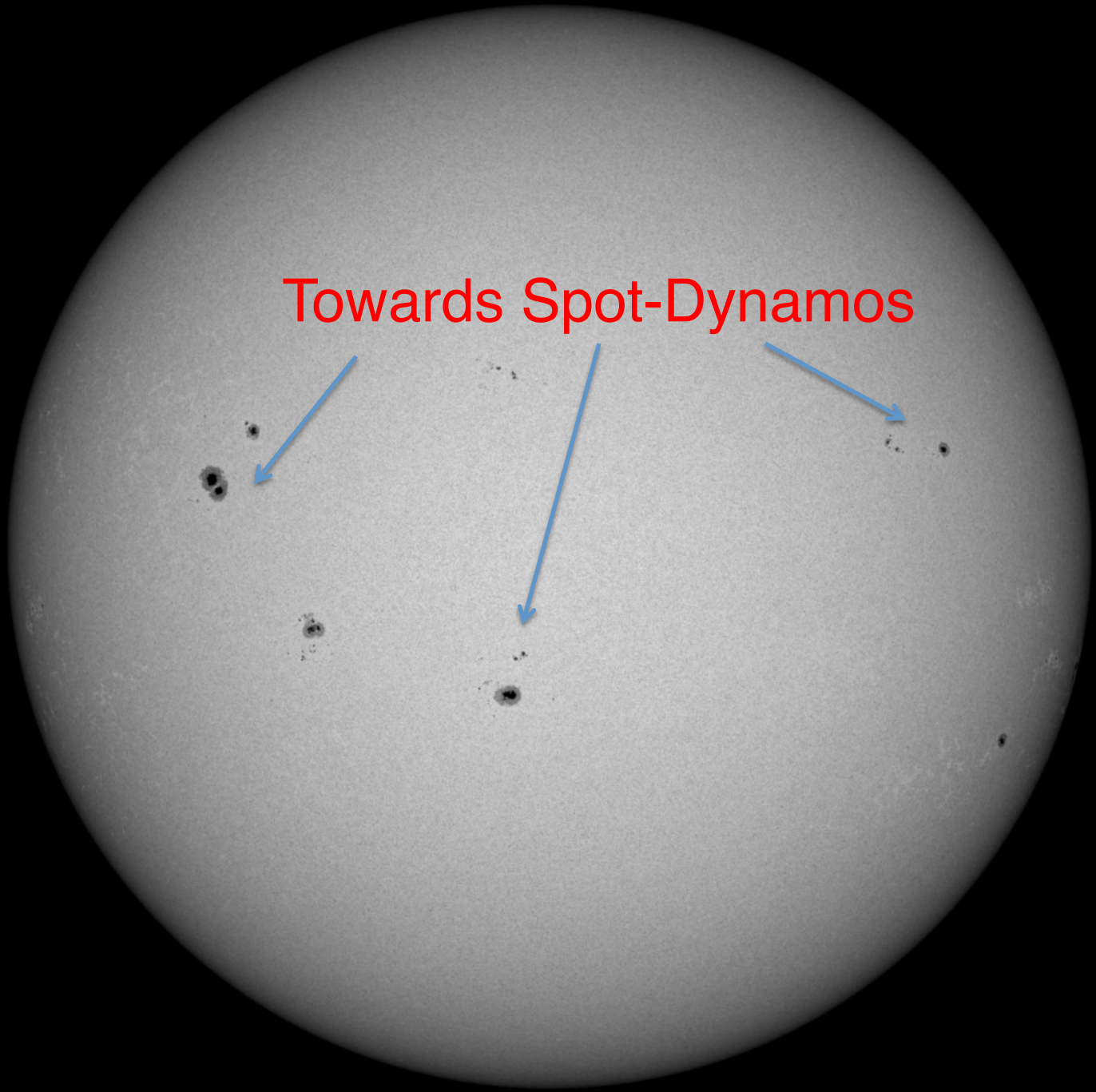
Towards Spot-Dynamos
SDO/HMI Quick-Look Continuum: 2013.12.12_21:16:30_TAI

Magnetic Wreath and Intermittency yielding flux emergence

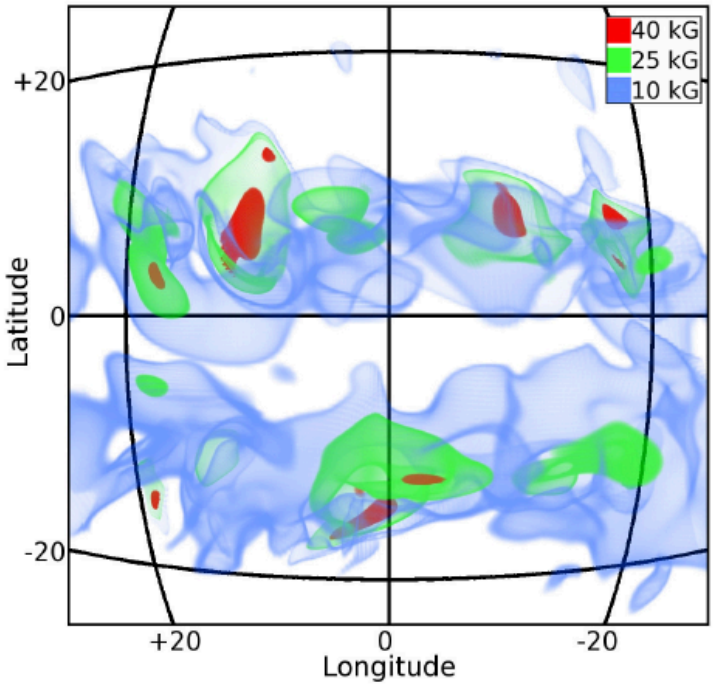

Figure 17. Three-dimensional volume renderings of isosurfaces of magnetic field amplitude in case S3. Blue surfaces have amplitudes of 10 kG, green surfaces represent 25 kG, and red surfaces indicate 40 kG fields. Grid lines indicate latitude and longitude at 0.72 $R_\odot$ as they would appear from the vantage point of the viewer. Small portions of the cores of these wreaths have been amplified to field strengths in excess of 40 kG while the majority of the wreaths exhibit fields of about 10 kG or roughly in equipartition with the mean kinetic energy density (see Figure 2).

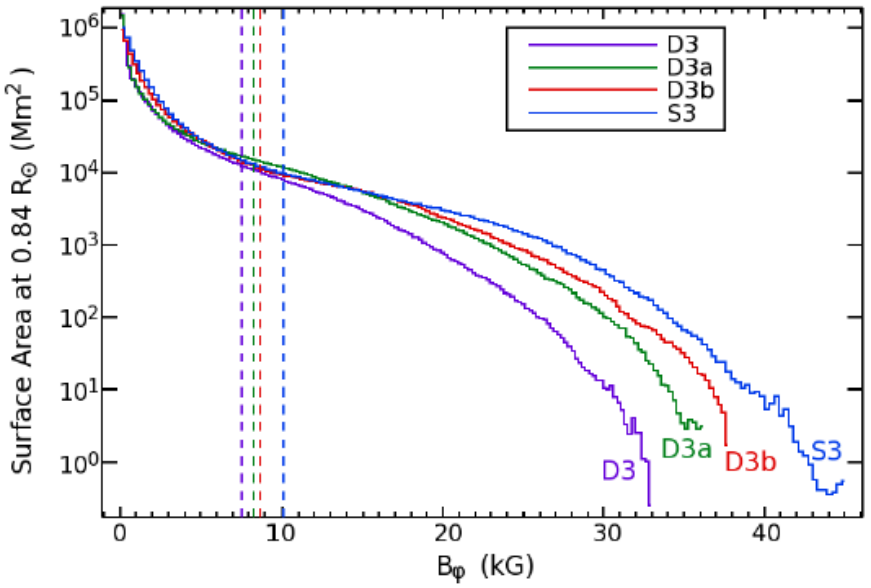

Figure 2. Probability distribution functions for unsigned B_ϕ at mid-convection zone for cases D3 (purple), D3a (green), D3b (red), and S3 (blue) showing the surface area covered by fields of a given magnitude. Distributions are averaged over about 300 days when fields are strong and as steady as possible. Dashed vertical lines show the field-strength at which equipartition is achieved with the maximum fluctuating kinetic energy (FKE) at mid-convection zone for each case. Case D3b shows a deficit of field in the 10 kG range, but an excess of surface area covered by extremely strong fields above 25 kG range, as well as higher peak field strengths. Case S3 shows significantly greater regions of fields in excess of 20 kG than all other cases.

Nelson et al. 2013, ApJ

Wreaths can generate Buoyant Loops

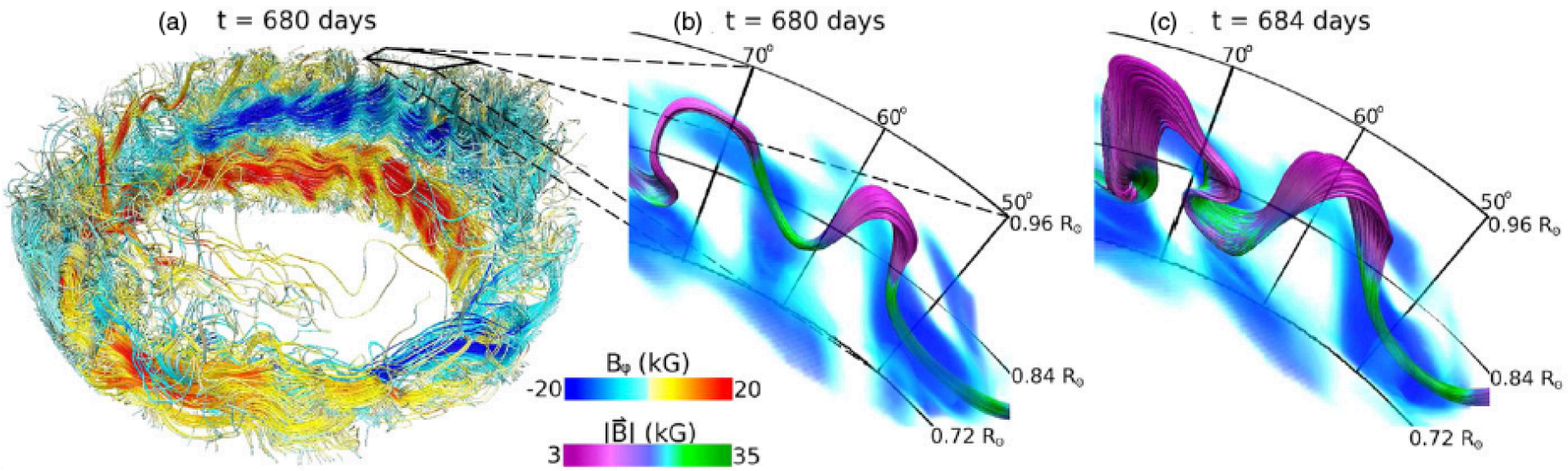

Nelson et al. 2011, 2013a, 2013b

Towards getting first “spot-dynamos”…

Statistic of Buoyant Loops

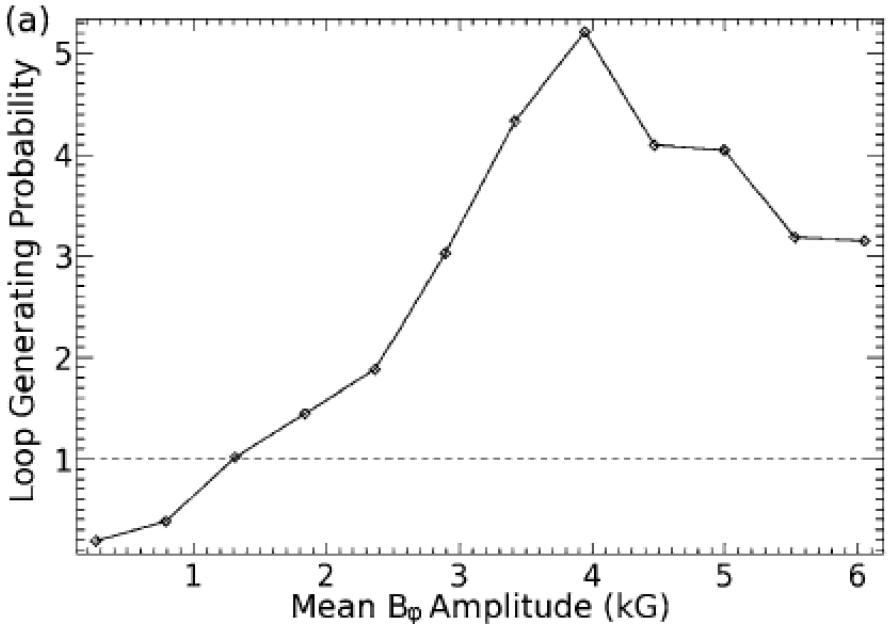

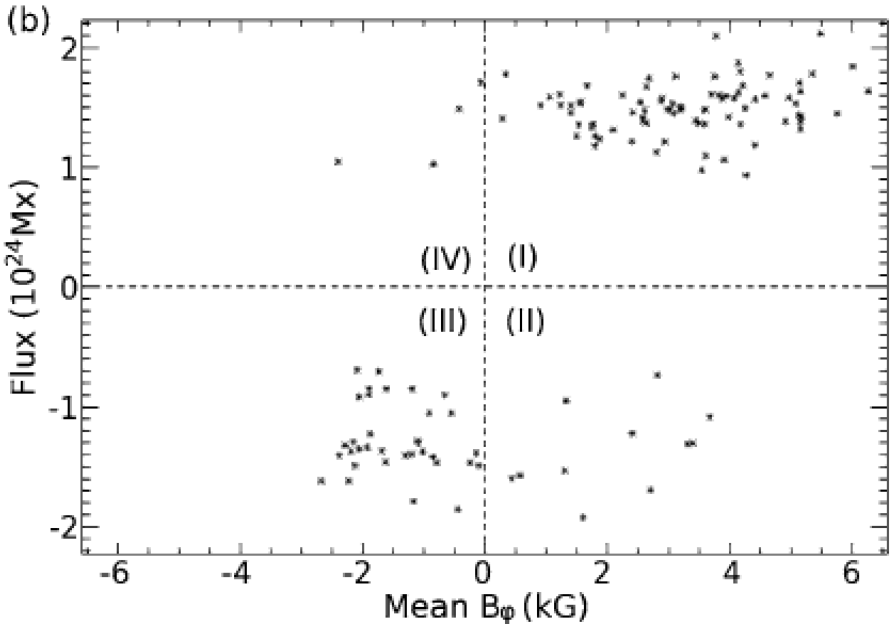

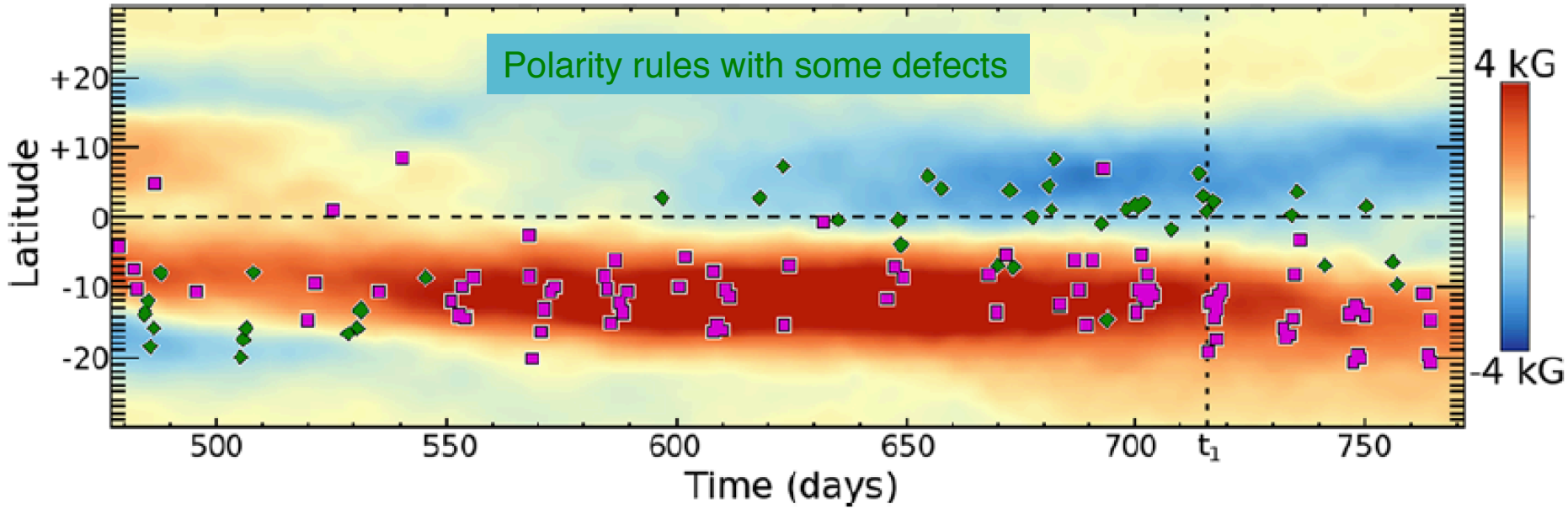

Nelson et al. 2013b

Conclusions

Convective velocities Vr roughly scales with cubic root of L/ρ_{meanCZ}
(star's luminosity devided by mean density in CZ)

$\Rightarrow$ Prograde vs retrograde state changes at different Ω_0
as spectral type is changed (since $Ro=V/2\Omega_0 L$ and V changes with spectral type)

$\Rightarrow$ Cylindrical vs conical vs shellular differential profiles
depends on Reynolds stresses & thermal (baroclinic)
effects/tachocline

$\Rightarrow$ Magnetic field B reduces or can even supress diff rot Ω

$\Rightarrow$ at high rotation rate we get magnetic wreaths that generate omega-loops as we lower diffusivity, cyclic dynamos easier to get

$\Rightarrow$ Multipolar or Dipolar magnetic bi-stability exist but
Multipolar fields seem to dominate at high stratification

$\Rightarrow$ Stratification and/or a tachocline may help getting equatorward
butterfly diagram (shift location of Ω and α-like effects)

STARS² project: Understanding Stellar Dynamics and Magnetism

3D MHD
High Performance
Simulations

Asterosismology/Magnetism
SoHO/Corot/Espadon/XMM

(Brun et al. 2002, 2004, 2005, 2006, 2007, Ballot et al. 2007, Browning et al. 2004, Jouve & Brun 2007 a,b, Zahn, Brun & Mathis 2007, Brown et al. 2007)

Massive Stars

Sun

Evolved Stars (RGB)

Young Suns

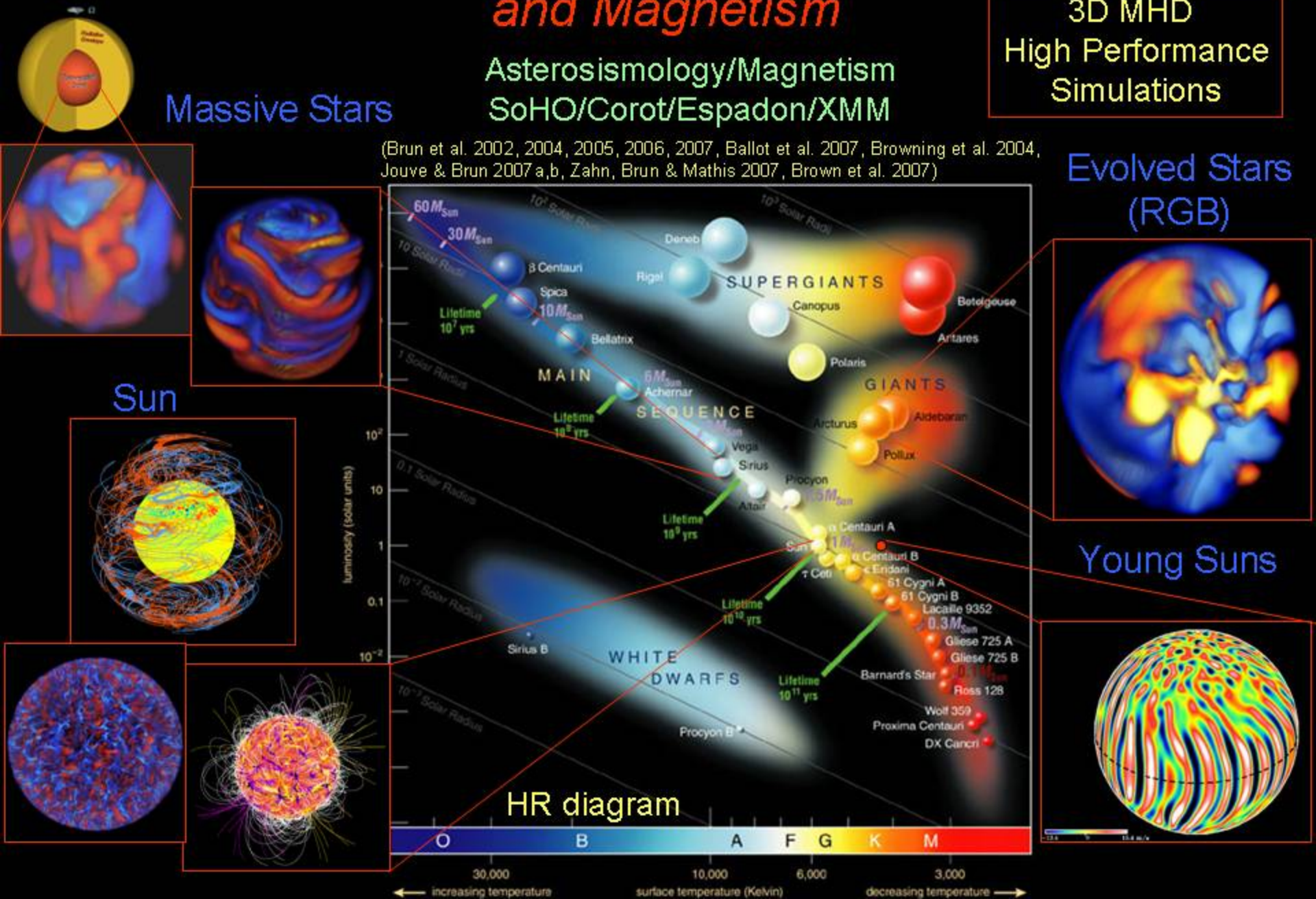

International Astronomical Union Symposium 328

Living Around Active Stars

Maresias, Brazil

17-21 October, 2016

iaustars328@gmail.com

Topics

Solar and Stellar Magnetism
Irradiance and Luminosity Variations
Solar and Stellar Winds
Extreme Events (Flares and Energetic Particles)
Heliosphere and Astropheres
Stellar Forcing of Planetary Atmospheres
Coupled Star-Planet Evolution
Space Climate Consequences
Exoplanets
Habitability

SOC Chairs

Dibyendu Nandi (India)
Sarah Gibson (USA)
Pascal Petit (France)

LOC Chairs

Adriana Valio
Emilia Correia
Alisson Dal Lago
Gustavo Guerrero
Jorge Lelendez

Tribute to Jean-Paul Zahn
(1935 – 2015)

A.S. Brun, Space-Inn School, 28/10/15